Joint conference

IMEKO TC 8, TC11, TC 24 & EUROLAB 2023

IMEKO

eurolab aisbl
European Federation of National Associations of Measurement, Testing and Analytical Laboratories

RELACRE
ASSOCIAÇÃO DE LABORATÓRIOS ACREDITADOS DE PORTUGAL

LNEC
LABORATÓRIO NACIONAL DE ENGENHARIA CIVIL

Message from the editors

We would like to introduce the congress attendees to the scientific program set up for the IMEKO TC8-TC11-TC24 Conference.

This IMEKO event has been designed to be an eminent forum for both researchers and professionals working in the fields of 'Traceability', 'Testing, Inspection and Certification', and 'Chemical Measurements'.

A good geographical diversity was achieved, with papers from 22 countries, across three continents. All contributions underwent a rigorous peer-review process to ensure a high scientific quality.

TC8 sessions covered digital twins, AI-traceability, reference materials, and standardization.
TC11 focused on digital transformation in TIC, innovation and validation of testing-methods, calibration, inspection and certification, quality management, conformity assessment, and use of reference materials in TIC Sector.
TC24 addressed the issues related to gas analysis for climate change and energy transition, chemical sensors, nanomaterials, and chemical measurements for health and biology,

The Conference Program was completed with three keynote lectures. The first, given by Damiano Petri (Metricode S.r.l), was entitled 'Digitization of laboratory processes: the ABC Bilance-Metricode case'. Then prof. Premysl Fitl (University of Chemistry and Technology - Prague) gave a lecture on 'Solid-state gas sensors and their applications in the field of metrology'. Finally, Sascha Eichstädt (Physikalisch-Technische Bundesanstalt (PTB), Germany) presented the latest advancements in the field of 'Digitalization of the Quality Infrastructure'.

In the frame of the conference, a Workshop on 'Sampling as laboratory activity' was held by Tatjana Tomic and Sandra Babic. During this workshop, the requirements of the ISO 17025:2017 standard related to sampling were discussed: identification of sampling risks, validation, and evaluation of sampling uncertainty as well as sampling quality control.

We anticipate that this event will inspire new studies in the field of measurements and instrumentation, to foster new collaborations, and to build active and cooperative groups in the fields of Traceability, Testing, Inspection and Certification, and Chemical Measurements.

Leonardo Iannucci
Marija Cundeva-Blajer
Thomas Wiedenhoefer

ISBN 978-972-8574-53-6

Published by RELACRE & EUROLAB aisbl December 2023

Table of contents

Welcome address

Dear Colleagues,

Welcome to the Joint Conference of IMEKO TC8, TC11, TC24 and EUROLAB aisbl, being held in Funchal, from 11 to 13 of October 2023 in the conference facilities at Hotel VIDAMAR, in the magnificent Island of Madeira in Portugal. Following the recent success of the Joint Conference held in Cavtat-Dubrovnik, Croatia, in 2022, and strengthened by the long tradition of cooperation between IMEKO Technical Committees, RELACRE (the Portuguese Association of Accredited Laboratories) hosts the 2023 Joint Conference, organized by IMEKO TC8, TC11, TC24 and EUROLAB aisbl. This event will bring together the TIC community, academia and industry, promoting the latest advancements in science and technology in many fields of metrology.

The joint event promoted by IMEKO TC8 (Traceability in Metrology), IMEKO TC11 (Measurement in Testing, Inspection and Certification) and IMEKO TC24 (Chemical Measurements), covers different aspects of interest of the wide scientific domains, bringing experts and professionals from all over the world to share ideas and knowledge about “New challenges and opportunities in traceability”, “Testing, Inspection and Certification for confidence and safety” and “New perspectives in Chemical measurements”.

It is also a great pleasure to meet you in Madeira Island, a Portuguese jewel discovered in the XV Century in the Atlantic Ocean, known for the nice tropical weather, a place full of authenticity where art, culture and nature provide incredible experiences and lasting memories. We hope that you will be amazed with the exotic colours of the flowers, the blue sea and the emerald green vegetation of this archipelago, enjoying the city of Funchal, famous for its hospitality, the gastronomical heritage and the vibrant environment all over the places.

The Executive Committee and the Local Organizing Committee will do their best to offer you a memorable Conference, hoping to create a great opportunity to share knowledge and new ideas improving the growing interest in Traceability, TIC industry and Chemical measurements. We hope that you will find the event technically fulfilling and highly entertaining and that it will be an opportunity for useful interactions and communications with colleagues from all over the world. A warm welcome to all of you coming to Madeira, for the 2023 IMEKO TC8, TC11, TC24 & EUROLAB joint Conference.

On behalf of the Organizing Committee

Michela Sega	***Álvaro Ribeiro***	***Tatjana Tomic***	***Laura Martin***
IMEKO TC8 Chairperson	*IMEKO TC11 Chairperson*	*IMEKO TC24 Chairperson*	*EUROLAB aisbl Secretary General*

About RELACRE

RELACRE was born in 1991, driven by the Portuguese Quality Institute and by some of the most relevant entities with laboratory activity in Portugal, creating conditions that did not exist until then, to act as a facilitator of synergies in a context of the growing economic activity of laboratories with accreditation. The constitution of RELACRE responded to a set of emerging challenges in the national context, following the dynamics of accreditation, and in the international context, after the foundation of EUROLAB (European confederation of laboratory associations) in 1990, constituting itself as the representative association of Portugal in this new organization and against the backdrop of the creation of the single European market. Since then, RELACRE has occupied an important space, responding to a growing need for shared resources and an independent space for dialogue and discussion of sectoral problems and potential solutions. This movement resulted in a strong institutional representation of the sector and, simultaneously, in the creation of bridges and a strong capacity for intervention in the European and international context, anticipating the importance that this aspect currently has for many of its members and for the laboratory community in Portugal.

About IMEKO

IMEKO is a non-governmental federation of 42 Member Organizations individually concerned with the advancement of measurement technology. Its fundamental objectives are the promotion of international interchange of scientific and technical information in the field of measurement and instrumentation the enhancement of international co-operation among scientists and engineers from research and industry. Founded in 1958, the Confederation has consultative status with UNESCO and UNIDO and is one of the five Sister Federations within FIACC: Five International Associations Co-ordinating Committee, further consisting of: IFAC- International Federation of Automatic Control, IFIP International Federation for Information Processing, IFORS International Federation of Operational Research Societies and IMACS International Association for Mathematics and Computers in Simulation.

About EUROLAB

EUROLAB was created in Brussels on April 27, 1990 on the basis of a memorandum of understanding, signed by delegations representing the private and public laboratories of 16 out of the 19 countries of the EEC and EFTA.

EUROLAB is since October 1998 a legal entity in the form of an international association under Belgian law (A.I.S.B.L. - Association Internationale Scientifique sans But Lucratif) setting it as the European Federation of National Associations of Measurement, Testing and Analytical Laboratories.

Organizing committee


Michela Sega

Álvaro Silva Ribeiro


Tatjana Tomic

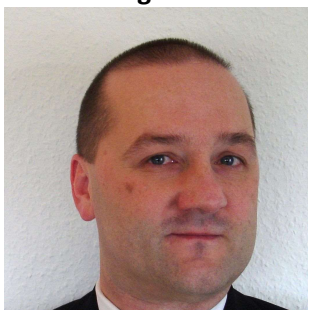
Thomas Wiedenhoefer


Marija Cundeva-Blajer


Leonardo Iannucci


Laura Martin

Mladen Jakovcic

Local Organizing committee

Álvaro Silva Ribeiro

Ana Duarte

Carla Estevens


Cila Silva


Catarina Martins

International Program Committee

TC8 - Traceability in Metrology	TC11 - Measurement in Testing, Inspection and Certification	TC24 – Chemical Measurements
Michela Sega *(Chair)*	Álvaro Silva Ribeiro *(Chair)*	Leonardo Iannucci *(Chair)*
Thomas Wiedenhoefer	Mladen Jakovcic	Aleksandra Aleksic
Sergio P. Oliveira	Marija Cundeva-Blajer	Carolina Andrade
Serhii V. Pronenko	Honglei Yang	Emma Angelini
	Admer Rey C. Dablio	Sandra Babic
	Agne Bertasiene	Ana Cop
	Antonio Shemakalu	Leila Es Sebar
	Christian Müller-Schöll	Přemysl Fitl
	Annette Röttger	Sabrina Grassini
	Rama Dasu Pittala	Katarina HafnerVuk
	Yoshitada Tanaka	Martin Hruska
	Rola Bou Khozam	Otta Jaroslav
	Shiv Kumar Jaiswal	Luca Lombardo
	Gertrud Mamiya	Zhechao Qu
	Ivana Ljevaković-Musladin	Michela Sega
	José Luis Prieto Calviño	Christable Tan
	Maria do Céu Lopes de Sousa Ferreira	Tatiana Tomic
	Paolo Emilio Roccato	Luisa Vigorelli
	Sanjay Yadav	
	Vedran Šimunovic	
	Yao Hejun	
	Bodan Velkovski	
	Kruno Milicevic	
	Gorana Baršić	
	Mare Srbinovska	
	Miryana Masheva	
	Kiril Demerdziev	
	Tzvetelin Gueorguiev	

Joint Conference of TC8, TC11 and TC24 Mottos

TC8, New challenges and opportunities in traceability

TC11, Testing, Inspection and Certification for confidence and safety

TC24, New perspectives in Chemical measurements

Topics

SUMMARY OF TOPICS TC8 Traceability in Metrology

- Digital twins
- Energy-related topics
- Traceability in AI, self learning systems and big data
- Metrological traceability in chemistry (primary reference methods and primary standards)
- Reference materials and certified reference materials
- International cooperation and SI traceability in chemistry, pharmacy and medicine
- Standardization

SUMMARY OF TOPICS TC11 Measurement in Testing, Inspection and Certification

- Management systems and Quality in the TIC sector
- Regulatory framework for quality, safety and security of products and services (agrifood, environment, health, cybersecurity, communication, construction, IoT, AI, among others)
- Innovation and validation of methods in testing, calibration, inspection and certification
- Sampling activities related to measurements in the TIC Sector
- Metrological traceability, measurement uncertainty and conformity assessment in TIC Sector
- Certification of reference materials and their use in laboratories
- Certification of products, processes, management systems and persons
- Digital transformation in testing, inspection and certification
- Measurements as an enabler of economic development
- Quality management and conformity assessment in TIC Sector
- SMART Metrology and TIC: Demands and new opportunities in the incorporation of Key Enabling Technologies (KET's)
- Other TIC issues

SUMMARY OF TOPICS TC24 Chemical Measurements

- Traceability and fundamental chemical metrology
- Chemical and biochemical sensors
- Separation techniques
- Gas-phase chemical measurements
- Measurements for Cultural Heritage
- Process Analytical Technology
- Validation, uncertainty and quality control in chemical measurements
- Chemical measurements for environment
- Chemical measurements for food and agriculture
- Chemical measurements for health and biomedical applications
- Data integrity and digitalization

Damiano Pietri

“Digitization of laboratory processes: the ABC Bilance-Metricode case”

Co-founder and President of Metricode s.r.l. which develops technologies to automate and digitalize industrial weighing processes by integrating them with hardware and industrial applications. Previously he was CEO in ABC Bilance s.r.l. and in charge of legal metrology and he is still the calibration laboratory manager. Damiano represented for four years an important Italian SME association being delegated for digital development issues both in Italy and Europe.

Přemysl Fitl

"Solid-state gas sensors and their applications in the field of metrology"

Přemysl Fitl has been working in field of chemical gas sensors since 2002. He is currently working at the University of Chemistry and Technology, Prague and the Institute of Physics of the CAS, where he works on the development of chemical gas sensors using thin film technologies and research on the preparation of thin films and nanostructured materials. He teaches courses focused on measurement and sensor technology. He is the author of 105 published scientific papers, 1 monograph and 2 patents. H-index 18. Since 2014 he is the Czech representative of TC24 in IMEKO organization.

Sascha Eichstädt

"Digitalization of the Quality Infrastructure"

Dr. Sascha Eichstädt is the leader of the department “Metrology for digital transformation” at the Physikalisch-Technische Bundesanstalt (PTB) since mid-2021. He received his Diploma in Mathematics in 2008 at the Humboldt University Berlin, and his PhD in Theoretical Physics in 2012 at the Technical University Berlin. He is a passionate metrologist since 2008 when he joined the group “Mathematical modelling and data analysis” at PTB to work on measurement uncertainty for time series. In 2017 he started his adventures in digital transformation of metrology as working group leader of the group “Coordination Digitalization” in the Presidential Staff of PTB. He chaired the EURAMET working group "Metrology for digital transformation” from 2020-2022. Sascha Eichstädt is chairing the OIML Digitalisation Task Group since 2022 and the IMEKO Technical Committee on Digitalisation since 2021

Special Sessions

IMEKO TC8 Traceability in Metrology

Digitalization in Traceability – new tools, new opportunities, new challenges

To provide a comprehensive understanding of the latest trends and technologies in digital supported traceability, challenges, and opportunities in implementing digital traceability solutions, and showcase success stories shall be presented and discussed.
In special keynote talks on topics e. g. from Blockchain Technology for Enhanced Traceability, Digital Calibration Certificates (DCC), Metrological Digital Twins (M-DT), smart supply-chain-management, AI and machine learning chances, changes and limitations of these new techniques shall be highlighted. You are invited to contribute by uploading an abstract of max. 250 words to the conference management system. Please state your interest in this special session.
We are aiming to get insights from industry experts and researchers on current developments, challenges, and barriers regarding digitalization in traceability, while uncovering opportunities for innovation and collaboration in this interactive workshop.

Keywords:

- *Digitalization in Traceability*
- *metrological digital twins*
- *smart supply-chain-management*
- *digital calibration certificates*
- *AI and ML*

IMEKO TC24 Chemical Measurements

Gas analysis for climate change and energy transition

The rise in atmospheric greenhouse gases is the primary driver of climate change. Closely monitoring the gas phase composition of the atmosphere is therefore critically important to understand and monitor climate change. Robust metrology for greenhouse gases monitoring in the air will be vital to achieve zero-pollution and carbon neutrality, ambitions laid out in strategies by both the European Union and the United Nations.
In striving towards environmental sustainability and a reliable energy network, it is vital to address outstanding fundamental challenges to establish renewable gases (e.g., Hydrogen, Ammonia, Biomethane) as a fuel source and as an energy vector. To ensure the safety and reliability of renewable gaseous fuels it is important to have robust, accurate measurements that can be traced to established standards.

Keywords:

- *Gas metrology*
- *Climate change and air quality*
- *Low-cost sensors*
- *Hydrogen*
- *Decarbonization*

Program

10-Oct		
19:00	**Welcome reception**	
11-Oct		
08:30	Registration	
09:00	Opening ceremony	
09:30	**Damiano Pietri** *"Digitization of laboratory processes: the ABC Bilance-Metricode case"*	
10:15	**Laura Martin** *"EUROLAB: an international collaboration towards the Lab of the Future"*	
10:40	Coffee & Networking	
Location	**Sunset III**	**Sunset II**
11:00	**Gas analysis for climate change and energy transition (part I)**	**Digital transformation in TIC and Digital Twins**
	#4 "Nanoporous Black Gold for Hydrogen Sensing"	*#22 "Validation methods in the preparation of Digital Calibration Certificates (DCCs)"*
	#8 "Climate change – cross-disciplinary metrology supporting its mitigation and control"	*#24 "The Digital Twin for frequency transfer traceability"*
	#14 "Preparation of Multicomponent Mixtures to Support Carbon Metrology"	*#28 "Digitalzations impact on Traceability in Metrology"*
	#21 "Enabling measurement of CO2 purity and composition: NPL's role as the UK National Metrology Institute"	*#34 "Progress with Digital Certificates of Analysis for Reference Materials and Traceability at NIST"*
12:30	Poster session	
13:00	**Lunch**	
14:00	**Přemysl Fitl** *"Solid-state gas sensors and their applications in the field of metrology"*	
14:45	**Workshop TC24** (Sampling as laboratory activity - by Tatjana Tomic and Sandra Babic)	
16:15	Coffee & Networking	
Location	**Sunset III**	**Sunset II**
16:30	**Gas analysis for climate change and energy transition (part II)**	**Gas-phase chemical measurements (part I)**
	#6 "Metrological Traceability in Environmental Gas Analysis – From SRP to TILSAM to d-TILSAM"	*#5 "Investigation of Surface Processes on Black Aluminium Layers for Sensor Applications"*
	#13 "Production of gaseous certified reference materials at INRiM for amount of substance fraction of CO2"	*#18 "Properties of black metal - lanthanide doped oxide sensitive layer toward multivariable gas sensor"*
	#27 "Traceable in-house preparation of RM CO2/N2 gas mixture using gravimetric standardized method"	*#17 "Surface decorated black metal active layers for gas sensors"*
17:30	**End of first day**	
18:30	Madeira wine in Funchal City Hall (Conference Bus from the hotel)	

12-Oct

08:30	Registration	
09:00	**Sascha Eichstädt** *"Digitalization of the Quality Infrastructure"*	
09:45	Invited Speaker (My Green Lab)	
10:10	**Workshop TC8** (Digitalization in Traceability – new tools, new opportunities, new challenges)	
11:30	Coffee & Networking	
Location	**Sunset III**	**Sunset II**
11:50	**Chemical measurements for health and biology**	**Innovation and validation of methods in testing, calibration, inspection and certification (part I)**
	#23 *"Metrological traceability of moisture content measurements in plant-origin bulk materials"*	*#25 "Traceability and method validation of a fully automated optical process to provide the on-site measurement of waste and bulk cargo volume"*
	#29 "Chemical measurents and their applications in health biomedical sciences"	*#30 "Implementation and Validation of Calibration Methods in the Area of High Frequencies"*
	#35 "Thin films gas sensors for biomedical applications"	*#31 "Extreme Impedance Calibrations: Enhancement of Metrology Infrastructure"*
	#37 "Novel approaches for measurements in dentistry"	#38*"The need to sensitize inspection and certification bodies in the use of decision rule to avoid poor decision making when interpreting results from certificates of analysis"*
13:00	**Lunch**	
14:45	Conference Photo	
15:00	Cultural visit (Conference Bus from the hotel)	
18:00	End of cultural visit	
19:30	Join in for Dinner (Conference Bus from the hotel)	
20:00	**Conference Dinner**	

13-Oct

09:00	TC8, TC11, TC24 meetings	
Location	**Sunset III**	**Sunset II**
10:00	**Gas-phase chemical measurements (part II)**	**Quality management, conformity assessment and use of reference materials in TIC Sector**
	#9 "Laser Direct Write Treatment of Black Metals for Gas Sensing Applications"	*#2 "Characterization of electronic waste materials by Instrumental Neutron Activation Analysis for Certified*
	#33 "On site measurements for the safeguard of metallic works of art"	#15 "Quality managment abd conformity assessment"
10:50	**Coffee & Networking**	
Location	**Sunset III**	**Sunset II**
11:10	**Gas analysis for climate change and energy transition (part III)**	**Innovation and validation of methods in testing, calibration, inspection and certification (part II)**
	#12 "Assessment of moisture absorption by anhydrous ethanol under different environmental conditions"	#39 *"Validation of a Method for the Extraction and Quantification of Water-Soluble Chloride in Cement by Ion Chromatography"*
	#26 "Preparation of stable isotope reference mixtures of CO2 in air global atmospheric monitoring"	*#3 "Experimental determination of the absolute roughness of concrete conducts in a water supply network"*
	#36 "Metrology for hydrogen vehicle 2: new reference materials and new sampling approaches applied to hydrogen fuel"	*#16 "Development of open-source tools for the digital and machine-readable calibration of flowmeters with numerical displays."*
		#20 "Analysis of flow rate measurement accuracy and traceability of flowmeters in field conditions using clamp-on ultrasonic flowmeters"
12:30	**Closing ceremony**	
13:00	**End of Conference**	

Session Chairs

11-Oct

Gas analysis for climate change and energy transition (part I)
Location: Sunset III
Time: 11:00
Chairs: Tatjana Tomic & Leonardo Iannucci

Digital transformation in TIC and Digital Twins
Location: Sunset II
Time: 11:00
Chairs: Marija Cundeva-Blajer & Thomas Wiedenhöfer

Gas analysis for climate change and energy transition (part II)
Location: Sunset III
Time: 16:30
Chairs: Zhechao Qu & Leonardo Iannucci

Gas-phase chemical measurements (part I)
Location: Sunset II
Time: 16:30
Chairs: Sabrina Grassini & Simon Peter Mukwaya

12-Oct

Chemical measurements for health and biology
Location: Sunset III
Time: 11:50
Chairs: Emma Angelini & Julio Brionizio

Innovation and validation of methods in testing, calibration, inspection and certification (part I)
Location: Sunset II
Time: 11:50
Chairs: Catarina Simões & Marija Cundeva-Blajer

13-Oct

Gas-phase chemical measurements (part II):
Location: Sunset III
Time: 10:00
Chairs: Sabrina Grassini & Tatjana Tomic

Quality management, conformity assessment and use of reference materials in TIC Sector
Location: Sunset II
Time: 10:00
Chairs: Álvaro Silva Ribeiro & Mladen Jakovcic

Gas analysis for climate change and energy transition (part III)
Location: Sunset III
Time: 11:20
Chairs: Francesca Durbiano & Martin Hruska

Innovation and validation of methods in testing, calibration, inspection and certification (part II)
Location: Sunset II
Time: 11:20
Chairs: Catarina Simões & Marija Cundeva-Blajer

Proceedings ("The following abstracts are related with presentations made by the Authors with valid registration in the Conference.")
#2

IMEKO TC8, TC11 and TC24 Joint Conference
October 11-13, 2023, Madeira, Portugal

CHARACTERIZATION OF ELECTRONIC WASTE MATERIALS BY INSTRUMENTAL NEUTRON ACTIVATION ANALYSIS FOR CERTIFIED REFERENCE MATERIAL PRODUCTION

M. Di Luzio[1]/Presenter, L. Bergamaschi[2], R. Jacimovic[3], G. D'Agostino[4]

[1] Istituto Nazionale di Ricerca Metrologica (INRIM), Pavia, Italy, m.diluzio@inrim.it
[2] Istituto Nazionale di Ricerca Metrologica (INRIM), Pavia, Italy, l.bergamaschi@inrim.it
[3] Jozef Stefan Institute (JSI), Ljubljana, Slovenia, radojko.jacimovic@ijs.si
[4] Istituto Nazionale di Ricerca Metrologica (INRIM), Pavia, Italy, g.dagostino@inrim.it

Abstract:
Recycling of Waste from Electrical and Electronic Equipment provides an accessible source to gather Technology Critical Elements which are in constant need. The main metrological challenge consists in the lack of Certified Reference Materials for this kind of matrices impeding to perform SI traceable and reliable analytical measurements on those heterogeneous materials.

This work describes the adoption of relative- and k_0-standardization of Instrumental Neutron Activation Analysis to quantify some of the Technology Critical Elements for certification in two Reference Material candidates.

Keywords: WEEE; INAA; Reference Material

1. INTRODUCTION

Electronic devices are ubiquitous within the European Union and their ever increasing demand is putting a lot of pressure on the supply chain, especially for what concerns materials defined as Technology Critical Elements (TCE). Waste from Electrical and Electronic Equipment (WEEE) can provide an accessible source to gather TCE; to this end, the European Union highly encourages practices involving more sensible waste management aiming to recycle those elements. However, a primary metrological obstacle to the recycling lies in the lack of Certified Reference Material (CRM) for this heterogeneous compound which makes difficult to perform SI traceable and reliable analytical measurements on waste samples.

Within the European project MetroCycleEU, samples from two WEEE materials from end-of-life Printed Circuit Boards (PCB) and Light-Emitting Diodes (LED) were prepared and characterized to be evaluated as candidates with the aim to produce the corresponding CRMs. The maximum allowed target standard uncertainty ($k = 1$) for the certified TCE mass fractions was fixed to 20%, including inhomogeneity and value assignment.

In detail, gathered materials were grinded to powder and analyzed by different analytical techniques to quantify interesting TCE present with mass fraction greater than 1 μg g^{-1}.

In this work the adoption of relative- and k_0-standardization of Instrumental Neutron Activation Analysis (INAA) to quantify TCE in samples of candidate CRMs is described. INAA provides suitable reference methods for bulk analysis preventing the dissolution of sample which is usually a challenging task for highly heterogeneous materials. The optimized INAA measurement procedures are reported and results for quantified TCE in both matrices are plotted on a sample-per-sample basis; major contributors to uncertainties are identified based on the provided uncertainty budgets, which also support SI traceability.

2. MEASUREMENT MODELS

INAA is an elemental analytical technique based on excitation of samples with a neutron flux and subsequent detection of γ-emissions from the produced radionuclides 0. Since neutrons and γ–rays have great penetration in matter, the technique is suitable for bulk analysis and allows to limit or completely avoid sample preparation.

The two main standardization methods adopted with INAA are referred to as (i) relative 0 and (ii) k_0 0; while the basic concept of the technique remains

the same they differ about the standardization element used for analysis. In the relative method a standard, containing the same element to be quantified, is co-irradiated with the measurement sample whereas in the k_0 method the co-irradiated standard contains a monitor element that is not necessarily the element to be quantified.

In the relative method a direct comparison between standard and sample is performed through the ratio of the corresponding count rate emissions. The k_0 method instead needs the knowledge of neutron flux parameters, alongside with specific composite nuclear constants, to relate data from the analyte element to the monitor element.

A general measurement model is described, suitable for both analytical methods, to measure the mass fraction of the analyte element, w_a, in the sample:

$$w_\mathrm{a} = \frac{C_\mathrm{s\,a}}{C_\mathrm{s\,m}} \frac{k_{0\,\mathrm{Au}}(\mathrm{m})}{k_{0\,\mathrm{Au}}(\mathrm{a})} k_\varepsilon\, k_\beta \frac{m_\mathrm{std}\,(1-\eta_\mathrm{std})}{m_\mathrm{sm}\,(1-\eta_\mathrm{sm})}\, w_\mathrm{m} \times \frac{G_{\mathrm{th\,m}} + \frac{G_{\mathrm{e\,m}}}{f}\left(\frac{Q_{0\,\mathrm{m}} - 0.429}{\bar{E}_{\mathrm{r\,m}}^{\alpha}} + \frac{0.429}{0.55^{\alpha}(2\alpha+1)}\right)}{G_{\mathrm{th\,a}} + \frac{G_{\mathrm{e\,a}}}{f}\left(\frac{Q_{0\,\mathrm{a}} - 0.429}{\bar{E}_{\mathrm{r\,a}}^{\alpha}} + \frac{0.429}{0.55^{\alpha}(2\alpha+1)}\right)}, \quad (1)$$

where subscript a, m, sm and std refer to the analyte element, monitor element, measurement sample and standard sample, respectively. The C_s parameter represents the count rate at saturation, $k_{0\,\mathrm{Au}}$ is the k_0 value, k_ε is the efficiency ratio between analyte and monitor, k_β is the correction due to neutron flux gradient for measurement and standard samples, G_th and G_e are neutron self-shielding corrections, f is the thermal to epithermal conventional flux ratio, Q_0 is the resonance integral $1/E$ to 2200 m s^{-1} cross section ratio, $\bar{E}_\mathrm{r}$ is the effective resonance energy, α is the deviation from the $1/E$ trend of the epithermal flux, m is the mass, η is the moisture correction and w is the mass fraction. Details of the measurement model and its validation can be found in 0 and 0, respectively.

The model reported in eq. **Error! Reference source not found.** is valid either for relative and k_0-method; however, in the first case some of the factors simplify completely or assume values close to 1 due to the adoption of the same element for analyte and monitor: this situation applies for $\frac{k_{0\,\mathrm{Au}}(\mathrm{m})}{k_{0\,\mathrm{Au}}(\mathrm{a})}$ and to some extent, k_ε and $\frac{G_{\mathrm{th\,m}} + \frac{G_{\mathrm{e\,m}}}{f}\left(\frac{Q_{0\,\mathrm{m}} - 0.429}{\bar{E}_{\mathrm{r\,m}}^{\alpha}} + \frac{0.429}{0.55^{\alpha}(2\alpha+1)}\right)}{G_{\mathrm{th\,a}} + \frac{G_{\mathrm{e\,a}}}{f}\left(\frac{Q_{0\,\mathrm{a}} - 0.429}{\bar{E}_{\mathrm{r\,a}}^{\alpha}} + \frac{0.429}{0.55^{\alpha}(2\alpha+1)}\right)}$. Accordingly, the combined uncertainty obtained via the relative method is expected to be lower with respect to a similar measurement performed with the k_0 method as long as the uncertainty on counting statistics is comparable and under control; the usual higher uncertainty of the k_0 method is due to the corrections needed for the analyte to monitor conversion which depend on results of detector and irradiation facility characterizations and literature values 0, all parameters that have little to no impact on the relative method.

3. EXPERIMENTAL

Materials recovered from WEEE and available within the MetroCycleEU project were measured to evaluate their suitability as candidate CRMs. Test batches obtained from end-of-life PCB and LED milled to a particle size below 200 μm were shipped to the Jozef Stefan Institute (JSI) and Istituto Nazionale di Ricerca Metrologica (INRIM) laboratories to perform INAA quantification of the critical elements Au, Co, La and Ta. The k_0-standardization was adopted by JSI and the relative-standardization was adopted by INRIM, respectively.

3.1. Printed Circuit Boards (PCB)

From the batch of PCB material delivered to JSI, 8 measurement samples (4 of about 0.20 g and 4 of about 0.30 g) were sealed into pure polyethylene ampoules while moisture content was assessed on a separated aliquot. For determination of short-lived radionuclides, 4 samples and corresponding Al-0.1%Au standards (ERM-EB530A alloy) were stacked together, fixed in polyethylene vial and irradiated for 30 seconds in the carousel facility (CF) of the TRIGA Mark II reactor with a thermal neutron flux of 1.1×10^{12} cm^{-2} s^{-1}. For determination of intermediate and long-lived radionuclides, 4 samples and corresponding Al-0.1%Au standards were prepared on the same way as above and irradiated for 1 hour in the CF of the TRIGA Mark II reactor. After short irradiation (30 seconds) samples were measured after 15, 25, 120 minutes, 24 hours and 15 days of cooling time on absolutely calibrated HPGe detectors (40% and 45 % relative efficiency). After long irradiation (1 hour) samples were measured after 4, 11 and 30 days of cooling time on the same detectors. For peak area evaluation, the HyperLab program was used. The values f = 22.54 and α = –0.0075, obtained from previous determinations using the Cd ratio method, were adopted as flux parameters.

From the batch of PCB material delivered to INRIM, 12 measurement samples of about 0.17 g each were prepared while moisture content was assessed on a separate aliquot by means of a thermo-balance. Standard samples were prepared by pipetting drops of Au, Co, La and Ta SI-traceable solutions; measurement and standard samples were

stacked in 3 irradiation containers and irradiated in the CF of TRIGA Mark II reactor of Pavia with a thermal neutron flux of 1.2×10^{12} cm^{-2} s^{-1}; the irradiation lasted 1 h with the reactor operating at 250 kW power. Spectra of measurement and standard samples were acquired at suitable counting positions (ranging from 200 mm to 20 mm) of a 50 % relative efficiency HPGe detector.

3.2. Light Emitting Diodes (LED)

From the batch of LED material delivered to JSI, 12 measurement samples (5 for short irradiation and 7 for long irradiation) of about 0.25 g each were sealed into pure polyethylene ampoules. The same procedure as mentioned above for PCB was applied, except for the long irradiation duration, which lasted 12 hours.

From the batch of LED material delivered to INRIM, 16 measurement samples of about 0.40 g each were prepared while moisture content was assessed on a separate aliquot by means of a thermo-balance. Standard samples were prepared by pipetting drops of Au, Co, La and Ta SI-traceable solutions; measurement and standard samples were stacked in 4 irradiation containers then split in two irradiations in the CF of TRIGA Mark II reactor of Pavia; the short irradiation, designed to limit the matrix activation for quantification of medium-lived nuclides (Au and La), lasted 30 min while the long irradiation, designed for quantification of long-lived nuclides (Co and Ta), lasted 3 h. Spectra of measurement and standard samples were acquired at suitable counting positions (ranging from 200 mm to 20 mm) of a 50 % and a 20 % relative efficiency HPGe detector.

4. RESULTS

Data collected in the k_0-NAA experiment performed at JSI were elaborated with the software package Kayzero for Windows V3.40, which includes effective solid angle algorithms for detection efficiency calculations. Results are provided with combined uncertainty considering all known contributors (k_0-related literature values 0, irradiation, decay and measuring times, sample mass, standard composition, flux parameters, detection efficiency and related corrections).

Data collected in the relative-NAA experiment performed at INRIM were elaborated with the aid of a homemade software implementing eq. **Error! Reference source not found.** to get mass fraction results of the investigated elements together with uncertainty budgets. Input parameters were provided from knowledge of the experimental setup (dimensions and content of samples, γ-counting distances, γ-peak net areas and times of the acquired spectra), previous measurements (detector efficiency characterization, flux parameters), and literature (activation and decay related parameters 0).

As anticipated, the relative method allows reaching an uncertainty significantly lower than the k_0-method.

4.1. Printed Circuit Boards (PCB)

5.

Mass fraction results concerning the quantification of Au, Co, La and Ta in the PCB samples and obtained by JSI and INRIM are hereafter reported. Additionally, relative differences with respect to the average of all mass fraction results concerning the same element, $\bar{w}$, are also given together with indication of the contribution to the combined uncertainty, I, of the three main macro-components obtained by grouping parameters related to (i) counting statistics, (ii) detection efficiency and (iii) the remaining ones, respectively.

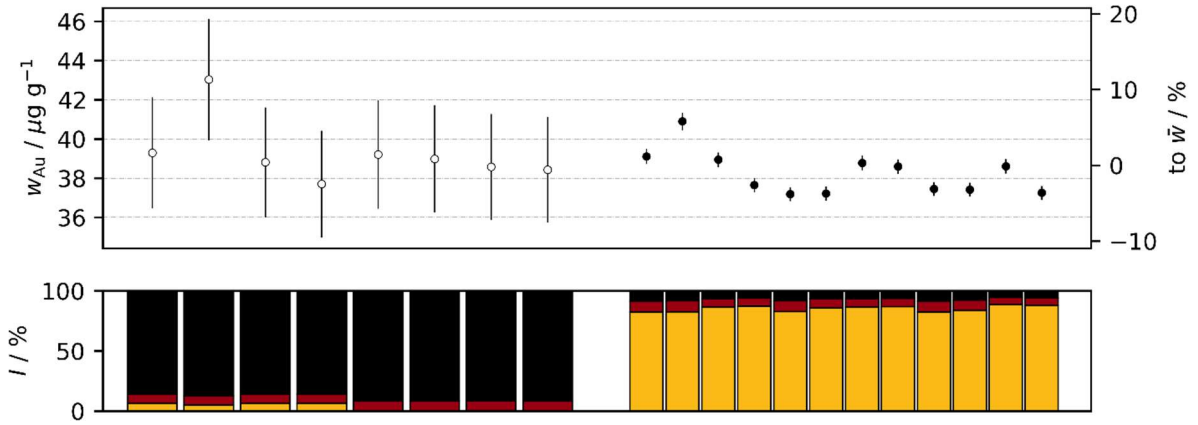

Figure 1: Au mass fractions measured on samples of the PCB material. White and black circles display results obtained with k_0-NAA and relative-NAA, respectively; errorbars indicate expanded uncertainty ($k = 2$). The bar chart at the

bottom reports the contributions to the uncertainty for the corresponding value: the highlighted macro-contributors are counting statistics (yellow), efficiency (red) and the remaining ones (black).

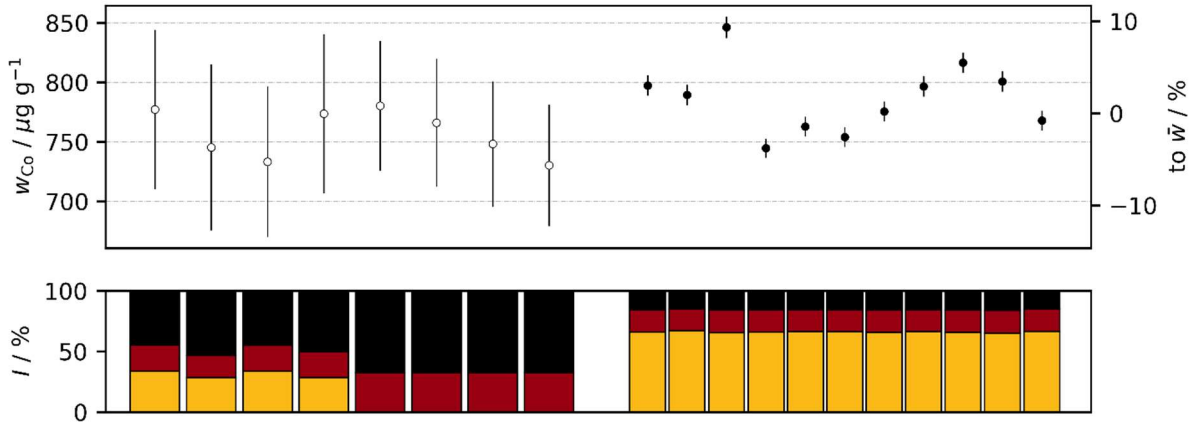

Figure 2: Co mass fractions measured on samples of the PCB material. White and black circles display results obtained with k_0-NAA and relative-NAA, respectively; errorbars indicate expanded uncertainty ($k = 2$). The bar chart at the bottom reports the contributions to the stated uncertainty for the corresponding value: the highlighted macro-contributors are counting statistics (yellow), efficiency (red) and the remaining ones (black).

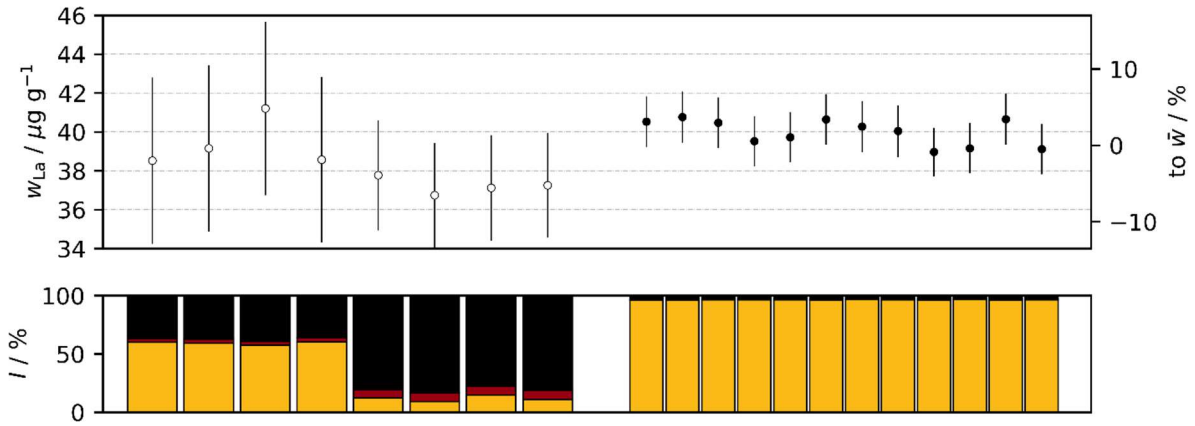

Figure 3: La mass fractions measured on samples of the PCB material. White and black circles display results obtained with k_0-NAA and relative-NAA, respectively; errorbars indicate expanded uncertainty ($k = 2$). The bar chart at the bottom reports the contributions to the stated uncertainty for the corresponding value: the highlighted macro-contributors are counting statistics (yellow), efficiency (red) and the remaining ones (black).

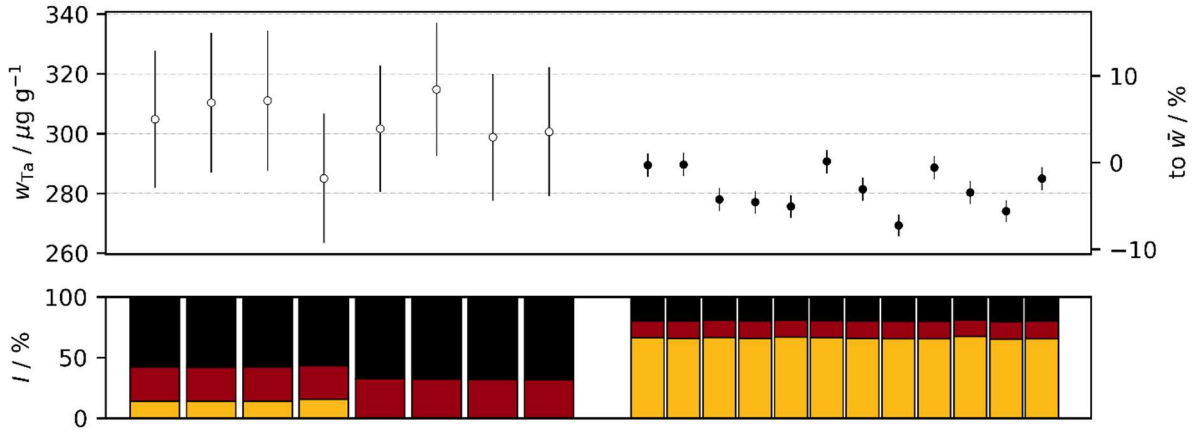

Figure 4: Ta mass fractions measured on samples of the PCB material. White and black circles display results obtained with k_0-NAA and relative-NAA, respectively; errorbars indicate expanded uncertainty ($k = 2$). The bar chart at the bottom reports the contributions to the stated uncertainty for the corresponding value: the highlighted macro-contributors are counting statistics (yellow), efficiency (red) and the remaining ones (black).

Data reported in Figure 1-Figure 4 display an overall agreement between results obtained with k_0 and relative methods. Non-homogeneities can better be appreciated from the less uncertain relative method data, but the variability, as denoted by the standard deviation, is within few percent.

5.1. Light Emitting Diodes (LED)

Mass fraction results concerning the quantification of Au, Co, La and Ta in the LED candidate material are hereafter reported; graphics maintain the same information of those related to PCB material shown previously.

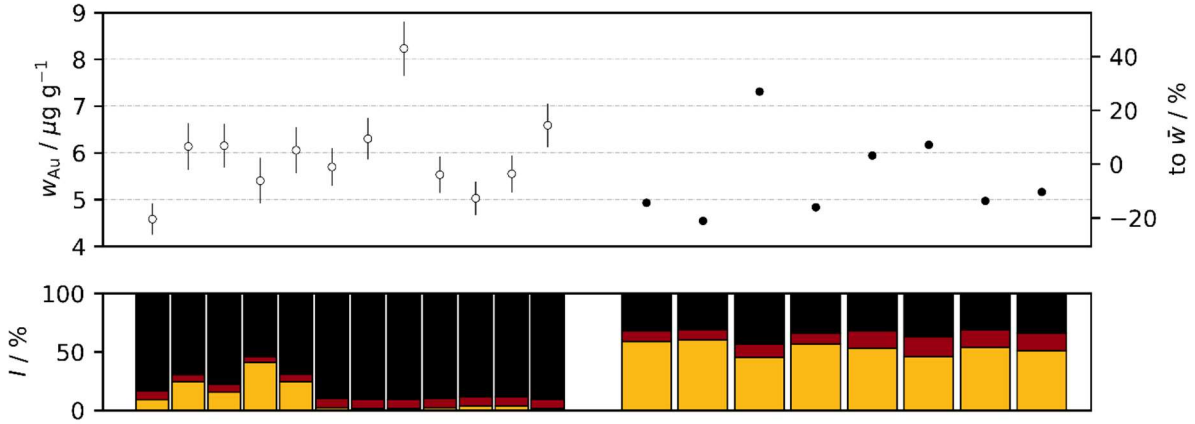

Figure 5: Au mass fractions measured on samples of the LED material. White and black circles display results obtained with k_0-NAA and relative-NAA, respectively; errorbars indicate expanded uncertainty ($k = 2$). The bar chart at the bottom reports the contributions to the stated uncertainty for the corresponding value: the highlighted macro-contributors are counting statistics (yellow), efficiency (red) and the remaining ones (black).

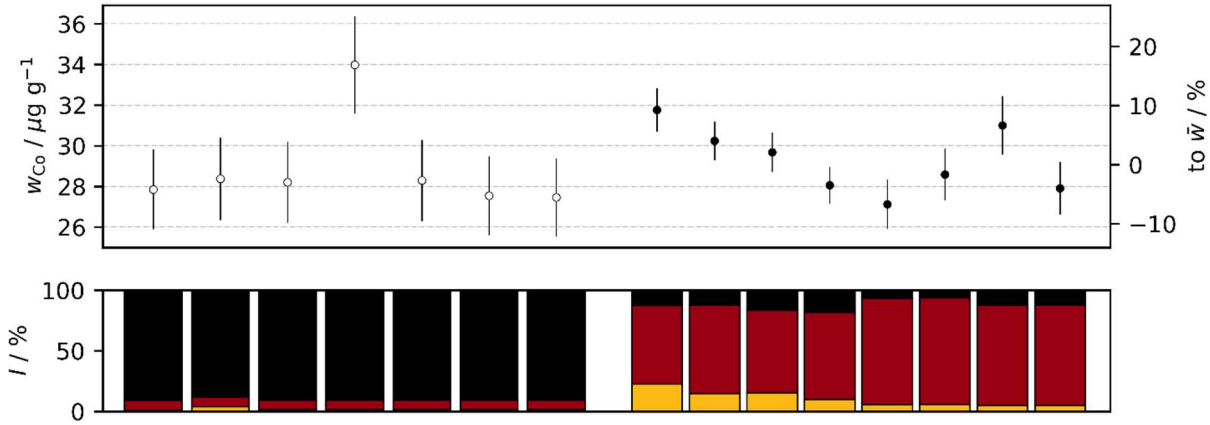

Figure 6: Co mass fractions measured on samples of the LED material. White and black circles display results obtained with k_0-NAA and relative-NAA, respectively; errorbars indicate expanded uncertainty ($k = 2$). The bar chart at the bottom reports the contributions to the stated uncertainty for the corresponding value: the highlighted macro-contributors are counting statistics (yellow), efficiency (red) and the remaining ones (black).

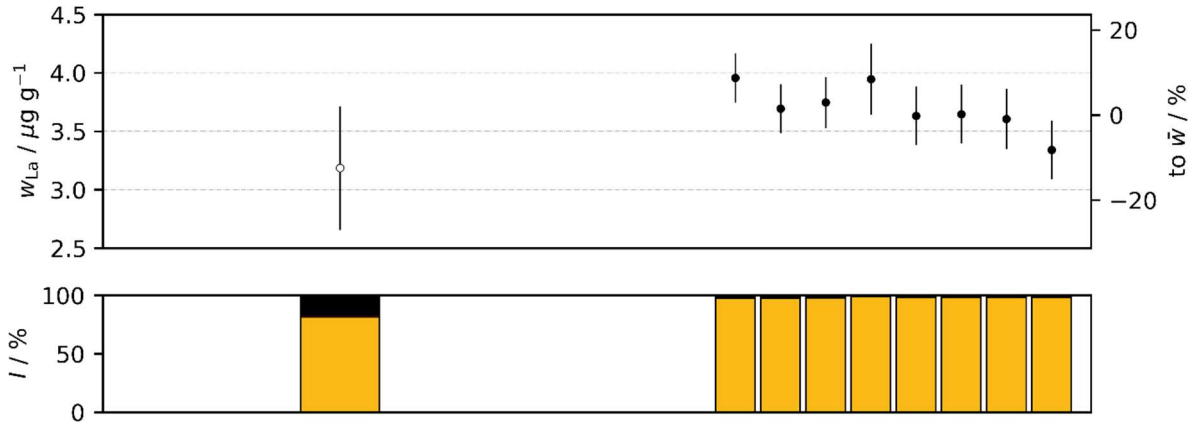

Figure 7: La mass fractions measured on samples of the LED material. White and black circles display results obtained with k_0-NAA and relative-NAA, respectively; errorbars indicate expanded uncertainty ($k = 2$). The bar chart at the bottom reports the contributions to the stated uncertainty for the corresponding value: the highlighted macro-contributors are counting statistics (yellow), efficiency (red) and the remaining ones (black).

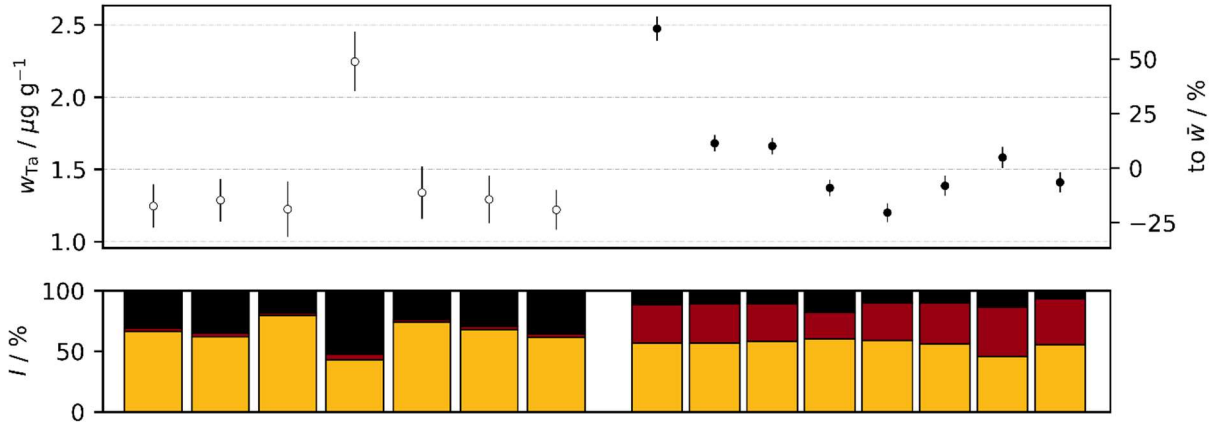

Figure 8: Ta mass fractions measured on samples of the LED material. White and black circles display results obtained with k_0-NAA and relative-NAA, respectively; errorbars indicate expanded uncertainty ($k = 2$). The bar chart at the bottom reports the contributions to the stated uncertainty for the corresponding value: the highlighted macro-contributors are counting statistics (yellow), efficiency (red) and the remaining ones (black).

Data reported in Figure 5-

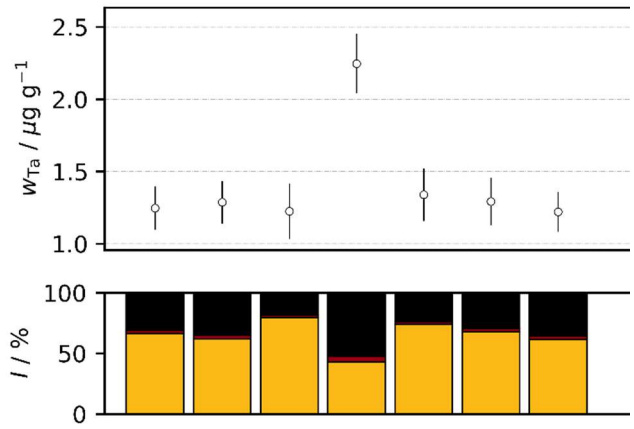

Figure 8 display a much more noticeable scattering of results especially for what concerns elements found at ppm level.

6. SUMMARY

Analysis on PCB and LED materials recovered from WEEE was performed with relative- and k_0-standardization methods of INAA technique in order to evaluate the suitability of these materials as a candidate WEEE CRM for Au, Co, La and Ta. The results did not show the presence of noticeable biases between the two standardization methods and confirmed that the measured PCB and LED materials are fit for purpose for the certification of Au, Co and La. For what concerns Ta, unacceptable non-homogeneities were highlighted in LED while La can be certified in PCB. Further studies will involve comparison with SI-traceable techniques based on completely different measurement principles for a broader consensus on the mass fraction values.

7. ACKNOWLEDGEMENTS

This project (20IND01 MetroCycleEU) has received funding from the EMPIR programme co-financed by the Participating States from the European Union's Horizon 2020 research and innovation programme.

8. REFERENCES

E. Witkowska, K. Szczepaniak, M. Biziuk, "Some applications of neutron activation analysis". Journal of Radioanalytical and Nuclear Chemistry, vol. 265, pp. 141-150, 2005. DOI: 10.1007/s10967-005-0799-1

R. R. Greenberg, P. Bode, E. N. Fernandes, "Neutron activation analysis: A primary method of measurement", Spectrochimica Acta Part B: Atomic Spectroscopy, vol. 66, pp. 193-241, 2011 DOI: 10.1016/j.sab.2010.12.011

F. De Corte, "The standardization of standardless NAA", Journal of Radioanalytical and Nuclear Chemistry, vol. 248, pp. 13-20, 2001. DOI: 10.1023/a:1010601403010

M. Di Luzio, M. Oddone, G. D'Agostino, "Developments of the k_0-NAA measurement model implemented in k0-INRIM software", Journal of Radioanalytical and Nuclear Chemistry, vol 331, pp. 4251-4258, 2022. DOI: 10.1007/s10967-022-08476-x

M. Blaauw, G. D'Agostino, M. Di Luzio, H. Manh Dung, R. Jacimovic, M. da Silva Dias, R. Semmler, R. van Sluijs, N. Pessoa Barradas, "The 2021 IAEA software intercomparison for k_0-INAA", Journal of Radioanalytical and Nuclear Chemistry, vol 332, pp. 3387-3400, 2023. DOI: 10.1007/s10967-022-08626-1

k_0-International Scientific Committee, database of recommended k_0-data, released August 24, 2020. http://www.kayzero.com/k0naa/k0naaorg/Nuclear_Data_SC/Entries/2020/8/24_Update_of_k0-database_I-128.html.

IMEKO TC8, TC11 and TC24 Joint Conference
October 11-13, 2023, Madeira, Portugal

EXPERIMENTAL DETERMINATION OF ABSOLUTE ROUGHNESS OF CONCRETE CONDUCTS IN A WATER SUPPLY NETWORK

L. Martins, A. Ribeiro, C. Simões, A. Pais, R. Mendes

LNEC – National Laboratory for Civil Engineering, Lisbon, Portugal, lfmartins@lnec.pt

Abstract:

This paper describes the experimental determination of the absolute roughness of concrete conducts in a pressurized water supply network related to agricultural irrigation. Based on the Colebrooke-White equation and using a Monte Carlo method, the following estimates and 95 % expanded measurement uncertainties were obtained for a circular concrete conduct with an inner diameter of 1,2 m: 0,060 mm ± 0,055 mm and 0,021 mm ± 0,024 mm, for a water flow Reynolds number, comprised between $1{,}7 \cdot 10^5$ and $5{,}1 \cdot 10^5$, respectively. The output probability distribution showed a non-symmetrical shape, and the volumetric flow and pressure drop measurements were identified as the main contributions to the obtained dispersion of roughness values.

Keywords: Hydraulics; Conduct; Concrete; Roughness

3 INTRODUCTION

Water supply networks have a massive role in our society in urban and rural areas. Water is a fundamental and essential resource for the subsistence and development of all countries and regions worldwide, justifying dedicated attention by United Nations (UN-Water) since the 1970s. These networks include several hydraulic elements such as reservoirs, dams, wells, and pumping and treatment stations, and usually have a high extension. Conducts are essential to the water transportation between the mentioned hydraulic elements, from an initial stage (collection) to the final stage (customer delivery).

From a design point of view, the friction of the water against the inner wall of conduct is a crucial issue due to the need for pumping to overcome the corresponding pressure drop along the water supply network, directly impacting construction and operation costs. The friction factor of conduct is directly related to its roughness. It is considered a complex problem in fluid mechanics, usually requiring an experimental approach under restricted conditions to obtain an accurate solution.

2 THEORETICAL BACKGROUND

In the studied hydraulic context, the conduct was considered rigid and straight, with a circular cross-section with an inner diameter D, subject to a gravitational field characterized by a g acceleration. Being V the average flow velocity inside the conduct and assuming a constant flow of a Newtonian fluid (water, in this case), the head loss, h, between two cross-sections separated by a distance L, is given by

$$h = f \cdot \frac{L}{D} \cdot \frac{V^2}{2 \cdot g}, \tag{2}$$

where f is the friction factor [1]. This dimensionless quantity is the function of the conduct roughness and the Reynolds number, Re, defined as

$$Re = \frac{V \cdot D}{v}, \tag{3}$$

being v the water kinematic viscosity (considered constant in the case of an isothermal flow) [1].

In this study, the absolute (equivalent) roughness, ε_s, is assumed homogenous and uniform along the conduct, expressing the dimensional irregularities of its inner surface and considering an equal sand grain diameter (in the first roughness studies in conducts, their inner surface was coated with standard sand with a known grain dimension). In this context, the quantity relative roughness is defined by the quotient between the equivalent roughness and the conduct inner diameter, ε_s/D.

The Colebrook-White equation [1] is an implicit function which allows determining (using interpolation tables, graphical diagrams, analytical or numerical approaches) the friction factor based on the relative roughness and the Reynolds number, i.e.

$$\frac{1}{\sqrt{f}} = -2 \log\left(\frac{\frac{\varepsilon_S}{D}}{I} + \frac{M}{Re \cdot \sqrt{f}}\right), \tag{4}$$

where $I = 10^{0,87}/2$ and $M = 10^{0,4}$. If the conduct friction factor is known, the Colebrook-White equation can be used to express the absolute (equivalent) roughness explicitly:

$$\varepsilon_s = D \cdot I\left(10^{-\frac{1}{2\sqrt{f}}} - \frac{M}{Re\cdot\sqrt{f}}\right). \quad (5)$$

By introducing the concept of equivalent hydrostatic pressure [1] in expression (1), the friction factor can be obtained from

$$f = \frac{2\cdot\Delta p\cdot D}{\rho\cdot L\cdot V^2}, \quad (6)$$

where ρ is the water density (for a given temperature and pressure inside the conduct), and Δp is the pressure drop between two cross-sections separated by a distance of L.

In summary, the measurement approach applied in this study for the determination of the absolute (equivalent) roughness is supported by knowledge about: (i) the water´s physical properties (known density and viscosity values from the literature, using pressure and temperature measurements); (ii) the conduct's dimensional properties (inner diameter and distance between two cross-sections); (iii) the average flow velocity (obtained from the volumetric flow measurements, q_v, knowing the inner diameter of the conduct), and; (iv) the pressure drop (based on pressure simultaneous measurements in two cross-sections of the conduct).

4 EXPERIMENTAL WORK

The following sections describe the hydraulic infrastructure where the studied concrete conduct is located, the applied experimental resources and the testing procedure.

a. Hydraulic infrastructure

The studied concrete conduct is part of a hydraulic infrastructure dedicated to agricultural irrigation at Alentejo (South region of Portugal), connecting two water reservoirs at different altitudes. Water pressurization is assured by a pumping station located near the lowest reservoir. Three measurement points were defined in this conduct (as shown in Figure 1): (i) the flow measurement near the highest reservoir; (ii) the pressure measurement in two air valves (1 and 2) installed in different cross-sections of the conduct, 804 meters away from each other, without any significant hydraulic elements between them.

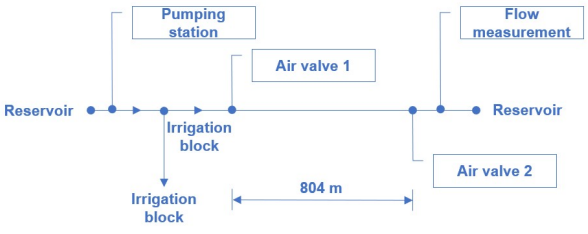

Figure 9: Schematic representation of the hydraulic infrastructure

b. Experimental resources

Table 1 mentions the measurement instruments used in the experimental work, namely, their main metrological features.

Table 1: Measurement instruments

Designation	Brand and model	Range and resolution
Pressure transducers with digital indicator	Druck; PDCR 910-1422	20 bar; 0,1 mbar
	Druck; ---	35 bar; 1 mbar
Ultrasonic flowmeter	Dynasonics; DXNP EHS-NN	1945 m^3/h; 0,01 m^3/h
Digital thermometer	Druck; DPI 605	0 ºC – 40 ºC; 0,01 ºC

These instruments are traceable to measurement standards which perform measurement units according to the International System of Units (SI) and were subjected to metrological confirmation, from which linear calibration curves were obtained for the case of the pressure measurement chains.

c. Testing procedure

Automatic data acquisition of flow, pressure and temperature measurements was defined, considering an acquisition period of five seconds during 10 minutes records.

The flowmeter was installed in the conduct considering its measurement principle (ultrasonic) and assuring the minimum recommended distance between sensors (see Figure 2), considering the conduct outer perimeter and wall thickness.

Figure 10: Flowmeter ultrasonic sensors installed in the conduct

Each pressure transducer was installed in the service plug of the air valve mounted in the conduct (see Figure 3) after water drainage and performing the measurement zero.

A water sample was collected before and after the test in one of these air valves to obtain the required temperature measurement.

Static pressure records were obtained at the beginning and end of the test without pump pressurization of the conduct. Seven volumetric flow testing steps were defined, from 550 m^3/h up

to 1750 m^3/h, and the corresponding dynamic pressure measurements were performed in the two cross-sections of the conduct at the air valves.

Figure 11: Connection of the pressure transducer to one of the conduct's air valve

5 RESULTS

In the performed test, a constant water temperature was observed (20,1 ºC) between the experimental campaign's beginning and end. Based on this information and in static pressure measurements performed in each air valve (shown in Table 2), average water density (998,30 kg/m^3) and kinematic viscosity ($1{,}0008 \cdot 10^{-6}$ m^2/s) values were obtained from the literature [2].

Table 2: Static pressure measurement results (average values and sample experimental standard deviations)

Static pressure	Air valve 1 /bar	Air valve 2 /bar
Test beginning	5,088 3 ± 0,008 6	1,769 6 ± 0,002 1
Test end	5,088 6 ± 0,001 5	1,769 4 ± 0,001 1

Table 3 presents the average values and sample experimental standard deviations related to the flow and dynamic pressure measurements.

Table 3: Dynamic pressure measurement results for each flow testing step

Volumetric flow /m^3/h	Dynamic pressure in air valve 1 /bar	Dynamic pressure in air valve 2 /bar
576 ± 34	5,096 3 ± 0,001 0	1,772 6 ± 0,000 6
765 ± 65	5,100 1 ± 0,000 9	1,773 7 ± 0,001 1
828 ± 71	5,100 5 ± 0,000 8	1,773 4 ± 0,001 0
1020 ± 100	5,106 5 ± 0,000 7	1,775 8 ± 0,000 9
1402 ± 139	5,122 1 ± 0,001 2	1,783 5 ± 0,000 6
1676 ± 134	5,140 7 ± 0,003 8	1,794 8 ± 0,001 5
1721 ± 117	5,139 3 ± 0,003 9	1,792 9 ± 0,001 4

Based on the results shown in Tables 2 and 3, the corresponding differential pressures and pressure drops were calculated (see Table 4) and used to determine the intermediate (average flow velocity, Reynolds number and friction factor) and output (roughness) quantities. The results are shown in Table 5 and Figure 4.

Table 4: Differential pressure and pressure drop estimates

Volumetric flow /m^3/h	Differential pressure in air valve 1 /bar	Differential pressure in air valve 2 /bar	Pressure drop /bar
576	0,007 9	0,003 1	0,004 8
765	0,011 7	0,004 2	0,007 5
828	0,012 1	0,003 9	0,008 2
1020	0,018 0	0,006 3	0,011 8
1402	0,033 6	0,014 0	0,019 7
1676	0,052 2	0,025 3	0,027 0
1721	0,050 9	0,023 4	0,027 5

Table 5: Estimates for the intermediate and output quantities

Flow velocity /m/s	Reynolds number	Friction factor	Roughness /mm
0,141	$1{,}7 \cdot 10^5$	0,072	0,060
0,188	$2{,}3 \cdot 10^5$	0,064	0,046
0,203	$2{,}4 \cdot 10^5$	0,059	0,039
0,251	$3{,}0 \cdot 10^5$	0,056	0,034
0,344	$4{,}1 \cdot 10^5$	0,049	0,025
0,412	$4{,}9 \cdot 10^5$	0,047	0,022
0,423	$5{,}1 \cdot 10^5$	0,046	0,021

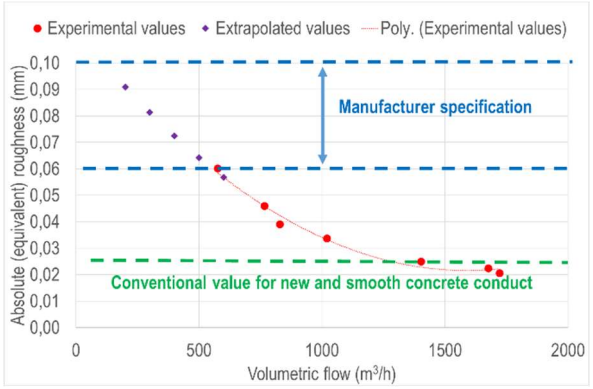

Figure 4: Relation between roughness and flow values

The determination of the measurement uncertainty related to the roughness estimates presented in Table 5 was performed using a Monte Carlo method (MCM) [3], considering the propagation of the measurement uncertainties (mentioned in Table 6) from the input quantities to the output quantity and the nonlinearity and complexity of the mathematical models involved, namely, the Colebrook-White equation. A total of 10^6 runs were performed to ensure a convergent solution for the roughness dispersion of values and a computational measurement uncertainty below 0,001 mm. The numerical simulation results are presented in Table 7.

Figure 5 shows an example of the roughness output probability distribution obtained by the MCM method, in this case, for an estimate equal to 0,023 mm.

Table 6: Probabilistic formulation of the input quantities

Uncertainty component	Type	Probability distribution	Standard uncertainty
$u(D)$	B	Gaussian	2,5 mm
$u(L)$	B	Gaussian	50 mm
$u(\rho)$	B	Gaussian	0,03 kg/m^3
$u(v)$	B	Gaussian	$2{,}9 \cdot 10^{-9}$ m^2/s
$u(q_v)$	A	Gaussian	34 m^3/h – 117 m^3/h
$u(p_1)$	A	Gaussian	0,7 mbar – 3,9 mbar
$u(p_2)$	A	Gaussian	0,6 mbar – 1,4 mbar

Table 7: Results of the MCM numerical simulations

Average /mm	Mode /mm	2,5 % and 97,5 % percentiles /mm	95 % expanded uncertainty /mm
0,063	0,054	0,019 ; 0,129	0,055
0,056	0,039	0,011 ; 0,123	0,056
0,043	0,033	0,011 ; 0,103	0,046
0,038	0,026	0,011 ; 0,092	0,041
0,028	0,022	0,008 ; 0,071	0,031
0,025	0,016	0,006 ; 0,063	0,028
0,023	0,017	0,006 ; 0,053	0,024

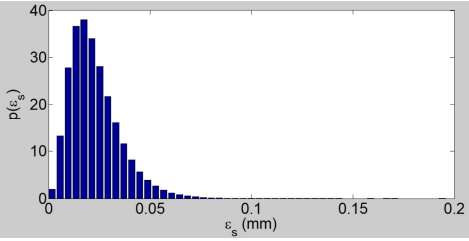

Figure 5: Example of the roughness output probability distribution

The same numerical routine was used to perform a sensitivity analysis of the input quantities to identify the main contributions to the roughness measurement uncertainty. Each input measurement uncertainty (mentioned in Table 6) was individually increased by 25 %, and the corresponding output measurement uncertainty increase was normalized. This analysis revealed that the volumetric flow quantity contributes to 53 % of the roughness uncertainty, while the pressure drop contributes to close to 44 %. The remaining input quantities have an individual contribution equal to or lower than 1 %.

6 CONCLUSIONS

The performed study allowed us to conclude that the absolute (equivalent) roughness of the concrete conduct (with a circular cross-section of 1,2 m inner diameter) is comprised between 0,060 mm and 0,021 mm, considering a water flow characterized by a Reynolds number between $1{,}7 \cdot 10^5$ and $5{,}1 \cdot 10^5$, respectively. The mentioned estimates include the additive pressure drop effect of joints and other hydraulic elements in the 804 m length conduct and of biofilm and other residues in its inner wall (expected to be reduced due to the short time of operation in agricultural irrigation).

95 % expanded measurement uncertainties varied between 0,055 mm and 0,024 mm, being related to the volumetric flow and pressure drop measurement uncertainties that are mainly originated by the hydraulic stability of the observed water flow in the conduct.

The application of the MCM allowed noticing the non-symmetrical geometrical shape of the roughness output probability distribution, which is justified by the proximity of the obtained estimates relative to the zero-roughness physical limit imposed by the Colebrook-White equation. This fact also explains the differences observed between: (i) the numerical estimates of the average and mode values shown in Table 7, and; (ii) the analytical (Table 5) and numerical (Table 7) roughness estimates.

The highest experimental roughness estimate (around 0,06 mm) is close to the expected value of the conduct's manufacturer for low volumetric flow (near 600 m^3/h). In comparison, the lowest roughness estimates are almost equal to the conventional value (0,025 mm) mentioned in the literature [4] for new and smooth concrete conduct, such as the one studied in this work.

A second-order polynomial (shown in Figure 4) can be fitted to the obtained experimental roughness and volumetric flow values, having a similar shape as the curves mentioned in hydraulic diagrams [1].

Future work will be dedicated to studying the relation between the equivalent roughness and the (non-equivalent) physical roughness directly measured in concrete conduct samples with an optical profilometer, for manufacturing quality control purposes.

7 REFERENCES

R. H. Sabersky, A. J. Acosta, E. G. Hauptmann, E. M. Gates, Fluid Flow – a first course in Fluid Mechanics. New Jersey: Prentice Hall, Ch. 5, pp. 187-202, 1999.

E. Lemmon, I. Bell, M. Huber, M. McLinden, "Thermophysical properties of fluid systems" in NIST Chemistry WebBook – NIST Standard Reference Database Number 69, 2023 Edition. Online [Accessed 20230602].

Evaluation of measurement data – Supplement 1 of the "Guide to the expression of uncertainty in measurement" – Propagation of distributions using a Monte Carlo Method. JCGM 101, Joint Committee for Guides in Metrology, 2008.

H. Ahmari, S. Kabir, Applied Fluid Mechanics Lab Manual. Mavs Open Press, 2019.

#7

IMEKO TC8, TC11 and TC24 Joint Conference
October 11-13, 2023, Madeira, Portugal

TRACEABLE AMMONIA QUANTIFICATION AND METROLOGICAL UNCERTAINTY EVALUATION IN A SHOCK TUBE

D. Zhu[1], S. Agarwal[1], B. Shu[1], R. Fernandes[1,2], Z. Qu[1]

[1] Department of Physical Chemistry, Physikalisch-Technische Bundesanstalt, Braunschweig, Germany
[2] Institute of Internal Combustion Engines, Technische Universität Braunschweig, Braunschweig, Germany
E-Mail (corresponding author): denghao.zhu.ext@ptb.de; zhechao.qu@ptb.de

Abstract:
This work emphasizes on the development of an ultra-rapid spectrally resolved tunable diode laser absorption spectroscopy (TDLAS)-based spectrometer with a scan frequency of 40 kHz for dynamic NH_3 quantification in a shock tube. Thanks to the high laser scan frequency, the NH_3 mole fraction at various stages during the dynamic process can be quantified. Besides, considering lacking metrology in shock tubes for dynamic studies, we comprehensively evaluated the uncertainty sources and budgets of thermodynamic parameters and species concentration based on *Guide to the expression of uncertainty in measurements* (GUM). The established metrological uncertainty evaluation method for shock tube experiments can be beneficial to provide traceable and high-quality data, which is vital for dynamic studies as well as chemical kinetic modelling.

Keywords: Ammonia; TDLAS; Shock tube; Uncertainty budget

1 INTRODUCTION

Ammonia is a promising zero-carbon fuel which has a comparable specific mass density to conventional fossil fuels. Compared to hydrogen, it has a 70% relatively higher specific volume density and higher boiling point, making it much easier to be liquefied and therefore significantly reducing the cost of storage and transportation. The volumetric hydrogen content of ammonia is also 70% relatively higher than hydrogen which means that ammonia is not only a good zero-carbon fuel but also a promising hydrogen carrier. A much narrower flammability limit of ammonia compared to hydrogen increases its safety property for daily usage. The "green" ammonia synthesized by "Power-to-X" technologies ensures life-cycle carbon neutrality of using ammonia and guides to the eventual "ammonia economy" [1].

When considering ammonia as a fuel to be applied on a large scale, fundamental thermodynamic studies are required. The shock tube is one of the typical facilities that can create a quasi-instantaneously and homogeneously high-temperature and pressure environment. It is commonly used for high-temperature chemistry validation where the thermal conversion process in shock tubes can be simulated using a zero-dimensional model. To get speciation data from shock tubes, diagnostic methods are required such as laser diagnostics, mass spectrometry, or gas chromatography. Among them, tunable laser diode laser absorption spectroscopy (TDLAS) is an *in-situ*, line-of-sight, and non-invasive measurement method with high time resolution and selectivity [2]. By coupling TDLAS to shock tubes, it is able to get highly accurate time-resolved speciation data within the time scales of only several hundred microseconds to several milliseconds.

Up to now, there are limited studies on speciation measurements of ammonia and ammonia fuel blends using TDLAS in shock tubes. Alturaifi et al. [3-5] conducted several experiments by coupling TDLAS to the shock tube for NH_3, N_2O and H_2O measurements during ammonia pyrolysis and oxidation. He and Zheng et al. [6-9] used TDLAS to measure NH_3, NO, CO, CO_2, H_2O and temperature during ammonia and ammonia fuel blends oxidation. At PTB (National Metrology Institute of Germany), we measured the time-resolved NO profiles for pure NH_3 and NH_3/H_2 fuel blends. Recently, we selected a new NH_3 absorption line and coupled it to the shock tube for NH_3 quantification [10-13].

The importance of quantifying ammonia in shock tube experiments is not only because it is the reactant, but also due to its sticky property, as well as the interest in evaluating unconsumed ammonia emissions. From the literature studies and our

previous works, there are still two concerns that are worthwhile for further investigations. Firstly, the NH_3 absorption cross-sections measurements in shock tubes were all based on the assumption that an unchanged NH_3 mole fraction before incident shock wave (T_1, P_1), to immediately after reflected shock wave (T_5, P_5). This assumption was obtained relying on the simulation results while has not been experimentally validated to our best knowledge. In our previous work, we already observed around 20% NH_3 decomposition at the first spectra (at 200 µs) after (T_5, P_5) at a temperature of 1933 K, therefore the cross-section measurements were limited to 1800 K. This reminds us of the importance of prerequisites for absorption cross-section measurements which merits more investigations. Secondly, there is still lacking metrological uncertainty evaluation methodology for speciation data measured in shock tubes by TDLAS although it has been used for several decades, which is particularly important in providing reliable experimental data.

Consequently, we upgraded our previous spectrometer by enhancing the scan frequency from previously 10 kHz to 40 kHz, and the corresponding data acquisition rate from 20 MS/s to 80 MS/s. The purpose is on the one hand to capture enough spectra at different stages during the dynamic process in shock tubes, especially regarding the ultra-short time duration of around 100 µs after the incident shock wave (T_2, P_2). On the other hand, we want to shorten the measurement time of the first spectra after the reflected shock wave (T_5, P_5) to minimize the potential pyrolysis of NH_3 at high temperatures. Based on the ultra-rapid TDLAS spectrometer, we quantified and compared the NH_3 mole fractions before the incident shock wave (T_1, P_1), after the incident shock wave (T_2, P_2) and immediately after the reflected shock wave (T_5, P_5) (within 25 µs). Also, we conducted comprehensive uncertainty evaluations on thermodynamic parameters and speciation mole fractions following the rules of *Guide to the expression of uncertainty in measurement* (GUM) [14].

2 METHODOLOGY

For TDLAS, the intensity of a monochromatic continuously tunable laser source transmitted through a gaseous sample is given by the Beer-Lambert law [15]:

$$I(\upsilon) = E(t) + I_0(\upsilon) \cdot T(t) \cdot exp[-\alpha(\upsilon)] \quad (1)$$

with the background emission $E(t)$ at time t, initial laser intensity $I_0(\upsilon)$, the spectrally broadband transmission losses $T(t)$, and the absorbance $\alpha(\upsilon)$.

The absorbance spectrum $\alpha(\upsilon)$ can be computed using the following equation:

$$\alpha(\nu) = -p \ln\left(\frac{I(\nu)-E(t)}{I_0(\nu)\cdot T(t)}\right) = \frac{S(T)\cdot p\cdot L\cdot g(\upsilon-\upsilon_0)\cdot x}{k_B\cdot T} \quad (2)$$

where $S(T)$ is the absorption line strength at gas temperature T, $g(\upsilon-\upsilon_0)$ is the area normalized (integrated area=1) line shape function (centered at the wavenumber υ_0), k_B is the Boltzmann constant, p is the total pressure, x is the NH_3 mole fraction, and L is the optical path length.

By integrating the absorbance spectrum, the NH_3 mole fraction can be obtained by the following equation without the necessity to solve the line shape function.

$$A=\int \alpha(\nu)=\frac{S(T)_{\mathrm{sum}}\cdot p\cdot L\cdot x}{k_B\cdot T} \quad (3)$$

3 EXPERIMENTAL SETUP

The schematic of the experimental setup is shown in Figure 1. The shock tube at PTB consists of a 3.5-meter driver section and a 4.5-meter driven section. The inner surface was electropolished with a diameter of 70 mm. A manometer (627F, MKS Instruments, PTB International System of Units (SI)-traceable) was installed on the top of the driven section near the diaphragm section to record the initial filling pressure. Five pressure sensors (Kistler model 603C) combined with charge amplifiers (Kistler model 5018A) were utilized for pressure measurements and shock velocity calculation.

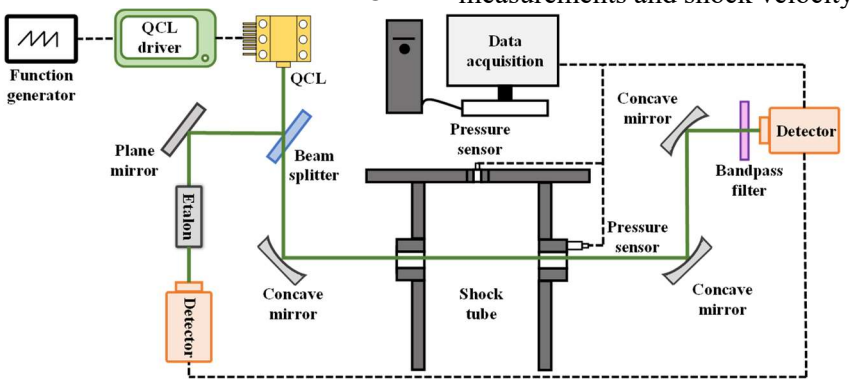

Figure 1. Schematic of the experimental setup

For laser diagnostics, two opposite CaF_2 windows were installed at the same plane as the fourth pressure sensor. The mid-infrared NH_3 laser centered at 1084.6 cm^{-1} is a continuous-wave distributed-feedback quantum cascade laser (CW-DFB-QCL, Alpes Lasers). The wavelength can be

tuned from 1083 to 1089 cm^{-1} by varying the current and/or temperature using a QCL driver (ITC4005QCL, Thorlabs). The laser current was modulated by a triangle-shaped ramp at a scan frequency up to 40 kHz supplied by a function generator (33500B, KEYSIGHT). From Figure 1, the laser beam was divided into two sub beams by a beam splitter (BSW711, Thorlabs). One was used to determine the dynamic laser tuning using a Germanium etalon (length 76.244 mm, traceable to PTB's length standard) before starting the measurements. The results of the etalon measurement were used to convert the x-axis of the measured spectra from the time to the wavenumbers domain. The other laser beam went through the optical windows with a path length of 7 cm via two concave mirrors (CM508-200-M01, focal length: 200 mm, Thorlabs) and was focused onto a photodetector (PVI-4TE-10, VIGO) by a concave mirror (CM508-050-M01, focal length: 50 mm, Thorlabs). A narrow bandpass filter (FB9000-500, Thorlabs) was placed in front of the detector to discriminate the signal against the background emission *E(t)* in Equation (1), e.g., thermal emission from the shock-heated gases. To match the ultra-rapid scan frequency, we upgraded the acquisition system with a new DAQ card (16-bit 80 MS/s, M2p.5943-x4, Spectrum Instrumentation).

The NH_3/Ar mixtures were prepared in a 50 L stainless steel tank using high quanlity pure NH_3 and pure Ar (HiQ 5.0, Linde). A manometer (627F, MKS Instruments, PTB SI-traceable) was installed on the top of the mixing tank to monitor the mixture pressure. Before preparing the mixtures, this tank was vacuumed overnight to a pressure below 1×10^{-7} mbar (TTR 91N, Leybold). When starting to prepare the mixture, a small amount of target gas first flushes the pipes twice to clean up residual gas. The mixtures were stirred by a magnetic stirrer (cyclone 300 ac, Büchiglasuster) for at least two hours to ensure homogeneity.

Table 1 shows the average mixture compositions and experimental conditions of three NH_3/Ar mixtures examined in this study. The ideal NH_3 mole fraction of Mixture 1, Mixture 2, and Mixture 3 is 0.5%, 1% and 1.5%, respectively. From Table 1, it can be found that the average NH_3 mole fraction is lower than the ideal value due to NH_3 adsorption effect, which will be discussed later.

Table 1. Average mixture compositions and experimental conditions

Mixture	x_{NH3}	x_{Ar}	P_1 /bar	T_1/K	P_2 /bar	T_2/K	P_5 /bar	T_5/K
1	0.0037	0.9963	0.0199-0.1177	295	0.2553-0.5543	603-1200	1.1502-1.7798	988-2394
2	0.0095	0.9905			0.2563-0.5492	597-1192	1.1589-1.7643	975-2374
3	0.0137	0.9863			0.2581-0.5880	620-1195	1.1711-1.8855	1027-2380

4 RESULTS AND DISCUSSIONS

a. Spectra

Figure 2 shows an exemplary pressure trace measured by the 4th pressure sensor and corresponding laser signal measured in a shock tube. The time zero is set as the arrival of the shock wave to the 5th pressure sensor. From Figure 2, two sharp pressure rises can be captured, indicating the arrival of the incident shock wave and reflected shock wave, respectively. The duration of the status (P_2, T_2) is quite short of around 100 µs. To get enough spectra at (P_2, T_2), the scan frequency was therefore enhanced to 40 kHz, namely 25 µs for a period. In this case, there are at least three complete spectra that can be captured. Besides, an ultra-rapid scan frequency was able to make the time duration of the first spectra at (P_5, T_5) as short as possible to reduce the possibility of pyrolysis at high temperature conditions.

Before starting the measurements, the etalon signal was firstly acquired to mark the relative laser wavelength. For each shot, the reference signal (I_0) and offset signal were recorded before filling the mixture. Then the transmitted signal (I_t) was automatically recorded trigged by the pressure signal. By using Equation (1-2) and transferring the time-domain to wavenumber-domain using etalon signal, the spectral absorbance at different stages can be calculated. Furthermore, the concentration can be quantified by integrating the absorbance spectra using Equation (3).

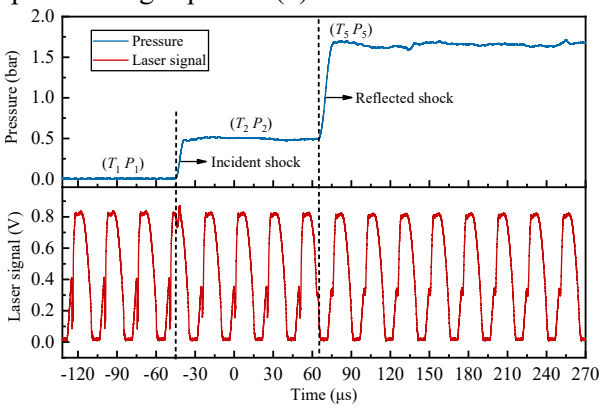

Figure 2. Exemplary pressure trace and laser signal

b. Metrological uncertainty evaluation

Although shock tube coupled with TDLAS have been widely applied for monitoring the dynamic speciation in the past decades, the uncertainty of the measurements is commonly analysed using the root sum squared method without a standard and metrological approach [3-5]. Given this, we conducted a comprehensive uncertainty evaluation using GUM Workbench® [14]. The coverage factor is given as 1.0 throughout the uncertainty evaluations in this study. For easier illustration, we took one case from Mixture 2 (P_1=0.0688 bar) as an example in the following steps.

Firstly, the heat capacity ratio of the mixture (γ) before incident shock wave is calculated by Equation (4),

$$\gamma = \frac{\sum C_{p_i} \cdot x_i}{\sum C_{v_i} \cdot x_i} \quad \text{(Eq.4)}$$

where x represents the mole fraction of the mixture composition; C_p and C_v represent the heat capacities at constant pressure and at constant volume, respectively.

The NH_3 mole fraction before incident shock wave ($x_{(P1,\ T1)}$) was calculated by Equation (3) including six relevant quantities. Specifically, k_B has a constant of 1.380649×10^{-23} J/K. The laser path length (L) is 7 cm, with an uncertainty of 1.1%. The absorption spectrum is averaged over 116 scans for the (P_1, T_1) period. The integral area of this averaged absorption spectrum ($A_{(P1,\ T1)}$) is 0.0984, with an uncertainty of 1.5% which includes the uncertainty of etalon measurements. The total line intensity ($S(T)_{(P1,\ T1)}$) of six transition lines at 295 K is 8.233×10^{-19} cm/mol, with an uncertainty of 10% from HITRAN [16]. The uncertainty of P_1 is 0.0001 bar according to the calibration certificate (PTB SI-traceable). The room temperature was controlled and measured at 295 K with an uncertainty of 0.5 K. As a result, $x_{(P1,\ T1)}$ is calculated to be 0.0101 with an uncertainty of 10.5%. Table 3 shows the uncertainty budgets of $x_{(P1,\ T1)}$. Clearly, the uncertainty of $S(T)_{(P1,\ T1)}$ accounts for a significantly greater contribution (96.6%) than other quantities, which indicates an efficient way to reduce the total uncertainty by reducing the uncertainty of the line intensity.

Other quantities for heat capacity calculation were obtained from the National Institute of Standards and Technology (NIST) database. Specifically, the C_p and C_v of NH_3 are 36.385 and 27.688 J/(mol·K), respectively, with an uncertainty of 0.25%. The C_p and C_v of Ar are 20.820 and 12.477 J/(mol·K), respectively, with an uncertainty of 0.15%. Overall, the heat capacity ratio γ of the mixture is 1.6608 with an uncertainty of 0.215%.

Secondly, the Mach number (M_a) of the shock front is another important parameter calculated by Equation (5),

$$M_a = \frac{u_s}{\sqrt{\frac{\gamma R}{\sum M_i x_i}_1}} \quad \text{(Eq.5)}$$

where u_s refers to the shock velocity; R is the gas constant; M is the molar mass.

The shock velocity has an uncertainty of 0.937 %. The gas constant R is defined as the Avogadro constant N_A (6.02214076×10^{23}) multiplied by k_B (8.31446261815324 J/(mol·K)). The molar mass of NH_3 and Ar were 17.0305 and 39.948 g/mol from NIST, respectively. Overall, the Mach number is 2.332 with an uncertainty of 0.943% where the uncertainty from shock velocity contributes 97.8%.

Thirdly, according to the gas dynamic equations based on one-dimensional shock wave coordinates, the pressures and temperatures (P_2, T_2, P_5, T_5) behind the incident and reflected shock waves can be calculated by Equation (6-9).

$$P_2 = P_1\left[1 + \frac{2\gamma}{\gamma+1}(M_a^2 - 1)\right] \quad \text{(Eq.6)}$$

$$T_2 = T_1\left[1 + \frac{2(\gamma-1)\gamma M_a^2+1}{(\gamma+1)^2 M_a^2}(M_a^2 - 1)\right] \quad \text{(Eq.7)}$$

$$P_5 = P_1\left[\frac{2\gamma M_a^2-(\gamma-1)}{\gamma+1}\right]\left[\frac{(3\gamma-1)M_a^2-2(\gamma-1)}{(\gamma-1)M_a^2+2}\right] \quad \text{(Eq.8)}$$

$$T_5 = T_1\frac{[2(\gamma-1)M_a^2+(3-\gamma)][(3\gamma-1)M_a^2-2(\gamma-1)]}{(\gamma+1)^2 M_a^2} \quad \text{(Eq.9)}$$

Based on the above analysis for the heat capacity ratio and Mach number, the uncertainties of P_2, T_2, P_5 and T_5 can be calculated to be 2.0%, 1.35%, 2.8% and 1.8%, respectively, as shown in Table 2. Combing the uncertainties of P_1 and T_1, it is evident that the uncertainties of thermodynamic parameters are increasing during the heating up process, of which the Mach number contributes the highest portion (over 90%) among all uncertainty sources.

Table 2. Uncertainty budgets of P_2, T_2, P_5 and T_5

Quantity		P_1	T_1	γ	Ma
Value		0.0688 bar	295 K	1.6608	2.332
Uncertainty (%)		0.15	0.17	0.215	0.9
P_2	Contribution (%)	0.6	-	0.1	99.3
	Value	**0.45 ± 0.008 bar (2.0%)**			
T_2	Contribution (%)	-	1.6	3.7	94.7
	Value	**735 ± 9.9 K (1.35%)**			
	Value	**1.636 ± 0.0458 bar (2.8%)**			
T_5	Contribution (%)	-	0.9	5.0	94.1

	Value	**1328 ± 23.9 K (1.8%)**

The NH_3 mole fraction at (P_2, T_2) and (P_5, T_5) can be calculated by Equation (3), the same method as for $x_{(P1, T1)}$. However, except for Boltzmann constant and path length, the values and uncertainties of the rest quantities have changed. As mentioned above, with an ultra-rapid scan frequency of 40 kHz, three complete spectra at (P_2, T_2) can be recorded and averaged. The area $A_{(P2, T2)}$ of the averaged absorbance is 0.0907 with an uncertainty of 1.5%. The line intensity at (P_2, T_2) is reduced to 3.098×10^{-19} cm/mol with an uncertainty of 10%. In a consequence, the NH_3 mole fraction at (P_2, T_2) is 0.0094 with an uncertainty of 10.5%.

To quantify the NH_3 mole fraction immediately after the reflected shock wave, we only used the first spectral absorbance to minimize the effect of possible pyrolysis with the growing time, especially for high temperature cases. With this ultra-rapid scan frequency, the largest time interval between the first scan and reflected shock wave is less than 25 μs, basically within 12.5 μs as only the first half period of the scan was considered. The line intensity at (P_5, T_5) is further reduced to 6.902×10^{-20} cm/mol with an uncertainty of 10%. As a result, the integrated absorbance $A_{(P5, T5)}$ is only about a half value compared to that at (P_1, T_1) or (P_2, T_2), leading to a larger uncertainty of 2%. Resultantly, the NH_3 mole fraction immediately after the reflected shock wave $x_{(P5, T5)}$ is 0.0099 with an uncertainty of 11%, which is 0.5% larger than that of $x_{(P1, T1)}$ and $x_{(P2, T2)}$ owing to a higher uncertainty in pressure, temperature, and integrated absorbance.

Table 3. Uncertainty budgets of NH_3 mole fraction at different stages

Quantity		k_B	L	$A_{(P1, T1)}$	$S(T)_{(P1, T1)}$	P_1	T_1
Value		1.380649×10^{-23} J/K	7 cm	0.0984	8.233×10^{-19} cm/mol	0.0688 bar	295 K
Uncertainty (%)		-	1.1	1.5	10	0.15	0.17
$x_{(P1, T1)}$	Contribution (%)	-	1.1	2.1	96.6	0.1	0.1
	Value	**0.0101 ± 0.0011 (10.5%)**					
Quantity		k_B	L	$A_{(P2, T2)}$	$S(T)_{(P2, T2)}$	P_2	T_2
Value		1.380649×10^{-23} J/K	7 cm	0.0907	3.098×10^{-19} cm/mol	0.45 bar	735 K
Uncertainty (%)		-	1.1	1.5	10	2.0	1.4
$x_{(P2, T2)}$	Contribution (%)	-	1.1	2.0	91.7	3.6	1.6
	Value	**0.0094 ± 0.0010 (10.5%)**					
Quantity		k_B	L	$A_{(P5, T5)}$	$S(T)_{(P5, T5)}$	P_5	T_5
Value		1.380649×10^{-23} J/K	7 cm	0.0427	6.902×10^{-20} cm/mol	1.636 bar	1328 K
Uncertainty (%)		-	1.1	2	10	2.8	1.8
$x_{(P5, T5)}$	Contribution (%)	-	1.0	3.4	86.3	6.6	2.7
	Value	**0.0099 ± 0.0011 (11%)**					

c. Ammonia quantification

The NH_3 mole fraction and corresponding uncertainties at (T_1, P_1), (T_2, P_2) and immediately after (T_5, P_5) of all cases for Mixture 1-3 are calculated by Equation (3), as shown in Figure 3. The dashed lines indicate the ideal mole fraction for mixture preparation. From Figure 3, when taking the measurement uncertainties into consideration, no evident NH_3 mole fraction variation can be observed, indicating no evident pyrolysis occurs during this dynamic process. Besides, it is concentration independent as three mixtures show consistent results. Note that this conclusion is only valid for the NH_3 mole fraction of the first spectra measured after the reflected shock wave, a time interval of less than 25 μs. As the time grows, the pyrolysis process will happen at such high T_5. Nevertheless, this study restricts the valid conditions of the assumption for cross-section measurements, especially for high temperatures. From Figure 3, another consistent phenomenon for three mixtures is that with the increase of P_1, the NH_3 mole fraction increases and then levels off when P_1 is larger than 0.06 bar. This result strongly indicates that at lower P_1, the relative NH_3 loss is larger. Especially for a low mole fraction mixture (e.g. Mixture 1), the largest relative NH_3 loss can be over 50% at the minimum P_1.

Note that before each experiment, we have used the same mixture as the experimental one to passivate the inner surface of the shock tube. Nonetheless, it is far from enough especially for low P_1 and low initial mole fraction mixtures. Some studies also used a specific higher concentration mixture as a compensation of NH_3 adsorption. However, this method also brings a risk that the NH_3 mole fraction after passivation is even higher than the target value. Up to now, there is still lacking golden standard passivation method for NH_3 studies in shock tubes. The difficulty is that the passivation process has a random nature, and highly depends on the initial pressure, mixture mole fraction, inner surface materials, passivation times, passivation time duration, vacuuming pumps and procedures. In

addition, the loss could also happen during the mixture preparation as NH_3 will also adsorb to the inner surface of the mixing tank, and it is quite difficult to monitor this process. Therefore, at least for low NH_3 mole fraction mixture and low P_1 conditions, it is strongly recommended to quantify the initial NH_3 mole fraction. A key quantity for thermodynamic parameters calculation, as well as an important input for modelling studies.

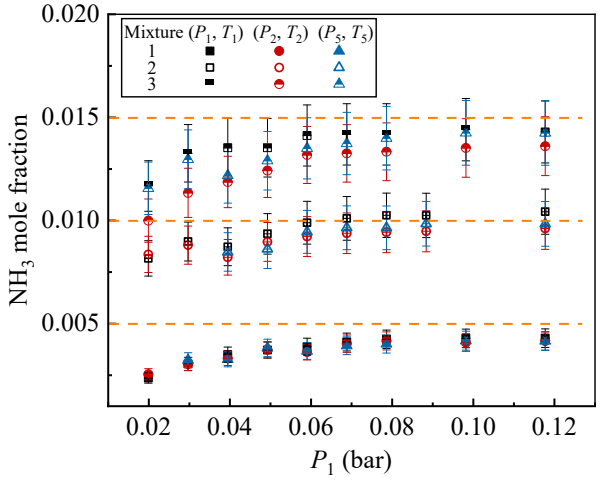

Figure 3. NH_3 mole fraction at (T_1, P_1), (T_2, P_2) and immediately after (T_5, P_5) of Mixture 1-3

5 SUMMARY

We developed an ultra-rapid TDLAS spectrometer (40 kHz scan frequency) and quantified the ammonia mole fraction before the incident shock wave (P_1, T_1), after the incident shock wave (P_2, T_2), and immediately after the reflected shock wave (P_5, T_5) (within 25 μs). No significant variation in NH_3 mole fraction was observed during the shock tube experiments, indicating no evident NH_3 pyrolysis during this dynamic process. This restricts the valid conditions for cross-section measurements. Additionally, we compared the NH_3 mole fraction at different P_1 values and found that NH_3 loss occurred, even with a passivation procedure, at lower P_1 (<0.06 bar in this study). For low NH_3 mole fraction mixtures, the largest relative NH_3 loss exceeded 50% at the minimum P_1 of 0.02 bar (ideally 0.5% NH_3 in the mixture). Therefore, it is strongly recommended to quantify the initial NH_3 mole fraction during shock tube experiments via an online *in situ* method, particularly for low NH_3 mole fraction mixtures and low P_1 conditions.

The uncertainties of thermodynamic parameters and the mole fraction of speciation measured by TDLAS in shock tubes have been metrologically evaluated. For the current study, the uncertainties of P_2, T_2, P_5 and T_5 are 2.0%, 1.35%, 2.8% and 1.8%, respectively. The uncertainties of NH_3 mole fraction at (P_1, T_1), (P_2, T_2), and immediately after (P_5, T_5) based on integrated absorbance are 10.5%, 10.5% and 11%, respectively. This methodology provides an insight into the uncertainty budgets of each quantity and can be generalized to other similar studies.

6 REFERENCES

M. Li, D. Zhu, X. He, K. Moshammer, R. Fernandes, B. Shu, Experimental and kinetic modeling study on auto-ignition properties of ammonia/ethanol blends at intermediate temperatures and high pressures, Proc. Combust. Inst. 39 (2022) 511-519.

R.K. Hanson, D.F. Davidson, Recent advances in laser absorption and shock tube methods for studies of combustion chemistry, Prog. Energy Combust. Sci. 44 (2014) 103-114.

S.A. Alturaifi, O. Mathieu, E. L. Petersen, An experimental and modeling study of ammonia pyrolysis, Combust. Flame. 235 (2022) 111694.

S.A. Alturaifi, O. Mathieu, E. L. Petersen, Shock-tube laser absorption measurements of N_2O time histories during ammonia oxidation, Fuel Commun. 10 (2022) 100050.

S.A. Alturaifi, O. Mathieu, E.L. Petersen, A shock-tube study of NH_3 and NH_3/H_2 oxidation using laser absorption of NH_3 and H_2O, Proc. Combust. Inst. 39 (2022) 233-241.

D. He, D. Zheng, Y. Du, J. Li, Y. Ding, Z. Peng, Laser-absorption-spectroscopy-based temperature and NH_3-concentration time-history measurements during the oxidation processes of the shock-heated reacting NH_3/H_2 mixtures, Combust. Flame. 245 (2022) 112349.

D. Zheng, D. He, Y. Du, Y. Ding, Z. Peng, Shock tube study of the interaction between ammonia and nitric oxide at high temperatures using laser absorption spectroscopy, Proc. Combust. Inst. 39 (2022) 4365-4375.

D. Zheng, D. He, Y. Du, Y. Ding, Z. Peng, Nitromethane as a nitric oxide precursor for studying high-temperature interactions between ammonia and nitric oxide in a shock tube, Combust. Flame. 250 (2023) 112644.

D. Zheng, D. He, Y. Du, J. Li, M. Zhang, Y. Ding, Z. Peng, Experimental study of the methane/hydrogen/ammonia and ethylene/ammonia oxidation: Multi-parameter measurements using a shock tube combined with laser absorption spectroscopy, Combust. Flame. 254 (2023) 112830.

D. Zhu, Z. Qu, M. Li, S. Agarwal, R. Fernandes, B. Shu, Investigation on the NO formation of ammonia oxidation in a shock tube applying tunable diode laser absorption spectroscopy, Combust. Flame. 246 (2022) 112389.

D. Zhu, L. Ruwe, S. Schmitt, B. Shu, K. Kohse-Höinghaus, A. Lucassen, Interactions in Ammonia and Hydrogen Oxidation Examined in a Flow Reactor and a Shock Tube, J. Phys. Chem. A 127 (2023) 2351-2366.

S. Agarwal, L. Seifert, D. Zhu, B. Shu, R. Fernandes, Z. Qu, Investigations on Pressure Broadening Coefficients of NO Lines in the 1←0 Band for N_2, CO_2, Ar, H_2, O_2 and He, Appl. Sci. 13 (2023).

D. Zhu, S. Agarwal, L. Seifert, B. Shu, R. Fernandes, Z. Qu, TDLAS spectrometer for the measurements of absorption cross-sections and absolute quantification of ammonia for dynamic processes at elevated temperature and pressure, Analyst (under review).

BIPM/ISO: Guide to the Expression of Uncertainty in Measurement, International Organization for Standardization, 1995, ISBN 92-67-20188-3.

Z. Qu, O. Werhahn, V. Ebert, Thermal Boundary Layer Effects on Line-of-Sight Tunable Diode Laser Absorption Spectroscopy (TDLAS) Gas Concentration Measurements, Appl. Spectrosc. 6 (2018) 853-862.

I. E. Gordon, L. S. Rothman, R. J. Hargreaves, R. Hashemi, E. V. Karlovets, F. M. Skinner, E. K. Conway, C. Hill, R. V. Kochanov and Y. Tan, et al., The HITRAN2020 molecular spectroscopic database, J. Quant. Spectrosc. Radiat. Transf. 277 (2022) 107949.

IMEKO TC8, TC11 and TC24 Joint Conference
October 11-13, 2023, Madeira, Portugal

ASSESSMENT OF MOISTURE ABSORPTION BY ANHYDROUS ETHANOL UNDER DIFFERENT ENVIRONMENTAL CONDITIONS

Valnei Smarçaro da Cunha; Romeu José Daroda; Júlio Dutra Brionizio*; Marcos Paulo Vicentim, Fernanda Figueiredo Nunes, Graziele Mozzer Pereira, Thais Fagundes da Silva

INMETRO – National Institute of Metrology, Quality and Technology. Av. N. Sra. das Graças, 50, Xerém, Duque de Caxias, RJ, Brazil, 25.250-020. *jdbrionizio@inmetro.gov.br

Abstract:
The main use of bioethanol in the world is as a fuel by adding it to gasoline. The addition of ethanol has many purposes, such as increasing gasoline octane number, reducing carbon dioxide emissions by fossil fuels, energy security and environmental sustainability. The suitable bioethanol for mixing in gasoline is the anhydrous one, which must contain up to a maximum of 1% (w/w) of water, according to ASTM D5798-21 [1]. Although it is well known that ethanol is a hygroscopic substance, a complete study addressing the rates of moisture absorption by the ethanol and its evaporation, or showing the influence of the environmental conditions on these factors cannot be found in literature. The assessment of these behaviours is fundamentally relevant for all the ethanol production and distribution chain in order to estimate how long an ethanol batch can be handled keeping the water content, or even to avoid significant loss of ethanol by evaporation, resulting in environmental problems and financial losses. In order to evaluate the ethanol behaviour under different environmental conditions, in this work, as a preliminary study, several environments with different relative humidities and temperatures were simulated in a climatic chamber, and their impact on the moisture absorption rate and/or on the ethanol evaporation were analysed in some anhydrous ethanol samples. It was also evaluated if moisture absorption or ethanol evaporation is the preferential process.

Keywords: ethanol; moisture; absorption; environmental conditions

1 INTRODUCTION

The use of bioethanol as automotive fuel has been considered as a renewable alternative biofuel in the last few years due to many reasons, especially those related to environmental sustainability, energy security, crude oil price volatility and limited availability of the non-renewable fossil fuel.

Brazil started using pure bioethanol as a fuel in internal combustion engines around 1925, and in 1931 the government determined a compulsory blend of at least 5% anhydrous ethanol in gasoline [2]. In 1975, the Brazilian automobile companies, through a government program called “Pro-álcool”, started producing engines running with pure ethanol (hydrated ethanol, containing around 5% w/w of water). Nowadays, Brazil has automobiles, called as flex vehicles, running with ethanol/gasoline blend in any ratio. In 2021, the flex vehicles represented 72.7% of the circulating automotive fleet in the country [3]. Also, Brazil is the second largest ethanol producer in the world, only behind USA. In 2021, U.S. and Brazilian production corresponded to, respectively, 55% and 27% of world production, which amounted 22.5 billion gallons [4].

The main use of bioethanol in the world is as a fuel by adding it to gasoline. The addition of ethanol has the main purpose of increasing gasoline octane number, instead of adding the toxic tetraethyl lead, which is prohibited in most countries. The suitable bioethanol for mixing in gasoline is the anhydrous one, which must contain up to a maximum of 1% (w/w) of water, according to ASTM D5798-21 [1]. In Brazil, the water specification regulated by the National Petroleum Agency (ANP) is limited to 0.4% (w/w), and in the European Union (EU) it is limited to 0.3% (w/w), as defined by the European Committee of Standardization (CEN). Standards from Brazil and USA demand that gasoline must contain up to 27% and 10% or 15% of ethanol, respectively.

It is well known that ethanol is a hygroscopic substance. However, a complete study addressing the rates of moisture absorption by the ethanol and its evaporation, or showing the influence of the environmental conditions on these factors cannot be found in literature. The assessment of these behaviours is fundamentally relevant for all the ethanol production and distribution chain in order to estimate how long an ethanol batch can be handled keeping adequate water content, or even to avoid

significant loss of ethanol by evaporation, resulting in environmental problems and financial losses. This knowledge has special interest not only to the fuel industry, but also to the pharmaceutical and cosmetic ones, for example.

Anhydrous ethanol plants are prevented from moisture raise both by storing the final product in well-sealed containers and by producing it with lower water content than specified by standards, even if it causes some increase in production costs [5]. On the other hand, in all the logistic process involved in anhydrous ethanol transportation before mixing it to gasoline, especially when transferring the ethanol from a container to another, care should be taken in order to avoid moisture raise due to the environment exposure, mainly during a wet day. Studies suggest that gasohol (ethanol blended with gasoline) is a viable fuel for automotive and power equipment, avoiding phase separation and corrosion problems, when the added ethanol contains less than 0.5% of water [6].

In order to evaluate the ethanol behaviour under different environmental conditions, environments with different relative humidities and temperatures were simulated in a climatic chamber, and their impact on the moisture absorption rate and/or on the ethanol evaporation were analysed in some anhydrous ethanol samples. It was also evaluated if moisture absorption or ethanol evaporation is the preferential process. The climatic conditions were precisely controlled and kept constant along a 32 h period test.

2 METHODOLOGY

For the evaluation of evaporation and moisture absorption by the anhydrous bioethanol fuel, it was used a 50 L sample, with 0.477 ± 0.004% of water, provided by a distillery. The sampling method and the determinations were performed as described in the following topics.

2.1. Sample Preparation

35.00 ± 0.05 g of anhydrous bioethanol fuel were inserted in a previously weighed 50 mL glass flasks with screw cap sealing. The surface area of the bioethanol fuel in the flask, sample portion which is in direct contact with the environment for vapour exchanges, was 1.52×10^{-3} m^2.

2.2. Sampling

Flasks containing the bioethanol samples were placed in a climatic chamber (Weiss Technik, WK3-340/40) and kept closed during about 15 h waiting for the complete relative humidity and temperature stabilization of the simulated environment. After the stabilization, the flasks were opened and kept static for periods between 5 min and 32 h, and then resealed. Twelve pre-defined time intervals were analysed for two samples, which resulted in 24 flasks placed in the chamber. The climatic conditions simulated by the chamber were maintained constant during the whole period, with fluctuations of less than ±0.25 °C and ±1.8 %rh.

2.3. Climatic Simulation

16 climatic conditions were simulated in the chamber by means of the combination of 04 different temperatures (10 °C, 20 °C, 30 °C and 40 °C) and 04 different relative humidities (30 %rh, 50 %rh, 70 %rh and 90 %rh). Inside the chamber, an airstream, which was temperature and humidity conditioned, flowed continuously through the test space by means of its large axial fan located at the rear panel. Both temperature and relative humidity were set and controlled by the software of the equipment. Before starting the tests, the inner space of the chamber was evaluated by means of nine thermometers in order to quantify its temperature stability and uniformity in the range from 10 ºC to 40 ºC. The obtained values were used as uncertainty sources of the temperature and relative humidity measurements. The expanded uncertainties of the 16 climatic conditions were 3.5 %rh and 0.6 ºC, with a confidence level of approximately 95%. It is important to point out that the evaporated substances from the samples are not accumulated in the inner of the chamber, since the air is constantly renewed. So, the effect of internal air saturation by ethanol vapor is discarded. All the simulations were performed at atmospheric pressure (101.3 kPa).

2.4. Temperature and Humidity Determination

The standard temperature within the climatic chamber was measured by a platinum resistance thermometer (PRT) of 100 Ω traceable to national standards. The PRT was connected to a digital indicator which was read by a home-made software. In order to keep the confidence of its readings, the resistance of the PRT was constantly checked and adjusted at the ice point. The standard relative humidity within the chamber was calculated for each test by means of the mean values of temperature and dew point temperature of the environmental conditions. The dew point temperatures were measured using a chilled-mirror hygrometer, which is considered as one of the most accurate and reliable methods of measuring dew/frost point temperatures [7]. For all the tests, the temperature and dew point temperature measurements were electronically obtained by means of software at short time intervals and, for the data processing, measurements at 30 s intervals were used. Figure 1 shows the dew-point hygrometer and the climatic chamber used in the experiments.

Figure 1: Dew-point hygrometer and the climatic chamber used in the experiments.

2.5. Moisture Determination

The moisture content of the bioethanol samples removed from the climatic chamber were measured by means of an accurate Karl Fischer coulometric titrator (Metrohm, Titrino 831). The apparatus uses a double platinum electrode, and the electrical current is generated by an electrode without diaphragm. A few drops of Hidranal Coulomat AG analytical solution (approximately 10 drops), which exact mass was weighted in a balance (Mettler Toledo, XS205), were directly injected in the titration vessel with a syringe. The sample analysis from each flask was performed in triplicate. The results are shown as percentage of water in bioethanol sample, given in mass basis (%, w/w), and the uncertainties are expressed as Relative Standard Deviation (RSD) from 06 replicates (%).

2.6. Determination of Mass Loss/Gain

This study was conducted by checking the sample weight before and after the period in which it was kept in the chamber. Thus, it was possible to analyse if there was preferably ethanol evaporation or moisture absorption, and to quantify this effect. The flasks had their weights measured once. The results are shown as percentage of weight loss/gain (%, w/w), and the uncertainties are expressed as Relative Deviation from the Mean (RDM) from 02 duplicates (%).

2.7. Influence of the Superficial Area on the Moisture Absorption and Ethanol Evaporation

This effect was evaluated by adding the same amount of bioethanol described before (35.00 $\pm$ 0.05 g, equivalent to 4.45 x 10^{-5} m^3) into previously weighed glass flasks with different internal areas. The surface areas of bioethanol in these flasks were 0.49, 1.52, 3.32, 4.66 and 6.94 x 10^{-3} m^2. The experiment was performed at 20 °C and 50 %rh for a fixed period of 24 h, as described in "Sampling" item.

3 RESULTS AND DISCUSSION

Regarding the analysis of the climatic conditions influence on the samples mass gain/loss, despite of the two competing effects that act inside the chamber, only mass loss was observed in all experiments, which means that evaporation occurs preferably than moisture absorption. Samples mass losses were observed in the first 5 min of sample exposure, especially under higher temperature conditions. At 30 °C and 40 °C, 5 min were enough to cause around 1% of mass loss; while at 10 °C, the same mass loss was reached only after 2 h of exposure.

Tan et al. [8] estimated that pure ethanol would have 40% of its volume as water after 24 h of air exposure, under uncontrolled and unspecified environmental conditions. A semi-quantitative study performed by that group showed a linear moisture absorption rate, at least up to 60 min of observation. However, according to Flores and Conde [9], moisture absorption should not take place up to 2 h of exposure under 25 °C and 40 %rh. These results obtained by Tan and al. and Flores and Conde were not confirmed in our experiments, as shown in the results and discussions below.

As shown in Figure 2, the bioethanol evaporation profile along the 32 h of exposure under any climatic condition presented a slight and positive 2nd order function correlation between the exposed time and mass loss, which means a constant increasing of the evaporation rate. After 32 h of exposure, samples mass loss was greater than 6%, reaching 23% when exposed to 40 °C at 30 %rh.

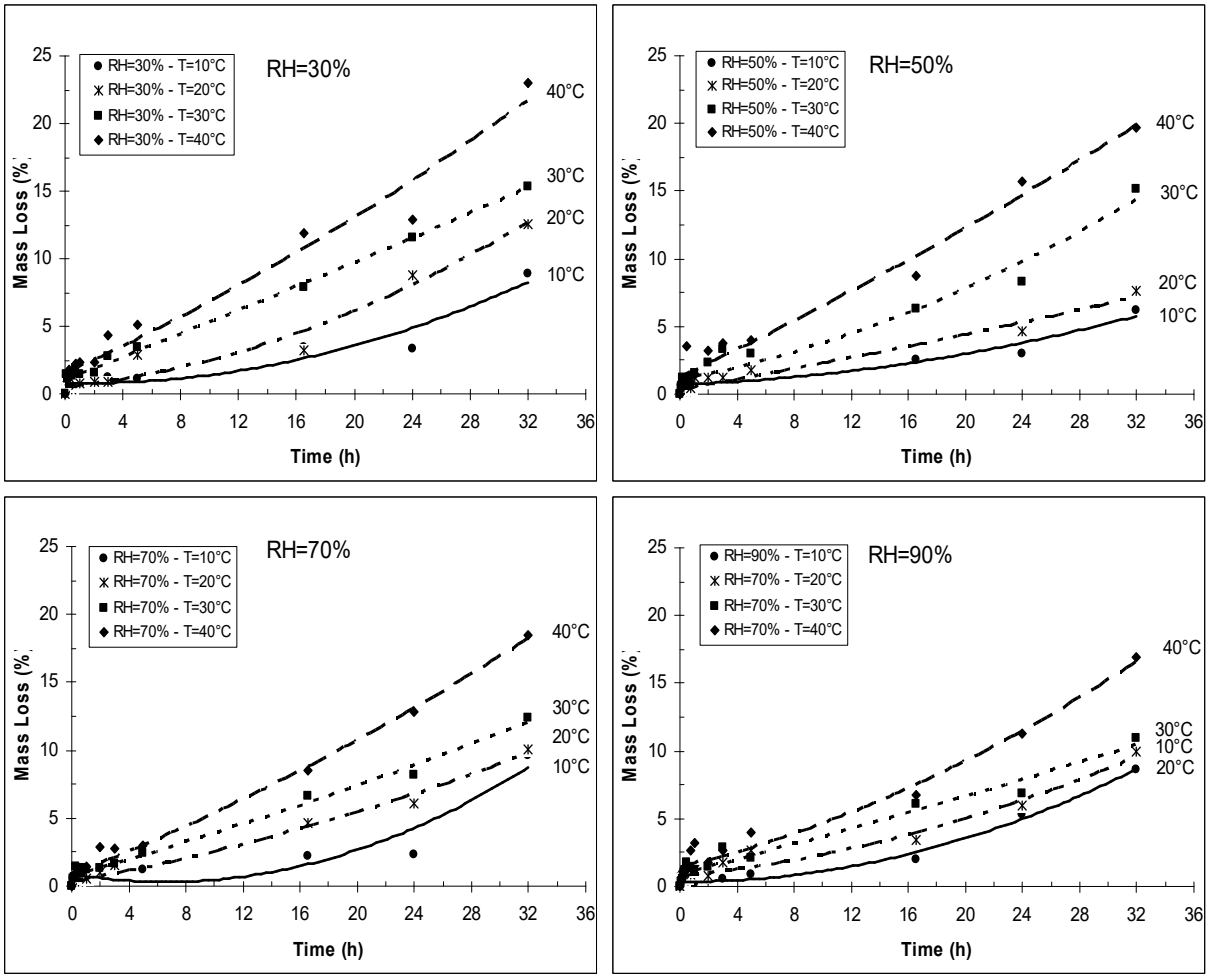

Figure 2: Profile of bioethanol evaporation along 32 h of exposure under different conditions of temperature and relative humidities. The average RDM observed for all the tested conditions was 7%.

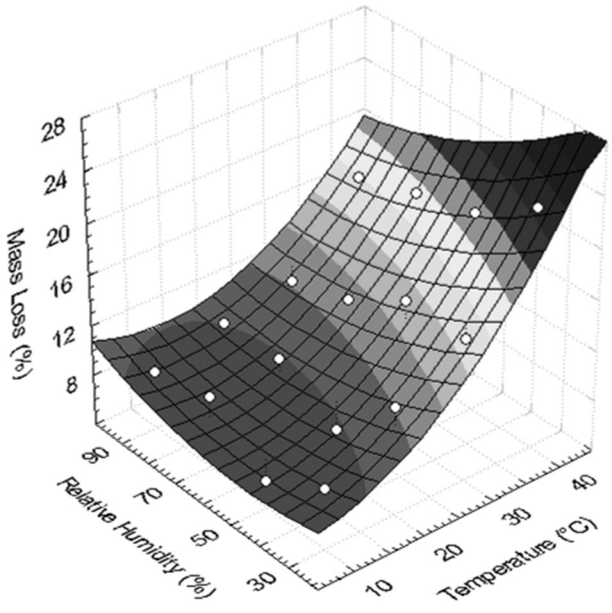

Figure 3: Surface plot demonstrating the effect of relative humidity and temperature on bioethanol evaporation. Mass losses presented herein refer to those obtained at 32 h of exposure. White dots represent the mass loss values determined experimentally.

Both temperature and relative humidity influenced on bioethanol evaporation, although temperature presented a more pronounced effect. For a better demonstration of the simultaneous effect of relative humidity and temperature on the evaporation, a 3D smooth surface plot was prepared, as shown in Figure 3. The mass loss values used to build this figure are those obtained at 32 h of experiment, since these values presented the highest differences. The surface plot is described by a mathematical model, which was analysed by ANOVA (analyses of variance) in order to statistically quantify the influence of temperature and relative humidity on the mass loss. The surface plot, which model explains 94.89% of the variability in mass loss, clearly shows that higher temperatures caused the greatest bioethanol evaporation, especially when associated to lower relative humidities. At lower temperatures, the relative humidity presented much less influence on the evaporation rate. The influence of temperature and relative humidity on the mass loss were estimated with a confidence level of 95%. Statistically, temperature (T) is the quantity that has more influence, providing variation due to the experimental treatment (F-ratio) equals to 154.80.

This value is at least 5 times greater than the variation provided by the relative humidity (RH) and other quantity combinations (RH = 10.30; T × T = 10.75; T × RH = 8.20; RH × RH = 1.67, which is not significant at 95% of confidence level).

3.1. Moisture Absorption

The hygroscopic characteristic of ethanol was observed since the first 5 min of experiment, when independently from the simulated climatic condition, the water content increased from 0.477 ± 0.004% to at least 0.55%. Even though, under most of the simulated climatic conditions, the tested bioethanol batch could be exposed up to 2 h without exceeding 1% of water content. This water content is the upper limit defined by the ASTM D5798-21 standard, which allows a bioethanol batch to be considered as "anhydrous" and permitted for mixing in gasoline. The highest moisture absorption rate was observed at 40 °C and 90 %rh. At this condition, the tested bioethanol batch could be exposed only up to 30 min in order to be in accordance with ASTM D5798-21. On the other hand, at 10 °C and 30 %rh or 50 %rh, the bioethanol water content reached only 0.72 ± 0.04% and 0.86 ± 0.02%, respectively, after 24 h of experiment. Figure 4 clearly shows that both temperature and especially relative humidity positively influenced the water content increasing of the bioethanol, but in order to get an improved demonstration of their simultaneous effect, a 3D smooth surface plot was designed and is shown in Figure 5.

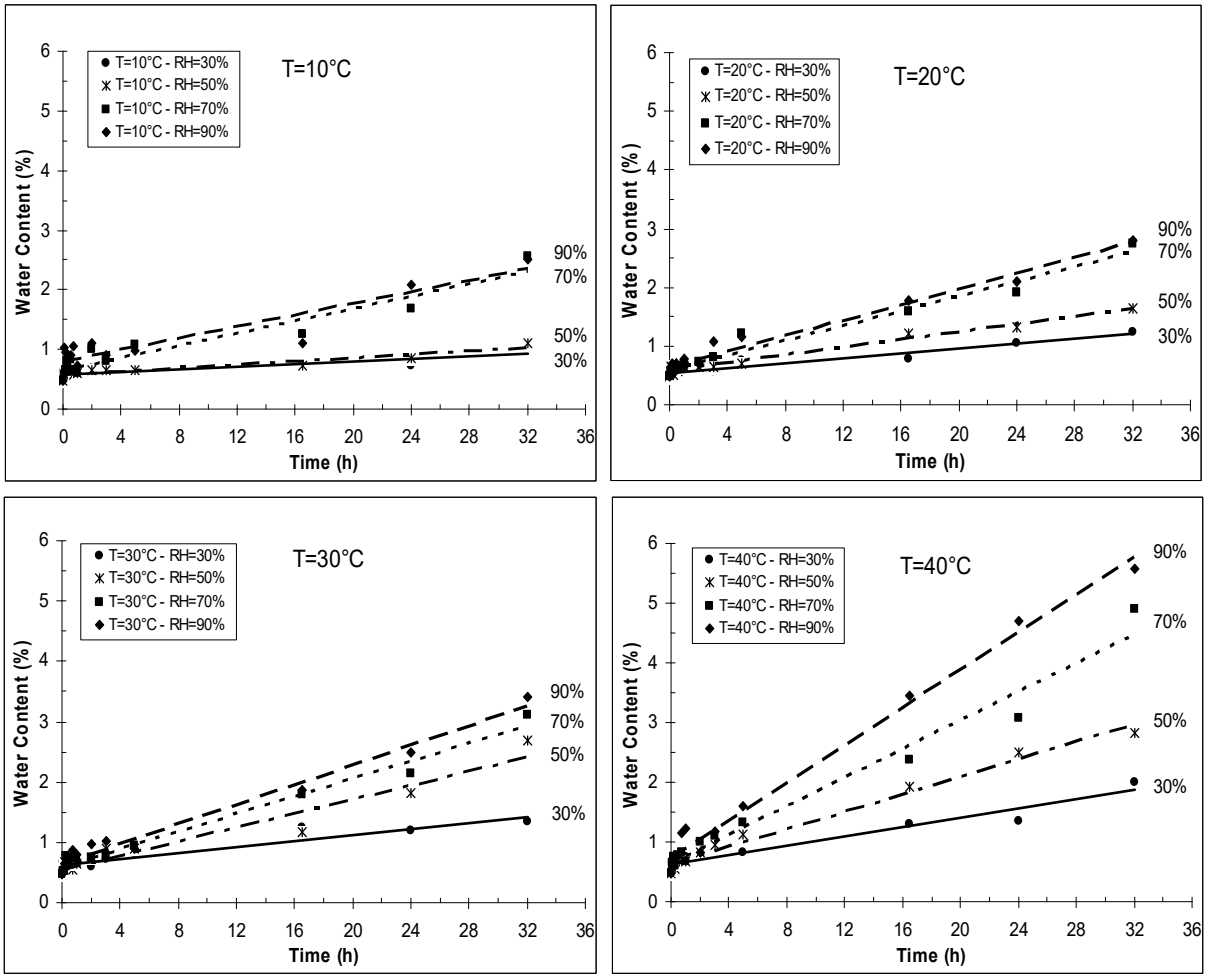

Figure 4: Profile of moisture absorption by bioethanol along 32 h of exposure under different conditions of temperature and relative humidity. The average RSD observed for all the tested conditions was 11%

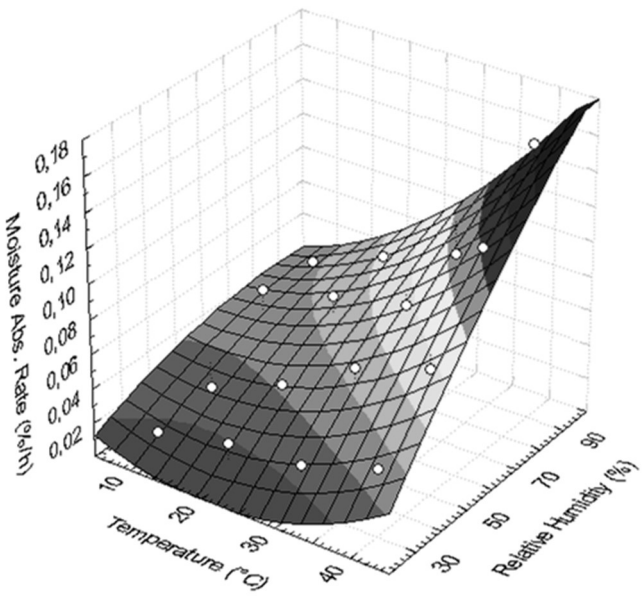

Figure 5: Surface plot demonstrating the effect of temperature and relative humidity on the moisture absorption rate by bioethanol. Mass losses presented herein refer to those obtained at 32 h of exposure. White dots represent the mass loss values determined experimentally.

4 SUMMARY

The results obtained in this work clearly shows that in an environment up to 30 ºC, independently of the relative humidity, the bioethanol can be exposed during at least 2 hours and still meet the specification of ASTM D5798-21 regarding the water content (maximum limit defined as 1%). At 40 ºC and above, the bioethanol keeps the ASTM specification only up to 30 min.

Regarding the ethanol evaporation (sample mass loss), the experiments show that only 10 min of exposure to any environmental conditions of relative humidity and temperature are enough to cause a mass loss of at least 1%.

It was also observed from the experimental results that there are two competing effects in the bioethanol fuel samples: mass loss by ethanol evaporation and moisture absorption, especially for higher relative humidities. However, the experiments showed that mass loss by ethanol evaporation occurs preferably than moisture absorption. These two phenomena need more detailed investigation, especially at elevated temperatures and relative humidities, since this is a preliminary study.

5 REFERENCES

American Society for Testing and Materials. “ASTM D5798-21: Standard specification for ethanol fuel blends flexible-fuel automotive spark-ignition engines”, 2021.

BNDES and CGEE. “Bioetanol de cana de açúcar: energia para o desenvolvimento sustentável”. 1st ed., Nov. 2008. Available online at: https://web.bndes.gov.br/bib/jspui/handle/1408/2002

Sindipeças/Abipeças. “Relatório da frota circulante”. Ed. 2022. Available online at: https://www.sindipecas.org.br/sindinews/Economia/2022/RelatorioFrotaCirculante_2022.pdf

Renewable Fuels Association (RFA). “2002 Ethanol Industry Outlook”. Available online at: https://d35t1syewk4d42.cloudfront.net/file/2145/RFA%202022%20Outlook.pdf.

J. D. van den Wall Bake, M. Junginger, A. Faaij, T. Poot, A. Walter. “Explaining the experience curve: Cost reductions of Brazilian ethanol from sugarcane". Biomass and Bioenergy, vol. 33, nº 4, p. 644–658, 2009.

C. A. L. Santos, L. C. O. Tiroel, E. C. Oliveira, N. L. Almeida. “O estado da arte da corrosão pelo etanol combustível”. INTERCORR 2018. Online: https://abraco.org.br/src/uploads/intercorr/2018/INTERCORR2018_207.pdf.

P. R. Wiederhold. “Water vapor measurement: methods and instrumentation”. Marcel Dekker, Inc. 1997.

B. Tan, P. Melius, P. Ziegler. “A simple gas chromatographic method for the study of organic solvents: Moisture analysis, hygroscopicity and evaporation. Journal of Chromatographic Science, vol. 20, nº 5, p. 213-217, 1982.

A. Flores, E. Conde. “Effect of the hygroscopic nature of pure ethanol in the accuracy of preparation of simulator solutions. Volpe National Transportation Systems Center. Cambridge, MA. Jun. 2004.

IMEKO TC8, TC11 and TC24 Joint Conference
October 11-13, 2023, Madeira, Portugal

PRODUCTION OF GASEOUS CERTIFIED REFERENCE MATERIALS AT INRiM FOR AMOUNT OF SUBSTANCE FRACTION OF CO_2

F. Durbiano[1]/Presenter, S. Pavarelli[2], F. Rolle[3], F.R. Pennecchi[4], M. Sega[5]

[1]INRiM, Torino, Italy, f.durbiano@inrim.it
[2]INRiM, Torino, Italy, s.pavarelli@inrim.it
[3]INRiM, Torino, Italy, f.rolle@inrim.it
[4]INRiM, Torino, Italy, f.pennecchi@inrim.it
[5] INRiM, Torino, Italy, m.sega@inrim.it

Abstract:

Due to the involvement of carbon dioxide (CO_2) in the global warming effects, INRiM is developing certified reference materials (CRMs) of CO_2 in synthetic air. The mixtures are prepared by gravimetry, a primary method, and verified by Non-Dispersive Infrared spectroscopy. The CO_2 amount fraction in the mixtures and its associated uncertainty are the certified properties of the CRMs. A corresponding stability study of the amount fraction of CO_2 is also ongoing.

Further work foresees the development of CRMs for the isotopic composition of CO_2 in air, after the participation in specific international comparisons.

Keywords: certified reference materials, gas mixtures, amount of substance fraction, CO_2

1. INTRODUCTION

The concentration trend of carbon dioxide (CO_2) in the atmosphere is increasing continuously and the average value in 2023 has reached 424.00 μmol/mol [1]. Accurate and sound determinations of the atmospheric concentration of the greenhouse gases (GHGs) enable the development of models to predict future scenarios and to implement effective measures to counteract global warming. For this purpose, it is very useful to have metrological references represented by gas mixtures with CO_2 concentration at the atmospheric level to ensure the reliability of the results and to have the possibility to compare them at the international level.

The use of Certified Reference Materials (CRMs) for the amount of substance fraction (amount fraction) of CO_2 in matrices of synthetic air is of utmost importance to achieve the comparability and traceability of data, which are essential features of measurement results in environmental and climate fields. CRMs can be used for the calibration of instrumentation that monitors the increasing values of CO_2 concentration in the atmosphere, thus contributing to undertake specific actions to mitigate climate change effects.

Moreover, discriminating between the CO_2 in the atmosphere due to anthropogenic activities and the CO_2 derived from natural sources is another pillar in the climate change studies. Stable isotopes of carbon in CO_2 represent effective markers. In this context, developing CRMs for the isotopic composition of CO_2 in air ($\delta^{13}C$-CO_2) enable to calibrate the instrumentation devoted to such determination.

The National Institute of Metrological Research (INRiM) has among its duties the development of CRMs as readily accessible measurement standards to establish the traceability of measurement results to the International System of Units (SI), in accordance with the focal point "Monitoring the environment and supporting the development of clean technologies" of the document "INRIM Metrology towards 2030" [2].

In this manuscript, the work carried out at INRiM for the preparation of reference gas mixtures which should become candidate CRMs for the amount fraction of CO_2 in air is presented. Moreover, a short description of the work in progress and scheduled for the production of CRMs related to the stable isotopic composition is reported.

2. MATERIALS AND METHODS

INRiM has a consolidated experience in the preparation of reference gas mixtures of CO_2 in synthetic air with an amount fraction similar to the concentration levels in the atmosphere. The candidate CRMs consist of reference gas mixtures contained in high-pressure 5 L aluminium alloy cylinders and accompanied by a certificate.

Considering the metrological traceability chain, the gas mixtures are prepared by gravimetry, a primary direct method, in accordance with the International Standard ISO 6142-1:2015 [3].

The gravimetric method used at INRiM consists in the introduction, in a preconditioned cylinder, of a specific mass of the analyte gas, in this case pure CO_2 or a CO_2 gas mixture and, successively, of the matrix gas by means of a proper filling station designed and realised at INRiM [4]. The various stages of gas injection are followed by an accurate weighing to determine the amount of gas actually introduced in each stage. The weighing is carried out using a mass comparator (Mettler Toledo PR 10003, Switzerland), according to the A-B-B-A double substitution scheme, in which A denotes the cylinder in which the mixture is being prepared and B is an identical but empty cylinder used to minimize the correction due to the buoyancy effect. As prescribed in [3], after their preparation the gas mixtures are verified against independent reference gas mixtures by means of a calibrated Non-Dispersive Infrared (NDIR) analyser (ABB URAS 14, Switzerland), following the requirements of the International Standard ISO 6143:2001 [5] to confirm the gravimetric value. A purity assessment of the parent gases is also required for the critical impurities. The International Standard ISO EN 17034:2016 [6] requires that CRMs, i.e., the reference gas mixtures in the present case, undergo stability assessments in order to track and examine how different environmental conditions or chemical reactions inside the cylinders can affect their composition.

Another requirement of [6] is related to the homogeneity assessments. The inter-units homogeneity assessment is not applicable in this case because every cylinder contains a stand-alone reference gas mixture specifically prepared. Besides, since these mixtures are composed of gases having similar densities and are not condensable, they are intrinsically homogeneous. Therefore, the intra-unit homogeneity study is not necessary.

The uncertainty budget for the value assigned to the amount fraction of CO_2 in synthetic air is described in [7].

From the perspective of the Guide to the Expression of Uncertainty in Measurement (GUM) [8], the uncertainty due to the stability, u_{stab}, is added to the uncertainty of characterization associated with the amount fraction of CO_2, u_{char}, so that the combined uncertainty associated to the CRM, u_{CRM}, results by the application of the law of propagation of uncertainty (Eq. 1):

$$u_{CRM} = \sqrt{u_{char}^2 + u_{stab}^2} \quad (1)$$

The expanded uncertainty is evaluated by considering a normal distribution associated with the measurement result, hence by multiplying the combined standard uncertainty by a coverage factor $k = 2$.

INRiM participated successfully in the international key comparisons CCQM-K52 (Carbon dioxide in synthetic air) [9] and CCQM-K120 (Carbon dioxide at background and urban level) [7], organised under the umbrella of the Consultative Committee for Amount of Substance: Metrology in Chemistry and Biology (CCQM) of the International Committee for Weights and Measures (CIPM). The CIPM Mutual Recognition Arrangement (CIPM MRA) is the framework through which National Metrology Institutes demonstrate the international equivalence of their measurement standards and the calibration and measurement certificates they issue [10]. The outcomes of this Arrangement are the internationally recognized Calibration and Measurement Capabilities (CMCs) of the participating institutes. Approved CMCs are publicly available from the CIPM MRA database (KCDB) [11]. On the basis of a successful participation in the measurement comparisons, it is possible for an institute to propose a CMC.

Further work is in progress at INRiM to establish a metrology traceability chain devoted to the determination of the isotopic composition of CO_2 in air (in terms of $\delta^{13}C$-CO_2), in order to develop the capability to produce CRMs also for this quantity. A stability study is ongoing and the participation in a specific international comparison in this measurement field is expected shortly. In this way, INRiM reference gas mixtures of CO_2 can become CRMs both for the amount fraction of CO_2 and for their isotopic composition, in order to enable the correct determination of the fraction of anthropogenic emissions of CO_2 in the atmosphere with respect to the carbon budget [12].

3. RESULTS AND DISCUSSION

At INRiM the value of the amount fraction associated with the candidate CRMs for CO_2 gas mixture is determined by the gravimetric method. The associated uncertainty, u_{char}, includes the sources due to the weighted masses of the parent gases, their purity and their molar masses.

In general, the average lifetime of a CRM of CO_2 gas mixtures is estimated to be about 5 years [13]. In order to assess the stability of the reference gas mixtures prepared at INRiM, in accordance with the requirements of [6], proper studies are carried out as follows. The gravimetric CO_2 amount fraction is considered as reference value and represents the time-zero value. Immediately after the preparation, the prepared mixture is verified by using the calibrated NDIR analyser to confirm the gravimetric preparation data. The verification is acceptable if

the gravimetric value and the analytical value are consistent within their respective expanded uncertainties. Periodically, the mixtures are verified following the same procedure. All these measurements are considered as independent. The uncertainty, u_{stab}, is evaluated as the standard deviation of the analytical values obtained during the study. This approach takes into account the dispersion of the values, which are affected also by the performance of the NDIR analyser.

In the following, an example of stability study carried out on a candidate CRM, identified as INRiM reference gas mixture 010 (cylinder serial number D370674) prepared in 2006, is presented. A graph of the measurement results versus time is reported in Figure 1. Such mixture of CO_2 in synthetic air has a CO_2 amount fraction of 359.65 µmol/mol with an associated combined standard uncertainty, u_{char}, of 0.46 µmol/mol.

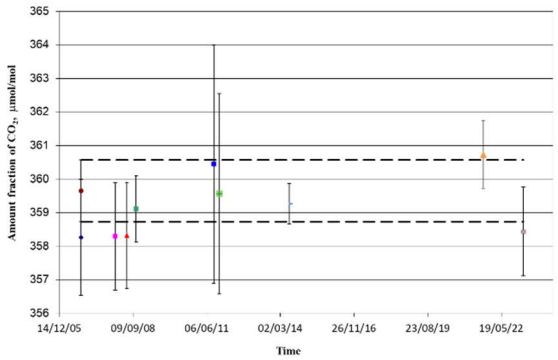

Figure 1. Stability assessment for the candidate CRM CO_2 INRiM reference gas mixture 010. The garnet-coloured circle represents the result obtained by the gravimetric method at time zero. The blue square represents the analytical value at time zero. The other coloured points are the analytical values in time. The black bars denote the associated expanded uncertainty (k = 2). The black dotted lines represent the expanded uncertainty associated with the gravimetric value reported as a reference for visualizing the consistency with the analytical data.

Table 1 shows how different lifetime values affect the u_{stab} value, and hence the combined standard uncertainties u_{CRM}. The corresponding expanded uncertainties are also reported considering a normal distribution and a coverage factor k = 2.

Table 1

Lifetime, year	u_{stab}, µmol/mol	u_{CRM}, µmol/mol	U_{CRM}, µmol/mol
1.5	0.79	0.91	1.8
5	0.85	0.97	1.9
8	0.78	0.91	1.8
17	0.90	1.01	2.0

The uncertainty associated with the analytical values is not explicitly considered for the evaluation of u_{stab}, as their dispersion is affected by the analytical method. Furthermore, the uncertainty associated with the analytical values may vary with time due to fluctuations and modifications of the experimental setup. About the latter, Figure 1 clearly shows that the values obtained from 2014 onwards present a reduced associated uncertainty. The study outcomes reported in Table 1 prove that gas mixtures of CO_2 at the atmospheric amount fraction show a long-in-time stability. An analogous study, carried out on similar mixtures, confirmed the same results. Currently, a 5-year stability assessment for the INRiM gas mixtures can be considered a suitable compromise, as in the case reported in [13], taking into account a conservative approach.

A second case refers to a more recent reference gas mixture, identified as STELLAR 022 (cylinder serial number 15914), prepared on April 2022 in the framework of the EMPIR Joint Research Project 19ENV05 "Stable isotope metrology to enable climate action and regulation – STELLAR". The stability study is ongoing and the data are shown in Figure 2. The mixture, prepared in a synthetic air matrix, has a CO_2 amount fraction of 404.72 µmol/mol with u_{char} of 0.20 µmol/mol. In this case, u_{stab}, calculated over one year, is 0.15 µmol/mol; u_{CRM} results of 0.25 µmol/mol. The corresponding U_{CRM} is 0.50 µmol/mol.

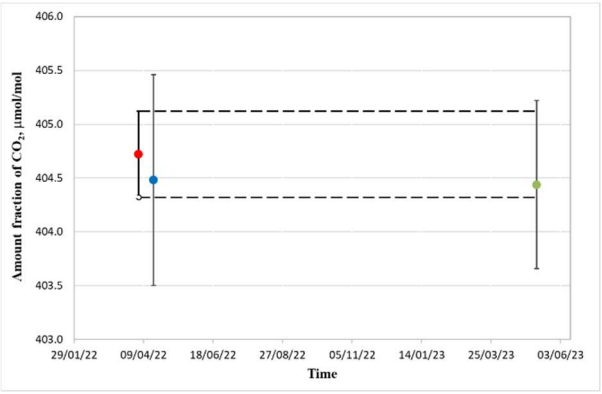

Figure 2. Stability assessment for the candidate CRM CO_2 reference gas mixture STELLAR 022. The red circle represents the result obtained by the gravimetric method at time zero. The blue circle represents the analytical value at time zero. The green circle denotes the analytical value of about one year later. The black bars denote the associated expanded uncertainty (k = 2). The black dotted lines represent the expanded uncertainty associated with the gravimetric value reported as a reference for visualizing the consistency with the analytical data.

For the reference gas mixture STELLAR 022, the isotopic composition was also determined. It has a $\delta^{13}C$ value of -41.87 ‰ with an associated expanded uncertainty (k = 2) of 0.30 ‰. The measurements were carried out by a Fourier-

Transform Infrared Spectrometer - FTIR (Nicolet iS50, ThermoFisher Scientific, USA) equipped with a mercury cadmium telluride (MCT) detector and a 2 m White type gas cell. This reference gas mixture was sent to the Max Planck Institute for Biogeochemistry (MPI-BGC) for the verification of the isotopic composition by isotope-ratio mass spectrometry (IRMS) and the value was consistent with the one reported by INRiM, within the declared uncertainty. Figure 3 shows some of the cylinders which were analysed at MPI-BGC for the validation of their isotopic composition.

Figure 3: Examples of INRiM reference gas mixtures for CO_2 amount fraction and isotopic composition.

4. SUMMARY

INRiM is working to become an official producer of CRMs for the amount fraction of CO_2 in synthetic air. Stability assessments have been carried out for the production of CRMs. Following the stability studies, a 5-year stability assessment for INRiM gas mixtures can be considered a suitable compromise taking into account a conservative approach. The submission of a specific CMC in the KCDB web resource is the next step. The outcome will be the activation of an internationally recognised service available to customers for the distribution of CRMs for this quantity within the CIPM MRA.

Moreover, INRiM started to study the stability of the isotopic composition value for some of the prepared reference gas mixtures. INRiM plans to take part in a programmed international comparison and, on the basis of a successful participation, a new CMC will be proposed also for isotopic composition.

5. REFERENCES

[1] Global Monitoring Laboratory, Carbon Cycle Greenhouse Gases, Trends in CO_2, https://gml.noaa.gov/ccgg/trends.

[2] INRIM Metrology towards 2030, https://www.inrim.it/it/chi-siamo/descrizione-dellente/documento-di-vision.

[3] ISO 6142-1:2015 Gas analysis — Preparation of calibration gas mixtures — Part 1: Gravimetric method for Class I mixtures.

[4] Amico di Meane E., Plassa M., Rolle F., Sega M., "Metrological traceability in gas analysis at I.N.Ri.M.: gravimetric primary gas mixtures", Accreditation and Quality Assurance, 14 (11) 2009, pp. 607-611.

[5] ISO 6143:2001 Gas analysis — Comparison methods for determining and checking the composition of calibration gas mixtures.

[6] ISO EN 17034:2016 General requirements for the competence of reference material producers.

[7] E. Flores, J. Viallon, T. Choteau, P. Moussay, F. Idrees, R. I. Wielgosz, J. Lee, E. Zalewska, G. Nieuwenkamp, A. van der Veen, "CCQM-K120 (Carbon dioxide at background and urban level)" Metrologia vol. 56, no. A1, 08001, 2019.

[8] Guide to the Expression of Uncertainty in Measurement (GUM), First edition, JCGM 100:2008. https://www.bipm.org/documents/20126/2071204/JCGM_100_2008_E.pdf

[9] R. M. Wessel1, A. M. H. van der Veen, P. R Ziel, P. Steele, R. Langenfelds, M. van der Schoot, D. Smeulders, L. Besley, V. Smarçao da Cunha, Z. Zhou, "International comparison CCQM-K52: Carbon dioxide in synthetic air" Metrologia, vol. 45, no. 1A, 08011, 2008.

[10] CIPM MRA-P-11, Overview and implementation of the CIPM, Version 1.3, 13/04/2023. https://www.bipm.org/documents/20126/43742162/CIPM-MRA-P-11.pdf

[11] Calibration and measurement capabilities in the context of the CIPM MRA, Guidelines for their review, acceptance and maintenance CIPM MRA-G-13, Version 1.2, 20/07/2022. https://www.bipm.org/documents/20126/43742162/CIPM-MRA-G-13.pdf/f8b8c429-42e0-4cf1-dc6c-bc60ab7f371a

[12] M. Zimnoch, J. Necki, L. Chmura, A. Jasek, D. Jelen, M. Galkowski, T. Kuc, Z. Gorczyca, J. Bartyzel, K. Rozanski "Quantification of carbon dioxide and methane emissions in urban areas: source apportionment based on atmospheric observations, Mitigation and Adaptation Strategies for Global Change" vol. 24, pp. 1051–1071, 2019.

[13] C. L. Zhao, P. P. Tans, "Estimating uncertainty of the WMO mole fraction scale for carbon dioxide in air" Journal of Geophysical Research, vol. 111, D08S09, 2006. doi:10.1029/2005JD006003

IMEKO TC8, TC11 and TC24 Joint Conference
October 11-13, 2023, Madeira, Portugal

PREPARATION OF MULTICOMPONENT MIXTURES TO SUPPORT CARBON METROLOGY

Florbela A. Dias[1], Cristina Palma[1], Carlos J. Costa[1]

[1] Instituto Português da Qualidade, Rua António Gião, 2, 2629-531 Caparica, Portugal, florbelad@ipq.pt

Abstract:
The Reference Gas Laboratory (LGR) of IPQ is participating in the project MetCCUS - Metrology for Carbon Capture Utilization and Storage under the new EPM (European Partnership on Metrology) Program.

The goal of this project is to develop a metrological infrastructure that enables monitoring and detection of carbon dioxide leaks in energy and industrial processes, in transport networks and also allow the support of a better understanding of the life cycle of carbon dioxide.

The contribution of LGR involves the preparation of certified reference materials (CRM) to allow the metrological traceability, providing support for the calibration and validation of instrumentation used in carbon capture processes.

Keywords: carbon metrology, multicomponent mixtures, gravimetric method, certification

1 INTRODUCTION

In recent years, the growing concern surrounding climate change has driven a substantial increase in environmental monitoring efforts. As a result, the demand for measurements with traceability has surged, aiming to ensure the reliability of data and minimize measurement uncertainties.

The Reference Gas Laboratory (LGR) at IPQ plays a pivotal role in this domain, responsible for producing, maintaining, and advancing national primary standard gaseous mixtures in strict accordance with ISO 17034 [1]. These mixtures are meticulously prepared using a gravimetric approach, following an internal procedure aligned with the international standard ISO 6142-1 [2], thereby guaranteeing the utmost accuracy. The certification of these gas mixtures adheres to the international standard ISO 6143 [3], leveraging analytical techniques such as gas chromatography (GC), paramagnetic moment, non-dispersive infrared spectroscopy (NDIR), and non-dispersive ultraviolet spectroscopy (NDUV).

The quality control of these measurements is fortified through active participation in projects and international comparisons. Furthermore, recognition and inclusion in the Bureau International des Poids et Mesures (BIPM) database of calibration and measurement capabilities (CMC) solidify their commitment to quality [4].

The LGR's latest contribution focuses on preparing multicomponent gaseous mixtures aimed at enhancing the accuracy, reliability, and traceability of carbon metrology measurements. Specifically, this paper outlines the work undertaken by LGR as part of the MetCCUS project. This project started on October 1, 2022, with the participation of 21 partners and will lasts for 36 months.

Under the MetCCUS project, the contribution of LGR involves the preparation of certified reference materials (CRM) to allow the measurement of impurities in CO2 with metrological traceability, providing support for methods validation and the calibration of instrumentation used in carbon capture processes. LGR had prepared the following bicomponent mixtures: SO_2 in CO_2 matrix and H_2S in CO_2 matrix; and two multicomponent mixtures SO_2+CO+O_2 in CO_2 and H_2S+CO+CH_4+O_2 in CO_2 matrix. This study successfully characterized four polluting gases and oxygen in CO_2 matrix within a cylinder under a pressure of approximately 40 bar, and it entailed an in-depth analysis of interferences and a stability study [5].

2 GAS MIXTURES PREPARATION

As previously mentioned, reference gas mixtures are prepared according to an internal procedure based on the gravimetric method outlined in ISO 6142-1 [2].

This section of ISO 6142 applies specifically to mixtures of gaseous or completely vaporized components, which can be introduced into the cylinder in either the gaseous or liquid state. The mixtures to be prepared can be either bicomponent or multicomponent.

This method describes the calculation of uncertainty associated with the molar fraction of each component. This uncertainty calculation requires the evaluation of contributions stemming from factors such as the weighing process, component purity, mixture stability, and final mixture verification.

During the preparation of gas mixtures, aluminium cylinders with a special coating are used to prevent the adsorption of mixture components on the inner walls.

Following the cylinder selection, a rigorous cleaning process is performed to ensure that any potential residues inside the cylinder do not impact the uncertainty of the composition of the final mixture. This step is particularly important when preparing mixtures with very low concentrations.

Another critical step in the filling process is the transfer of gases from the parent cylinder, for each component, to the cylinder where the mixture is being prepared. The addition of each gas is carried out at a filling station equipped with electronically polished tubes, valves, vacuum and pressure meters, and oil-free turbo molecular vacuum pumps. The amount of gas added to the cylinder is carefully controlled using a balance (Figure 1).

Figure 12: Filling station and comparative balance

The accurate mass of each gas component added to the cylinder is determined using a mass comparator, utilizing calibrated masses that are traceable to the national standard. The traceability of the gas composition to the international system of units (SI) is ensured through the use of calibrated instrumentation.

By utilizing the results from the purity analysis certificates of the initial gases and the data obtained through the weighing process, the exact composition of the mixture and the associated uncertainties (relating to the various molar fractions obtained) can be calculated.

IPQ prepared a bicomponent gas mixture and a multicomponent gas mixture in a carbon dioxide matrix using the gravimetric method, with the following nominal molar fractions: SO_2 (20×10^{-6} mol/mol), H_2S (10×10^{-6} mol/mol) CO (750×10^{-6} mol/mol), CH_4 (2×10^{-2} mol/mol) and O_2 (1×10^{-2} mol/mol).

Once prepared, the gas mixture underwent a homogenization process. The cylinder containing the mixture was placed in a rolling system for approximately an hour (Figure 2).

Figure 2: Rolling cylinder system

3 GAS MIXTURES CERTIFICATION

The composition of the gas mixture is determined through an individual analysis of the molar fraction of each component. The procedure for determining the molar fraction is described in the international standard ISO 6143 [3]. The analytical method used is a comparative method, as it employs primary reference standards to establish the calibration curve. The specific analytical methods used are gas chromatography (GC), paramagnetic moment, non-dispersive infrared spectroscopy (NDIR), and non-dispersive ultraviolet spectroscopy (NDUV). The final results are presented together with their respective uncertainties in accordance with the Guide to the Expression of Uncertainty in Measurement [6].

The produced gas mixtures are certified using specific analysers for SO_2, H_2S, CO, CH_4 and O_2. In each certification, the molar fraction of each component in the prepared mixture is determined by comparing the equipment's response to the standards used, in accordance with the gas under analysis, within appropriate measurement intervals.

The certification process takes place using an automated multichannel sampling system, to which all the cylinders to be analysed are connected (Figure 3).

Figure 3: Certification of Gas Mixtures Facility

During the analysis, the cylinders are automatically selected, enabling the individual circulation of gas through the analyser. This system employs the purpose-built IPQAnaliseQui software, which manages the sampling process and records all measurements taken by the analyser. Ultimately, all the gathered data, including records of standard and sample analyses, are entered into a spreadsheet and adjusted with zero and pressure measurements.

The calibration function determination is carried out using the XGENLINE program developed by the NPL - National Physical Laboratory. This software calculates the most suitable low-degree polynomial calibration function (1, 2, 3 or 4) for a set of measurement data (X, Y), considering the uncertainties and covariances associated with the data. Hence, the determined calibration function is employed to derive estimates of the molar fraction values for the samples under analysis and their corresponding associated uncertainties.

4 INTERFERENT STUDY

The study of interferents was conducted using certified reference material (Table 1).

Table 7: PSM / CRM used for the study of interferents

Interferent Gas	PSM /CRM (mol/mol)	Analytical method
H_2S	CRM412061 (9,2±0,5) x10^{-6}	NDUV
SO_2	VSL4910 (25,00±0,37) x10^{-6}	NDIR
CO	CRM034916 (823±4) x10^{-6}	NDIR
O_2	VSL8612 (1,003±0,019) x10^{-2}	Paramagnetic
CH_4 / ar	CRM015377 (2,49±0,02) x10^{-2}	NDIR
CO_2	CRM034907 (20,01±0,05) x10^{-2}	NDIR
CH_4 / N_2	PSM202534 (2,501±0,012) x10^{-2}	NDIR

SO_2 Analyser

Measurements of SO_2, H_2S, CO, CH_4, O_2, and CO_2 standards were conducted on the SO_2 analyser. The results obtained during the SO_2 analyser tests are presented in Table 2. *Zero* is the reading of the analyser when the zero cleaning gas is passing, which is nitrogen. *Reading* is the value when the sample gas is passing. *S* is the standard deviation of the measurements.

The *Zero* value of the analyser does not have to be zero because the calculations are carried out with the zero correction and the analytical method is a comparative method according to ISO 6143.

Table 2: Results of interferents on the SO_2 analyser

Cylinder	Molar Fraction mol/mol	Zero mV	Reading mV	S mV
CRM412061 (H_2S)	9,2x10^{-6}	-2560,95	-2556,61	0,6686
VSL4910 (SO_2)	25,00x10^{-6}	-2553,19	-2249,54	0,6123
CRM034916 (CO)	823x10^{-6}	-2547,53	-2546,61	0,5344
VSL8612 (O_2)	1,003x10^{-2}	-2545,11	-2544,24	0,5266
CRM015377 (CH_4 / ar)	2,49x10^{-2}	***-2543,55***	***7314,06***	0,6940
CRM034907 (CO_2)	20,01x10^{-2}	-2531,41	-2540,10	0,8063
PSM202534 (CH_4 / N_2)	2,501x10^{-2}	---	---	---

We can observe that for the gases H_2S, CO, O_2 and CO_2, the zero in the table is similar to the reading. We consider that the values are similar when the difference between the reading and the zero is less than 10 mV. This indicates that these gases do not interfere with the SO_2 gas reading on the SO_2 analyser. On the other hand, we have CH_4 gas interfering with the SO_2 sensor.

H_2S Analyser

Measurements of SO_2, H_2S, CO, CH_4, O_2, and CO_2 standards were conducted on the H_2S analyser. The results obtained during the H_2S analyser tests are presented in Table 3.

Table 3: Results of interferents on the H_2S analyser

We can observe that for the gases CO, O_2, CH_4 and CO_2, the zero in the table is similar to the reading. This indicates that these gases do not interfere with the H_2S gas reading on the H_2S analyser. On the other hand, we have SO_2 gas interfering with the H_2S sensor.

CO Analyser

Measurements of SO_2, H_2S, CO, CH_4, O_2, and CO_2 standards were conducted on the CO analyser. The results obtained during the CO analyser tests are presented in Table 4.

Table 4 – Results of interferents on the CO analyser

Cylinder	Molar Fraction mol/mol	Zero mV	Reading mV	S mV
CRM412061 (H_2S)	$9{,}2x10^{-6}$	2180,90	2179,85	0,378
VSL4910 (SO_2)	$25{,}00x10^{-6}$	2179,17	2178,70	0,382
CRM034916 (CO)	$823x10^{-6}$	2179,00	7819,40	0,665
VSL8612 (O_2)	$1{,}003x10^{-2}$	2180,19	2178,71	0,419
CRM015377 (CH_4 / ar)	$2{,}49x10^{-2}$	*2179,03*	*2147,72*	0,459
CRM034907 (CO_2)	$20{,}01x10^{-2}$	2178,36	2170,43	0,356
PSM202534 (CH_4 / N_2)	$2{,}501x10^{-2}$	---	---	---

We can observe that for the gases SO_2, H_2S, O_2 and CO_2, the zero in the table is similar to the reading. This indicates that these gases do not interfere with the CO gas reading on the CO analyser. Methane gas interferes with the CO analyser (NDIR) however the interference is negligible within the measurement uncertainty.

O_2 Analyser

Measurements of SO_2, H_2S, CO, CH_4, O_2, and CO_2 standards were conducted on the O_2 analyser. The results obtained during the O_2 analyser tests are presented in Table 5.

Table 5 – Results of interferents on the O_2 analyser

Cylinder	Molar Fraction mol/mol	Zero mV	Reading mV	S mV
CRM412061 (H_2S)	$9{,}2x10^{-6}$	-1054,93	-548,592	4,8925
VSL4910 (SO_2)	$25{,}00x10^{-6}$	***-1036,35***	***781,121***	8,3786
CRM034916 (CO)	$823x10^{-6}$	-1030,93	-1028,56	6,3142
VSL8612 (O_2)	$1{,}003x10^{-2}$	-1027,85	-1025,05	7,1555
CRM015377 (CH_4 / ar)	$2{,}49x10^{-2}$	---	---	---
CRM034907 (CO_2)	$20{,}01x10^{-2}$	-1024,66	-1022,14	4,8874
PSM202534 (CH_4 / N_2)	$2{,}501x10^{-2}$	-2458,53	-2456,86	8,4032

We can observe that for the gases SO_2, H_2S, CO, O_2 and CO_2, the zero in the table is similar to the reading. This indicates that these gases do not interfere with the O_2 gas reading on the O_2 analyser.

CH_4 Analyser

Measurements of SO_2, H_2S, CO, CH_4, O_2, and CO_2 standards were conducted on the CH_4 analyser. The results obtained during the CH_4 analyser tests are presented in Table 6.

Table 6 – Results of interferents on the CH_4 analyser.

Cylinder	Molar Fraction mol/mol	Zero mV	Reading mV	S mV
CRM412061 (H_2S)	$9{,}2x10^{-6}$	2079,21	2078,47	0,190
VSL4910 (SO_2)	$25{,}00x10^{-6}$	2079,33	2080,43	0,201
CRM034916 (CO)	$823x10^{-6}$	2079,44	2079,35	0,203
VSL8612 (O_2)	$1{,}003x10^{-2}$	2079,87	2079,67	0,222
CRM015377 (CH_4 / ar)	$2{,}49x10^{-2}$	2079,72	5944,30	0,292
CRM034907 (CO_2)	$20{,}01x10^{-2}$	2081,01	2078,70	0,208
PSM202534 (CH_4 / N_2)	$2{,}501x10^{-2}$	---	---	---

We can observe that for the gases SO_2, H_2S, CO, O_2 and CO_2, the zero in the table is similar to the reading. This indicates that these gases do not interfere with the CH_4 gas reading on the CH_4 analyser.

5 RESULTS

Four gas mixtures were carefully prepared for analysis, including two binary combinations of SO_2 in a carbon dioxide matrix, designated as PRM408326 and PRM108593. Furthermore, two mixtures composed of H_2S in CO_2, labelled as PRM108595 and PRM108596, were also carefully assembled. This study facilitated the comprehensive

characterization of these four mixtures, each contained within individual cylinders maintained at an approximate pressure of 40 bar.

Furthermore, two multicomponent mixtures were prepared in a CO_2 matrix, PRM308978 with the impurities SO_2, CO and O_2; and PRM202557, with the impurities H_2S, CO, O_2, and CH_4 at the previously mentioned molar fractions. These mixtures were contained within two cylinders at an approximate pressure of 40 bar each.

a. Results for the SO_2 Mixtures

The binary mixtures PRM408326 and PRM108593 were certified using the SO_2 analyser with the standards presented in Table 7.

Table 7 – Standards used for SO_2 Component Certification.

Standards Used	*x* mol/mol	*U* mol/mol
VSL9159	2,554E-05	3,7E-07
VSL7897	2,992E-04	9,3E-07
VSL7886	1,001E-03	3,2E-06

Table 8 shows the results of the analysis of the SO_2 component, in the two prepared binary mixtures, PRM408326 and PRM108593.

Table 8 – Results of the analysis of the SO_2 component, in the prepared binary mixtures.

Results PRM408326 – SO_2		
Data	***x*** **10^{-6} mol/mol**	***U*** **10^{-6} mol/mol**
2023-09-04	19,52	0,51

Results PRM108593 – SO_2		
Data	***x*** **10^{-6} mol/mol**	***U*** **10^{-6} mol/mol**
2023-09-04	20,71	0,50

b. Results for the H_2S Mixtures

The binary mixtures PRM108595 and PRM108596 were certified using the H_2S analyser with the standards presented in Table 9.

Table 9 – Standards used for H_2S Component Certification.

Standards Used	*x* mol/mol	*U* mol/mol
NPL0274	4,610E-06	4,6E-06
VSL4408	5,000E-06	5,0E-06
VSL4982	1,001E-05	1,0E-05
VSL4427	5,000E-05	5,0E-05

Table 9 shows the results of the analysis of the H_2S component, in the two prepared binary mixtures, PRM108595 and PRM108596.

Table 10 – Results of the analysis of the H_2S component, in the prepared binary mixtures.

Results PRM108595 – H_2S		
Data	***x*** **10^{-6} mol/mol**	***U*** **10^{-6} mol/mol**
2023-09-11	9,97	0,48

Results PRM108596 – H_2S		
Data	***x*** **10^{-6} mol/mol**	***U*** **10^{-6} mol/mol**
2023-09-11	9,64	0,47

c. Results for the Multicomponent Mixtures

The multicomponent mixtures PRM308978 and PRM202557 were certified using the SO_2, H_2S, CO, CH_4 and O_2 analysers with the standards presented in Table 11.

Table 11 – Standards Used for Certification of the Components.

Standards Used	*x* mol/mol	*U* mol/mol
SO_2		
VSL9159	2,554E-05	3,7E-07
PSM502546	5,005E-05	4,0E-07
VSL7897	2,992E-04	9,3E-07
VSL7886	1,001E-03	3,2E-06
H_2S		
NPL0274	4,610E-06	3,4E-07
VSL4408	5,000E-06	3,7E-07
VSL4982	1,001E-05	3,2E-07
VSL0536	2,000E-04	3,0E-06

PSM402577	5,0020E-04	5,0E-06
NMI8601	5,5010E-04	5,2E-06
NMI8622	7,0050E-04	2,0E-06
NMI3707	8,0030E-04	2,3E-06
NPL1720	9,9940E-04	3,7E-06
CH_4		
NPL273	4,999E-03	1,9E-05
VSL6039	5,001E-03	1,8E-05
PSM202534	2,501E-02	1,2E-02
VSL6037	5,006E-02	1,0E-04
O_2		
VSL3704	5,000E-03	4,3E-04
VSL8612	1,003E-02	1,9E-04
VSL8554	1,003E-01	2,6E-04

6 SUMMARY

Under the MetCCUS project, the contribution of LGR involves the preparation of certified reference materials (CRM) to allow the measurement of impurities in CO_2 with metrological traceability, providing support for the calibration and validation of instrumentation used in carbon capture processes.

We can conclude that methane gas interferes with the SO_2 sensor when using the NDIR analytical method. Also, SO_2 gas interferes with the H_2S sensor when using the NDUV analytical method. Methane gas interferes with the CO analyser (NDIR) however the interference is negligible within the measurement uncertainty. Therefore, two multicomponent mixtures were prepared taking this information into account. One mixture does not contain SO_2 and the other does not contain CH_4 and H_2S.

Four bicomponent and two multi-component mixtures in CO_2 matrix were prepared, with uncertainties within expectations.

The results of the molar fractions of the multicomponent mixtures PRM308978 (SO_2+CO+O_2 in CO_2) and PRM202557 (H_2S+CO+CH_4+O_2 in CO_2) are presented in Table 12.

Table 12 – Molar fractions of the multicomponent mixtures in CO_2

PRM308978 2023-09-19		
Component in a Carbon Dioxide Matrix.	***x*** **mol/mol**	***U*** **mol/mol**
SO_2	14,26 x 10^{-6}	0,46 x 10^{-6}
CO	666,1 x 10^{-6}	2,7 x 10^{-6}
O_2	0,594 x 10^{-2}	0,027 x 10^{-2}
PRM202557 2023-09-20		
Component in a Carbon Dioxide Matrix.	***x*** **mol/mol**	***U*** **mol/mol**
H_2S	9,83 x 10^{-6}	0,48 x 10^{-6}
CO	669,5 x 10^{-6}	2,7 x 10^{-6}
CH_4	1,9685 x 10^{-2}	0,0060 x 10^{-2}
O_2	0,586 x 10^{-2}	0,027 x 10^{-2}

A stability study will be carried out in order to have data to establish the shelf life of the different mixtures.

In the future, we intend to extend this study to mixtures with more components. To obtain more information regarding what is intended in the project, we intend to analyse these mixtures using other analytical methods to avoid the interferences.

7 REFERENCES

ISO/IEC 17034:2016 General requirements for the competence of reference material producers;

ISO 6142-1:2015 – Gas analysis – Preparation of calibration gas mixtures – Part 1: Gravimetric method for Class I mixtures;

ISO 6143:2001 – Gas analysis – Comparison methods for determining and checking the composition of calibration gas mixtures;

https://www.bipm.org/kcdb/;

ISO 13528:2022 – Statistical methods for use in proficiency testing by interlaboratory comparisons;

Evaluation of measurement data – Guide to the expression of uncertainty in measurement JCGM 100:2008 (GUM 1995 with minor corrections).

IMEKO TC8, TC11 and TC24 Joint Conference
October 11-13, 2023, Madeira, Portugal

DEVELOPMENT OF OPEN-SOURCE TOOLS FOR THE DIGITAL AND MACHINE-READABLE CALIBRATION OF FLOWMETERS WITH NUMERICAL DISPLAYS

G. Esteves Coelho/Presenter[1], A. Pinheiro[2],A. Silva Ribeiro[3], C. Simões[4], L. Martins[5]

[1] Laboratório Nacional de Engenharia Civil, Lisboa, Portugal, gfcoelho@lnec.pt
[2] Laboratório Nacional de Engenharia Civil, Lisboa, Portugal, apinheiro@lnec.pt
[3] Laboratório Nacional de Engenharia Civil, Lisboa, Portugal, asribeiro@lnec.pt
[4] Laboratório Nacional de Engenharia Civil, Lisboa, Portugal, csimoes@lnec.pt
[5] Laboratório Nacional de Engenharia Civil, Lisboa, Portugal, lfmartins@lnec.pt

Abstract:
This paper presents a methodology for obtaining digital machine-readable measurements from numerical displays images. The proposed method provides means to automate and digitalize a previously manual and labour-intensive laboratory procedure for flowmeters calibration.

The proposed method allows to obtain machine-readable readings from remote numerical displays with available-off-the-shelf hardware and open-source software. By using smartphones for remote image capture and streaming and the Tesseract open-source OCR engine, is possible to leverage the infrastructure's digital transition, improve procedures efficiency and effectiveness while promoting sustainable actions with cost reductions.

Keywords: Metrology; Automation; Process efficiency; Machine-readable data; Open-source programming.

1 INTRODUCTION

The Industrial 4.0 era and particularly the Industrial Internet of Things (IIoT) lead to an unprecedented ability to use different types of sensors and generate enormous amount of measurement data, requiring traceability. The heterogeneous nature of the equipment and the laboratory with inadequate Information Technology (IT) penetration, is often the bottleneck for a fully digitalized calibration process.

The development and establishment of digital processes and digital infrastructures offers enormous potential for overall calibration process efficiency. However, this process is often doomed to manual interaction and is usually labour-intensive. Nevertheless, it is possible to reduce human interaction and increase process efficiency and effectiveness by increasing the infrastructure's IT penetration, towards a fully digital and machine-readable calibration process.

The current accessibility to technology combined with the maturity of open-source software, including Artificial Intelligence (AI), allows the introduction and interoperability of digital processes with available off-the-shelf hardware and custom software, with reduced financial investments. The method proposed for the calibration of flowmeters with numerical displays, aims to aggregate and automate in a single computer all the data collection and storage of a typical decentralized and manual calibration process, gathering images remotely with cameras (image synchronization is also discussed), followed by pre-processing the images and obtaining the machine-readable readings from the numerical displays by means of Optical Character Recognition (OCR).

This method is scalable to virtually any number of cameras and can be applied to both laboratory calibration and *in-situ* measurement processes. The software is developed with open-software solutions implemented in Python, with OpenCV for image pre-processing and Tesseract for OCR engine implementation.

2 INFRASTRUCTURE DESCRIPTION

The Unit of Hydraulic Metrology (UHM) is a R&DI infrastructure jointly coordinated by the Department of Hydraulics and Environment (DHA) and the Scientific Instrumentation Center (CIC) of LNEC, with competence and capabilities to develop research in Hydrology and Hydraulics and to provide traceability to instrumentation and systems applied in a wide range of measurement quantities,

namely, flow rate (mass and volumetric), flow speed, volume, level, and precipitation.

The laboratory infrastructure (figure 1) has several hydraulic test benches allowing to establish different conditions to obtain flow rate by the primary gravimetric measurement using two weighing platforms (reaching 3 ton and 30 ton of mass) and the measurement of time using universal time counters, all traceable to the primary standards of IPQ (Portuguese Institute for Quality, the Portuguese National Metrology Institute). The main experimental facility as the following operational capabilities:

- volumetric flow rate $\leq$ 0.500 m^3/s;
- mass flow rate $\leq$ 400 kg/s;
- nominal diameter $\leq$ DN 400;
- maximum operating pressure $\leq$ 1.0 MPa;
- power $\leq$ 250 kW of electric power groups;
- power $\leq$ 75 kW for electric pumps not coupled to drive motors.

This Unit supports the skills that allow LNEC-UHM to be a Designated Institute for the flow rate and flow speed for liquids, according to the international recognition accepted by the BIPM in 2021 and confirmed by EURAMET in 2022. The management of UHM is developed according to the LNEC Quality Management System complying with the requirements of the ISO/IEC 17025 standard [1].

The R&DI develops methods and apply processes to provide traceability and to perform metrological characterization related with several types of measuring instruments, namely, ultrasonic flowmeters, turbine meters, positive displacement flowmeters, differential pressure flowmeters, rotameters, mass flowmeters, Parshall flumes, among others [2-5].

This infrastructure has human resources and technologies capable of promoting hydraulic metrology services and metrological information management, in a variety of areas of water resources management (water supply, undue inflow, agricultural uses and wastewater treatment), and in different frameworks (management entities, industry, manufacturers, and customers).

Figure 13: UHM infrastructure overview

3 THE DIGITAL TRANSITION CHALLENGE AND IMPLEMENTATION

The previous described infrastructure has been subject to successive equipment modernization to foster and leverage the digital technologies and transition. More recently, the infrastructure's automation legacy system was upgrade in the perspective of the Industry 4.0 and towards the Industrial Internet of Things (IIoT) [6]. The integration of standard industrial communication protocols and modern technologies leverages the infrastructure's automation capabilities and big data analysis, aiming to improve efficiency and effectiveness of the calibration procedures, the auditing process and the infrastructure's maintenance actions.

In the same perspective, the work presented here aims to contribute to the modernization of this infrastructure and contribute to the ongoing digital transition.

The main goal with this work is to acquire the measurements from the flowmeter under calibration in a machine-readable format to able to collect the measurements directly in a digital media or support (e.g. spreadsheet). However, given the wide range

of flowmeters devices that are currently calibrated at this infrastructure, with diverse interfaces and different numerical displays, a one-size-fits-all solution approach is difficult to reach. Additionally, the remote location of the equipment in the plant usually restricts the use of cables and wired devices to obtain the measurements of the flowmeters under calibration. Nevertheless, the majority of the flowmeter's devices are at least equipped with one numerical display that enables the measurement by inspection.

To tackle these issues, the proposed approach general principle employs imaging devices to capture the remote images from the numerical displays in real-time and obtain the measurements in a numerical machine-readable format by means of Optical Character Recognition (OCR).

In figure 2 the implemented system architecture is presented. From left to right: Near the flowmeter under calibration an imaging device (such as smartphone) is installed. The imaging device is positioned in order to obtain an image of the flowmeter's numerical display; The image is stream over Wi-Fi to a local PC; The PC implements the OCR engine and image processing and also provides Network Time Protocol (NTP) for clock synchronization between the capturing devices and the PC; The OCR engine converts the numerical display from the image to machine-readable numbers format that can be stored in digital support such as spreadsheets files.

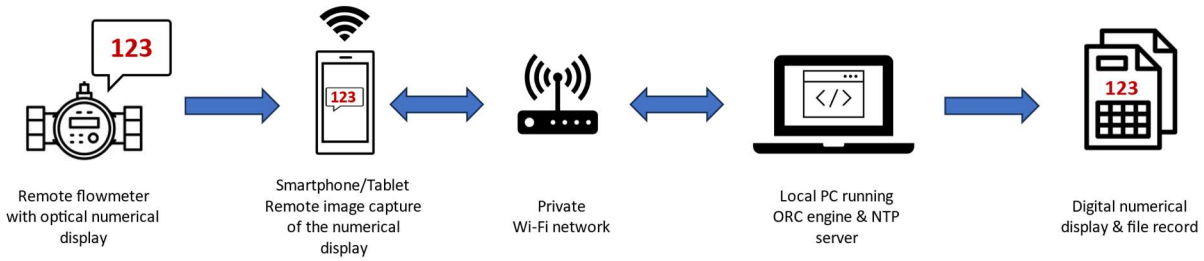

Figure 14: System implementation architecture

a. Experimental system implementation

The remote flowmeter's numerical display can be capture with available off-the-shelf smartphones, considering that these devices have good image quality with low optical distortion and are Wi-Fi capable. The smartphone is mounted in a tripod with the camera properly facing the flowmeter's numerical display, as depicted in figures 3 and 4.

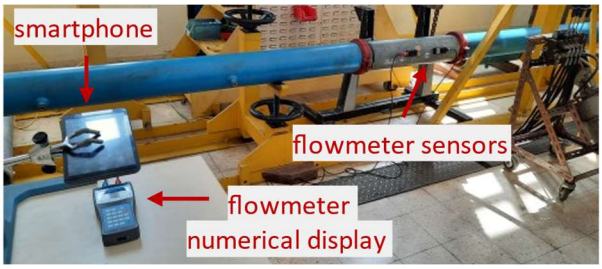

Figure 15: Experimental setup example for ultrasonic flowmeter calibration at the UHM plant

There are several implementations and software available to stream the video from a smartphone to a PC. In this case we used the android IP Webcam app (available in Google Play), that provides unicast video streaming with session validation capabilities. Although, private Wi-Fi network are available at UHM´s infrastructure, the later option is used *in-situ* calibrations environments where private networks are not available, and communications security are mandatory.

Figure 16: Close up of the flowmeter's numerical display and the smartphone for image streaming

Although the image processing is conducted in an asynchronous model by design, the NTP synchronization of the devices provides means of measurement synchronization between the flowmeter and the standard measurement and provides traceability and auditability of the overall process. For this purpose, the image streaming is time stamped locally in the smartphone device and the PC provides another time stamp for the measurements during the calibration process. In order to provide a temporal reference of the entire process, the capturing devices (smartphones) and the image processing unit (PC) are time synchronized with the same NTP server. This NTP

server is provided from the PC to have the same time reference.

With the IP Webcam app installed in the smartphone, the video stream is accessed through the device's IP. This configuration provides a real-time video stream of the remote flowmeter's numerical display to a PC located in our monitoring and command room, see figure 17.

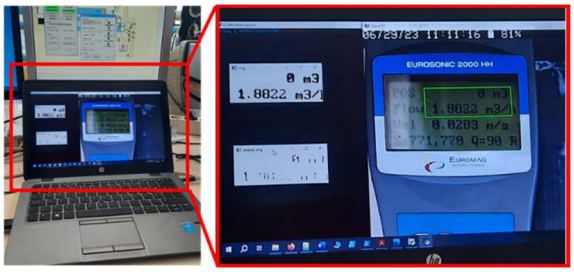

Figure 17: Remote image of the flowmeter display in the PC in the monitoring and command room

The image processing application and OCR engine was developed in Python with fully open-source software: using OpenCV for the image pre-processing and using Tesseract for the OCR engine.

The first step is to is to create a bounding box around the area of numbers of interest in the image, namely in the area corresponding to the measurement of the flowmeter. Since the OCR engine is sensitive to the image quality, e.g., light exposure, display contrast and especially the presence of light reflections in the display surface, the next step the numerical display image is converted in binary (black and white) video format. This step is needed to achieve adequate confidence levels from the OCR results. With the binary image output (see figure 18), the operator can evaluate the appropriate image quality to send to OCR engine.

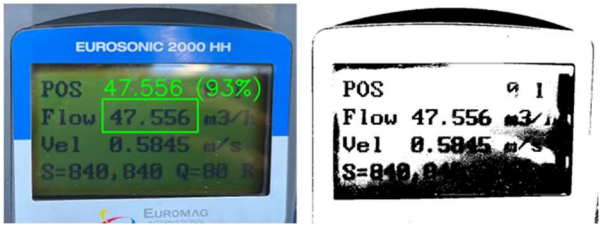

Figure 18: (left) Original image of the flowmeter numerical display with OCR results overlayed and (right) corresponding binary image

With a single command in the PC, the binary image is sent to Tesseract OCR engine, where the machine-readable of the numerical display from the OCR engine is overlayed in the image along with the confidence value (see figure 18). The digital information of the OCR's numerical display and the corresponding confidence value is stored in a spreadsheet file, along with the PC time stamp and the original processed picture stored path, for auditing purposes.

4 RESULTS

To assess the proposed methodology, several pictures of the flowmeter's numerical displays were acquired in different angles and light conditions and evaluated with the OCR engine. In general, the results show that the implemented OCR engine is adequate to convert the numerical measurements from the numerical display to machine-readable format, to the majority of the flowmeters under calibration.

In figure 19 an example of the numerical display of an ultrasonic flowmeter (model eurosonic 2000 HH) is presented. The OCR results are overlayed in the picture showing the obtained numerical conversion (left) and a confidence level of the OCR (right). Figure 8 shows the binary image output of the pre-processed image in the bounding box of figure 7 before sending to the OCR engine to obtain the measurements in machine-readable format.

Figure 19: OCR result and confidence overlayed in the numerical display image

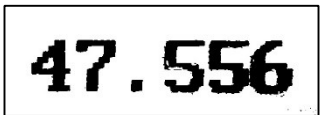

Figure 20: Binary image output of the pre-processed image of interest in figure 7

With proper display's contrast and light conditions, the OCR results in a correct numerical conversion. However, in the presence of low brightness and/or light reflections, the conversions results are inadequate as expected. This is an inevitable limitation of the OCR engine, nonetheless it can be mitigated by assuring a fair quality of the images before applying it to the OCR engine. To implement this, the image stream is preprocessed to obtain the binary counter part of the images. Image binarization enables to obtain the best contrast between the background and the

numbers to be converted and provide useful information to the operator about the quality of the image stream in the OCR's perspective.

Figure 21 shows an example of OCR output results in presence of adverse light conditions. In this case, although the image appears to be in fair conditions for human interpretation, the OCR engine outputs the incorrect numerical measurements when the binary image quality is inferior (see figure 22).

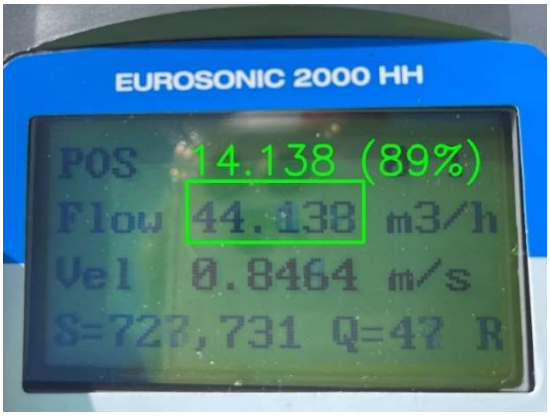

Figure 21: Influence of light reflections in the OCR output

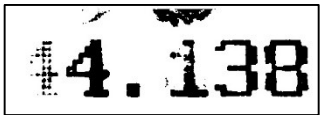

Figure 22: Binary image output in the presence of adverse light effects

Consequently, image pre-processing is also used in the early stage of the smartphone positioning in front of the numerical display of the flowmeter under calibration, to achieve the best possible quality of the image stream to the OCR engine.

Nevertheless, the OCR can also output incorrect values due to limitation in the OCR model. The case presented in figure 23 is an example of the incorrect identification of the zero value, even in good light conditions (see figure 24). This is a limitation of the current OCR engine for the slashed zero "Ø" that is incorrectly converted to number "6". This problem only affects displays using slashed zero and is further discussed in section 5. However, the confidence low values give some insight of this limitation, and for this reason the OCR output is always evaluated and stored along with the confidence values to detect and potentially manage these situations.

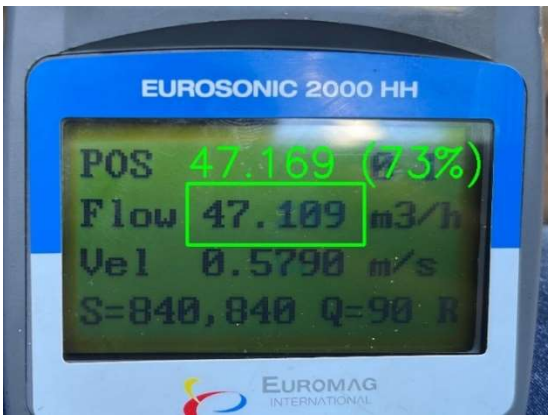

Figure 23: Slashed zero OCR engine problem

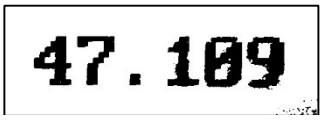

Figure 24: Corresponding binary image

5 DISCUSSION AND FUTURE WORK

A solution to automate and digitalize a manual and labour-intensive laboratory procedure was presented. With available off-the-shelf hardware (smartphone and laptop) and open-source software was possible to develop and implement a new tool that enables to read remote numerical displays of a flowmeter and obtain its measurements in a machine-readable format ready to store directly in a computer with minimal human interaction.

The results showed that its possible to improve laboratory procedure efficiency and effectiveness with minimal financial investment. The proposed solution also promotes sustainable practices, important in the digital transformation, by reducing intermediate processes that are usually supported by pen-and-paper methods.

Since the image streaming is implemented over standard ethernet protocols, this method is scalable to any number of smartphones and feasible for calibration of multiple flowmeters simultaneously.

Although the laboratory procedure for flowmeter's calibration usually requires human interaction, there are some procedures that is desirable to automate to further increment the process efficiency. Since the process for the calibration of a flowmeter device involves gathering simultaneous and synchronous measurements (both the device under calibration and the standard measurement), future work addresses further reduction in human interaction towards a semi-automated procedure. In order assure the OCR best performance, one potential improvement is to implement a threshold approach to the confidence level of the OCR output by implementing a while-loop with a time-out mechanism: The flowmeter

measurements are only accepted based on the OCR's confidence level threshold that in turn triggers the standard measurement (standard measurements are obtained in machine-readable format and in real-time) and both measurements are obtained simultaneously.

To reduce the influence of adverse light conditions resulting in the poor OCR performance, on solution is to use artificial and controlled light environment, combined with low reflective backgrounds.

The problem regarding the slashed zero mismatch is a well-know and documented issue in the Tesseract open-source community. To solve this issue adequate OCR models are need. These models can be obtained directly from the open-source community or by training new OCR models with adequate training data. Nevertheless, as already stated this limitation only affects the measurements with devices that employs this specific type of numerical font.

6 REFERENCES

A. S. Ribeiro, L. Dias, A. C. Martins, H. Dimas, R. Mendes, "Flow measurement traceability used to improve water management", Test & Measurement 2018 International Conference. NLA – South Africa, Western Cape (South Africa), 2018

M. A. Silva, C. Amado, A. S. Ribeiro, D. Loureiro, "Uncertainty evaluation in time-dependent measurements", Measurement 196, 2022. : DOI:10.1016/j.measurement.2022.111196

A. Ribeiro, D. Loureiro, M. C. Almeida, M. Cox, J. A. Sousa, M. Silva, L. Martins, R. Brito, A. C. Soares, "Uncertainty evaluation of totalization of flow and volume measurements in drinking water supply networks", FLOMEKO 2019 – 18th International Flow Measurement Conference, 26-28 June, LNEC, Lisboa (Portugal), 2019.

C. Simões, A. S. Ribeiro, M. C. Almeida, D. Covas, "Uncertainty evaluation related with the fitting of probability distributions to rainfall experimental data", IMEKO XXIII World Congress (IMEKO 2021) - Measurement: sparking tomorrow's smart revolution. Yokohama (Japan). 30Aug.–3Sep, 2021.

R. S. Brito, M. C. Almeida, A. Ribeiro, "Enhancing hydraulic data reliability in sewers", Water Practice & Technology Vol 17 No 1, 431, 2022 DOI: 10.2166/wpt.2021.093.

G. E. Coelho; A. S. Ribeiro;J. dos Reis, J.; C. Simões, – "Industry 4.0 Legacy Systems Integration Case Study", IMEKO TC11 & TC24 Joint Hybrid Conference, Dubrovnik, Croatia, October 17-19, 2022.

IMEKO TC8, TC11 and TC24 Joint Conference
October 11-13, 2023, Madeira, Portugal

ANALYSIS OF FLOW RATE MEASUREMENT ACCURACY AND TRACEABILITY OF FLOWMETERS IN FIELD CONDITIONS USING CLAMP-ON ULTRASONIC FLOWMETERS

C. Simões[1], A. Ribeiro[2], M. Almeida[3], Dídia Covas[4]

[1] LNEC – National Laboratory for Civil Engineering, Lisbon, Portugal, csimoes@lnec.pt
[2] LNEC – National Laboratory for Civil Engineering, Lisbon, Portugal, asribeiro@lnec.pt
[3] LNEC – National Laboratory for Civil Engineering, Lisbon, Portugal, mcalmeida@lnec.pt
[4] CERIS, Instituto Superior Técnico, Universidade de Lisboa, Av. Rovisco Pais 1, 1049-001 Lisboa, Portugal, didia.covas@tecnico.ulisboa.pt

Abstract:
This study examines the traceability and measurement uncertainty of *in situ* hydraulic calibration using clamp-on ultrasonic flowmeters as a reference. The procedure compares the equipment readings with the reference ones. Measurement uncertainty evaluation uses GUM formulation, considering the linearity conditions of the mathematical models applied. Experimental values are used to test the procedure and its suitability for actual cases where the expected accuracy needs to be achieved.

Keywords: Flow measurement; clamp-on ultrasonic flowmeter; measurement uncertainty; traceability; measurement accuracy.

1 INTRODUCTION

Many hydraulic infrastructures (e.g. supply pipes, drainage systems, pumping stations) have installed flowmeters to collect and provide data for monitoring and control systems and for the efficient management of systems, thus, requiring traceability. It is common to find flowmeters installed in pipes with physical constrains that prevent their removal for calibration in metrology laboratories, being needed to find alternative solutions to evaluate the accuracy of measurement equipment *in situ* using portable reference flowmeters.

Clamp-on ultrasonic flowmeters are a viable alternative for assessing the measurement accuracy in these locations, even if performance is lower when compared to metrology laboratories. An additional undeniable difficulty is to ensure stable flow conditions to define steps for testing. Thus, the basic principle of traceability is achieved, allowing to compare a reference standard and equipment to be calibrated. The method is based on the statistical analysis of time series.

This approach has the merit of incorporating the influence of local setup and flow conditions in the traceability evaluation, not considered in a laboratory setup with optimized calibration conditions.

This process of calibration has some advantages. It is non-invasive, since the quantities of interest (flow rate and velocity) are not disturbed, avoiding pressure drops in the pipe. Calibration equipment installation and readjustment are also easier. The procedure must follow specific rules to ensure the quality of the data using this method. The rules are related to the fluid characteristics, the installation setup, and the pipe characteristics.

The operation procedure of a clamp-on ultrasonic flowmeter, based on the transit-time differential method, requires an initial configuration using data related to the liquid (e.g., the type of liquid and its temperature) and pipe (e.g., material, coatings, outer diameter, and wall thickness allowing to calculate inner diameter). Thus, the measurement procedure includes estimates of influence quantities (temperature, length, outside perimeter and wall thickness). Usually, these systems can provide the distance between a couple of transducers, given the data mentioned above.

The relation of the setup conditions with these influence quantities allow to consider that the main sources of error are the following: existing irregularities of the pipe along the sections; installation of the transducers; properties of the fluid; and acoustic characteristics.

Flow behaviour and regimes of this type of flowmeters in non-laboratory conditions are

typically not under control, and there is a need to study how, under those conditions, it is possible to provide traceability to the equipment under evaluation and, how the accuracy is affected in the comparison process and how it is possible to get correction functions and to assess its uncertainty from time series of flow data.

This paper describes how, under dynamic conditions, the contributions of the uncertainty sources are evaluated and propagated through probability distribution functions to calculate the measurement uncertainty. This information is crucial in determining whether calibrated equipment is suitable for a particular purpose and its impact on the measurement system.

2 CLAMP-ON ULTRASONIC FLOWMETER

A. Description and characteristics

The concept of ultrasonic flowmeters for liquids was firstly presented by [1].

Sanderson [2] highlighted the problems encountered using traditional flowmeters and suggested the of ultrasonic flowmeters, which are not in contact with the fluid.

The performance of ultrasonic flowmeters with two pairs of transducers emitting and receiving ultrasonic signals has been largely experimentally studied [3]. Lynnworth [4] compared various types of ultrasonic flowmeters, their measurement processes and transducer mounting mechanisms.

When using ultrasonic flowmeters, depending on the propagation route of the ultrasonic waves, the measurement methods can be divided of two types: the Z-path method (the transmission method) and the V-path method (the reflection method).

The method applied by clamp-on ultrasonic flowmeters is the reflection method. An advantage of the reflection method is its ability to consistently obtain correct measurement values even when some flowing components move perpendicularly to the flow direction. However, since the ultrasonic wave propagation route is approximately twice the course length with the transmission method, a more considerable propagation loss occurs.

Figure 1 shows the schematic diagram of transit-time clamp-on ultrasonic flowmeters configured in a V-path arrangement, without being in contact with the fluid, as they are clamped on the outer side of an existing pipe, not disturbing the fluid flow.

The measuring principle consists of the upstream transducer transmitting an ultrasonic signal that travels in the fluid flow direction and reaches the downstream transducer [6-7]. After that, the downstream transducer transmits an ultrasonic signal which travels backwards, that is in the opposite direction to the fluid flow, and is received by the upstream transducer. This difference, called time of flight of both signals, is estimated and used to compute the velocity of the fluid integrated over the acoustic path. The integration of the fluid velocity in the pipe cross-section allows the estimation (i.e. measurement) of the flow rate.

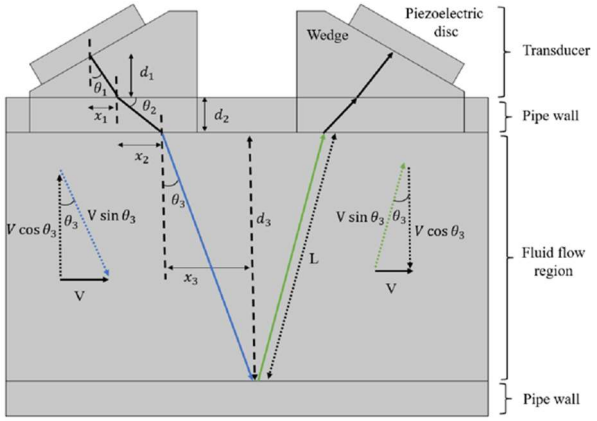

Legend:
θ_1, θ_2, θ_3: the angle of the ultrasonic wave in the wedge, pipe wall and the fluid, respectively;
d_1: the vertical distance travelled by the wave in the wedge;
d_2: the pipe thickness;
d_3: the inner diameter of the pipe;
v: the fluid flow velocity;
x_1, x_2, x_3: the horizontal distances travelled by the wave in the wedge, pipe wall and fluid, respectively.

Figure 25: Schematic of the V-path method for Clamp-on ultrasonic flowmeters, adopted by [5].

b. Mathematical models

The flow rate – Q can be calculated by means of Equation 1, based on the cross-sectional area of the pipe, A:

$$Q = v_a \cdot A = \left(\frac{v}{K}\right)\frac{\pi \cdot {d_3}^2}{4} \tag{7}$$

where (see Figure 1): d_3 is the inner pipe diameter; v is the velocity of the fluid integrated over the acoustic path; v_a is the velocity integrated over the pipe cross-section; K is a flow profile correction factor.

A clamp-on ultrasonic flowmeter transit-time, with single-path, and reflection transmitted indirectly measures the average velocity along the acoustic path, v, not the average flow velocity v_a needed to calculate the flow rate. The mathematical models associated with calculating v (Equation 2) and v_a (Equation 3) are presented below:

$$v = \frac{\Delta t}{t_{up} + t_{down} - 2t_{delay}}\left(\frac{c_{wedge}}{sin_{\theta 1}}\right) \tag{8}$$

and

$$v_a = K\frac{\Delta t}{t_{up} + t_{down} - 2t_{delay}}\left(\frac{c_{wedge}}{sin_{\theta 1}}\right) \tag{9}$$

considering $\Delta t = t_{\mathrm{up}} - t_{\mathrm{down}}$, where t_{up} corresponds to the total time taken by the wave to propagate inside both transducers and the fluid for a wave which is propagating in the opposite direction of the fluid flow; t_{down} corresponds to the total time taken by the wave to propagate inside both transducers and the fluid for a wave propagating in the direction of the fluid flow; t_{delay} corresponds to the time taken by the wave to propagate inside the wedge and pipe wall; and c_{wedge} is to the speed of sound in the wedge. To obtain the inner diameter of the pipe's cross-sectional area, the values of two quantities are usually measured: the wall thickness, t; and the pipe cross-section the perimeter, P.

The outer diameter, d_{ext}, is obtained from the perimeter estimate,

$$d_{\mathrm{ext}} = \frac{P}{\pi} \tag{10}$$

and the inner diameter, d_3, is given by,

$$d_3 = d_{\mathrm{ext}} - 2\,t = \frac{P}{\pi} - 2\,t. \tag{11}$$

c. Traceability chain

The metrological activity requires resources of a metrology infrastructure to perform experimental comparisons with reference instruments with higher accuracy and traceability to SI.

Hydraulic Metrology Laboratory of the National Laboratory for Civil Engineering (HML-LNEC) has four closed conduits test rigs installed in parallel with lengths of 15 m, with nominal diameters from DN 80 to DN 400, as shown in Figure 2.

Each test rig has an electromagnetic flowmeter and is connected to two weighing platforms capable of storing from 1.7 and 17.6 ton of water. Additionally, it has a, underground water supply tank with 340 m^3, and three vertical axis pumps controlled using variable speed drives, capable of operating under the following conditions: volumetric flow rate ≤ 0,500 m^3/s; and mass flow rate ≤ 400 kg/s.

Figure 26: Hydraulic Metrology Laboratory (view).

Laboratory conditions are controlled with the aid of flow straighteners upstream, adjustable joint connections upstream, regulating valves, flow diverting systems and full bore shut-off valves.

The primary gravimetric flow rate measurement functional model is based on the measurement of mass using the weighing platforms and the measurement of time interval using universal time counters, being traceable to the Portuguese IPQ (the Portuguese National Metrology Institute) for the quantities of mass and time.

This facility allows the calibration of different types of flowmeters and counters, providing reference conditions for the measurement of mass flow rate and volumetric flow rate, and flow speed, being the reference obtained from the primary gravimetric standard (e.g. for electromagnetic flowmeters) or the secondary electromagnetic flowmeters (e.g. for the ultrasonic flowmeters), with best measurement capabilities reaching 0.05 % to 0.3 %.

It should be mentioned that HML-LNEC was recognized, since 2023, by EURAMET as the Portuguese Designated Institute for the measurement of liquid flow rate and flow velocities.

The calibration performed *in situ* is intended to provide traceability to the SI by establishing a traceability chain able to give confidence to the measurements obtained with the calibrated equipment. This is achieved using a clamp-on ultrasonic flowmeter of the Hydraulic Metrology Laboratory of LNEC, used as transfer standard.

The chain is obtained through comparisons with standards of higher accuracy to the top level of primary international standards of BIPM.

In this specific case, there are five levels, the lower one is between the equipment to be calibrated

and the secondary standard (electromagnetic flowmeter); the next one represents the internal calibration of these secondary standards with the primary gravimetric system, which considers the flow rate traceable to mass and time measurement standards. These two internal standards are traceable to the Portuguese NMI followed by the traceability to BIPM. Figure 3 shows the traceability chain related with the calibration *in situ* performed by HML-LNEC.

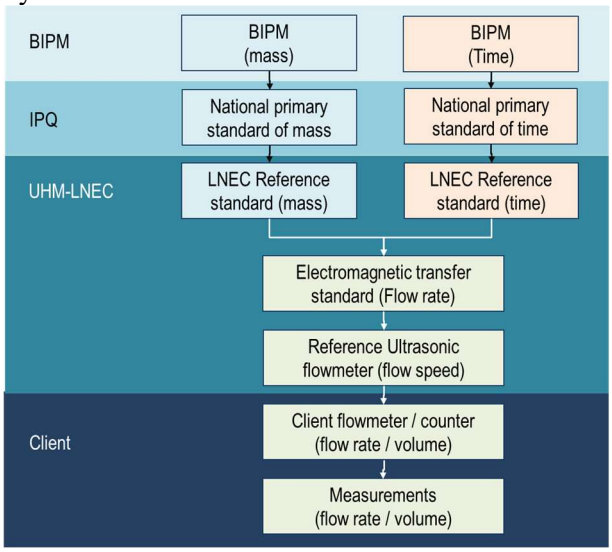

Figure 3 – Traceability chain adapted to *in situ* calibration procedures of HML-LNEC.

3 DATA ACQUISITION APPROACH

The proposed method uses clamp-on ultrasonic flowmeters as reference standard in on-site calibrations.

The traceability chain internal first step is to calibrate the electromagnetic transfer standard using the primary gravimetric method [8].

The second internal step to establish the traceability of the clamp-on ultrasonic flowmeters is obtained in the LNEC hydraulic metrology laboratory facilities, under ideal conditions, where the transducers are mounted in the clean (not painted) surface of a reference pipe (whose internal geometry is also evaluated using a 3D coordinate measuring machine) and the setup assures good acoustic coupling between the transducer faces and the pipe surface.

The calibration method consists of a direct comparison between the readings of the clamp-on ultrasonic flowmeter and of an electromagnetic flowmeter used as a standard. In laboratory conditions, the major influencing factors that affect the uncertainty of clamp-on flowmeters are the area of the measurement cross-section [7], the velocity profile, the path-velocity measurement, and the resolution and repeatability.

The clamp-on ultrasonic flowmeters also require the definition of operational parameters to be able to properly use internal algorithms. These includes operational data regarding the fluid (e.g. the type of fluid) and the installation pipe (e.g. material, coatings, inner diameter and wall thickness) with which the signal conditioner calculates the appropriate distance of the transducers.

The third internal step of the traceability chain is obtained by performing the calibration procedure *in situ*. This process is highly dependent on the nature of the flow and its operational conditions, sometimes allowing to change its magnitude using valves and other elements in the pipeline, but often without any means to change the conditions of the flow. The approach usually followed considers the sample observation of more than 20 pairs of readings (reference flow rate, Q_S, and equipment's flow rate, Q_R), if it is possible to change the flow magnitude in three or more steps and, at least, 50 pairs of readings otherwise. Typically, both readings are taken in intervals of 10 or 15 s, to capture the dynamics of the flow. The procedure usually generates two time series, being required to process the data to assure synchronization.

The practice of this approach shows that, In many cases, non-ideal conditions can affect the quality of readings, always requiring some caution about measurement results, examples of these conditions are::

- unknown inner condition of the pipe, often with encrustations (see Figure 4);
- upstream flow disturbances due to pipe tightness;
- the pipe is not working in closed conditions.

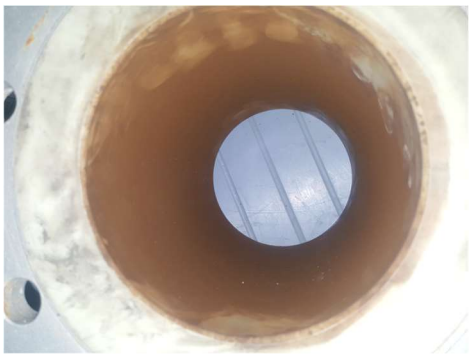

Figure 4: Inner pipe with encrustations

Other factors can be mentioned as affecting the performance of flowmeters in local setups:

- distortion in the fluid flow profile due to disturbances related to bends, contractions, expansions, valves and pumps, air bubbles or fluid contamination; and
- unknown pipe condition, such as, pipe roughness or incrustation due to corrosion on the inner side of the piping and parametric errors .

a. Uncertainty analysis

The general method used for the evaluation of measurement uncertainty is presented in [9], known as the GUM, firstly published by ISO, IEC and other organizations in 1993. This method states that, for a functional relation *f* of the type,:

$$y = f(x_1, \dots, x_n) \tag{12}$$

being *y* the output quantity calculated from *n* input quantities, x_i. The development of the function as a 1st order Taylor series gives the formulation for the measurement standard uncertainty of the output quantity, *u(y)*:

$$u^2(y) = \sum_{i=1}^{n} \left(\frac{\partial f}{\partial x_i}\right)^2 u^2(x_i) + 2\sum_{i=1}^{n-1}\sum_{j=i+1}^{n} \left(\frac{\partial f}{\partial x_i}\right)\left(\frac{\partial f}{\partial x_j}\right) u(x_i, x_j) \tag{13}$$

The first part of the second term of Equation 7 is related to the variance of each input quantity, whereas the second part of the second term is related to the contributions resulting from the correlation between input quantities, providing an exact solution only for linear functions. For non-linear mathematical models, computational approaches are used.

For the studied *in situ* calibration method, the starting point for the mathematical model is given for the average calibration error, $\bar{\varepsilon}$:

$$\bar{\varepsilon} = \frac{\Sigma(Q_{r,i} - Q_{s,i})}{n} \tag{14}$$

where $Q_{r,i}$ represents the readings obtained with the flowmeter to be calibrated, $Q_{s,i}$ represents the readings of the reference flow rate (clamp-on ultrasonic flowmeter) and *n* is the number of pairs of observations.

This mathematical model should also include the contributions for the uncertainty budget related with the time dependent method. Taking into account another variable associated with the data time series, $\delta\varepsilon_{\Delta t}$, the mathematical model is described as follows:

$$\bar{\varepsilon} = \frac{\Sigma(Q_{r,i} - Q_{s,i})}{n} + \delta\varepsilon_{\Delta t}. \tag{15}$$

This equation can be simplified considering,

$$(Q_{r,i} - Q_{s,i}) = \Delta Q_i. \tag{16}$$

being the uncertainty of the differences obtained using Equation (7),

$$u^2(\Delta Q_i) = u^2(Q_{r,i}) + u^2(Q_{s,i}). \tag{17}$$

and that the uncertainty of each difference value has identical uncertainty given by Equation (14) being calculated using Equation (15),

$$u(\Delta Q_i) = u(\Delta Q). \tag{18}$$

$$u^2(\Delta Q_i) = u^2(Q_r) + u^2(Q_s). \tag{19}$$

Regarding the uncertainty associated with the measurement of the reference flow rate, $u^2(Q_s)$, it should be noted that the contributions for uncertainty are included in the calibration certificate associated with the clamp-on ultrasonic flowmeter.

The uncertainty associated with the flow rate to be calibrated, $u^2(Q_r)$, can be estimated considering the following sources of uncertainty:

- *repeatability*, $\delta Q_{r,\mathrm{rep}}$, given by the calibration error experimental standard deviation of the mean;
- *resolution* of the equipment associated with the measurable quantity, $\delta Q_{r,\mathrm{res}}$; and
- *stability*, $\delta Q_{r,\mathrm{sta}}$, obtained from the magnitude of variation of the measurement results of the flow rate to be calibrated.

The combined uncertainty is given by,

$$u^2(Q_r) = u^2(\delta Q_{r,\mathrm{rep}}) + u^2(\delta Q_{r,\mathrm{res}}) + u^2(\delta Q_{r,\mathrm{sta}}) \tag{20}$$

Using the approach mentioned above, the mathematical model (Equation 11) using the equivalent formula (Equation 12) generates Equation (17) and the respective uncertainty (Equation 18).

$$\bar{\varepsilon} = \frac{\Sigma(\Delta Q_i)}{n} + \delta\varepsilon_{\Delta t}, \tag{21}$$

$$u^2(\bar{\varepsilon}) = \sum_{i=1}^{n} \frac{u^2(\Delta Q_i)}{n^2} + u^2(\delta\varepsilon_{\Delta T}). \tag{22}$$

Applying the simplified relation given by Equation (14) results in:

$$u^2(\bar{\varepsilon}) = \frac{1}{n^2}\sum_{i=1}^{n} u^2(\Delta Q_i) + u^2(\delta\varepsilon_{\Delta T}), \tag{23}$$

and,

$$u^2(\bar{\varepsilon}) = \frac{u^2(\Delta Q)}{n} + u^2(\delta\varepsilon_{\Delta T}). \tag{24}$$

To determine the uncertainty associated with the deviation associated with the data time series, $\delta\varepsilon_{\Delta T}$, the following sources of uncertainty are considered (shown Equation 16): acquisition method, $\delta\varepsilon_{\mathrm{met}}$; synchronization, $\delta\varepsilon_{\mathrm{sinc}}$; and *repeatability,* $\delta\varepsilon_{\mathrm{rep}}$, obtained through the experimental standard deviation of the mean error of calibration.

$$u^2(\Sigma\delta\varepsilon_{\Delta T}) = u^2(\delta\varepsilon_{\mathrm{met}}) + u^2(\delta\varepsilon_{\mathrm{sinc}}) + u^2(\delta\varepsilon_{\mathrm{rep}}) \tag{25}$$

B. Case study and data

The case study corresponds to the hydraulic calibration carried out *in situ* without control of the flow, being used a sample of 25 pairs of reference flow rate, $Q_{s,i}$, and read flow rate, $Q_{r,i}$, shown in Figure 5. Figure 6 shows the time variation of the error of calibration (difference between readings and reference values). For the remaining calibration levels, the evaluation of the measurement uncertainties is performed in the same way.

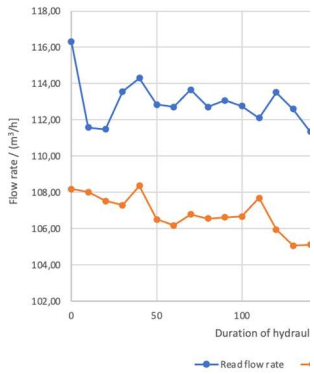

Figure 5: Reference flow rate and readings of flow rate of the hydraulic equipment under calibration.

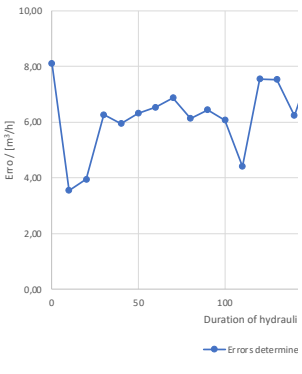

Figure 6: Errors obtained in the hydraulic calibration.

To calculate the standard uncertainty, $u(\bar{\varepsilon})$, using Equation (19), the contributions of the input quantities needed to be determined applying Probability Distribution Functions (PDF) and their parameters are presented in Table 1 and Table 2, respectively.

Table 8: PDF's of input quantities related to Q_r

Quantity	PDF	Parameters
$\delta Q_{r,\text{sta}}$	Uniform	$[-0{,}1; +0{,}1]$
$\delta Q_{r,\text{res}}$	Uniform	$[-5 \cdot 10^{-3}; +5 \cdot 10^{-3}]$
$\delta Q_{r,\text{rep}}$	Normal	$N(\mu;\sigma) = N(0; 0{,}33)$

Table 9: PDF's of input quantities related to $\delta\varepsilon_{\Delta T}$

Quantity	PDF	Parameters
$\delta\varepsilon_{\text{met}}$	Uniform	$[-0{,}2; +0{,}2]$
$\delta\varepsilon_{\text{sinc}}$	Normal	$N(\mu;\sigma) = N(0; 0{,}1)$
$\delta\varepsilon_{\text{rep}}$	Normal	$N(\mu;\sigma) = N(0; 0{,}32)$

Using the values presented in Table 1, the value of the standard uncertainty of the clamp-on ultrasonic flowmeter (taken from the calibration certificate), $u(Q_{s,i}) = 6{,}9 \cdot 10^{-2}$ m³/h, and by applying Equation 14, an estimate of the standard uncertainty associated with average calibration error the can be obtained given by:

$$u(\bar{\varepsilon}) = 0{,}07 \text{ m}^3/\text{h} \quad (26)$$

The expanded uncertainty, $U_{95}(\bar{\varepsilon})$, is calculated by,

$$U_{95}(\bar{\varepsilon}) = k_{95} \cdot u(\bar{\varepsilon}) \quad (13)$$

with k_{95} being the expansion factor. Using a value of 2.05 for this parameter (an alternative could be used considering a t-student PDF with the degrees of freedom analysis based on the Welch-Satterthwaite formula, as described in the GUM), the expanded uncertainty is:

$$U_{95}(\bar{\varepsilon}) = 0{,}15 \text{ m}^3/\text{h} \quad (14)$$

4 CONCLUSIONS

This study allowed to assess the accuracy of the results of hydraulic calibration tests performed *in situ* using a clamp-on ultrasonic flowmeter as a reference.

The measurement uncertainty related to the average calibration error was determined using the conventional Uncertainty Propagation Law, showing that in non-ideal conditions (sometimes it is complicated to obtain data variability), HML-LNEC has instrumentation necessary to meet the accuracy requirements associated with this type of test. These accuracy requirements are achievable through careful statistical analysis, by using numerical methods, for the uncertainty evaluation, reflecting that the quality of the measurement result depends on this analysis.

Considering that the approach presented for the quantification of uncertainty sources associated with calculating the measurement uncertainty of the average calibration error is presented in a simplified way, it is expected that other sources of uncertainty will be quantified in future work. Additionally, it is also planned to study approaches based on FDP and the uncertainty associated with its parameters as an alternative to the method presented herein.

5 REFERENCES

J. Kritz, "An ultrasonic flowmeter for liquids", International Society of Automation, vol. 10, 1955.

M. L. Sanderson, "Electromagnetic and ultrasonic flowmeters: their present states and future possibilities", Electronics and Power, vol. 28, pp. 161-164, 1982. DOI: 10.1049/ep.1982.0071

E. Thompson, "Two beam ultrasonic flow measurement", Imperial College of Science and Technology, University of London, 1978.

L. C. Lynnworth, "Ultrasonic flowmeters", Transactions of the Institute of Measurement and Control, vol. 3, pp. 217-223, 1981. DOI: 10.1177/014233128100300405

M. Ali, "Evaluation of clamp-on ultrasonic liquid flowmeters", University of Western Ontario, 2022.

A. Scwery, T. Staubli, A. Abgottspon, "Field and laboratory experience with a clamp-on acoustic transit time flowmeter", 2012.

ISO 12242, "Measurement of fluid flow in closed conduits – Ultrasonic transit-time meters for liquid", 2012.

ISO 20456, "Measurement of fluid flow in closed conduits – Guidance for the use of electromagnetic flowmeters for conductive liquids", 2017.

JCGM 100, "Evaluation of measurement data. guide to the expression of uncertainty in measurement (GUM 1995 with minor corrections)", 2008.

IMEKO TC8, TC11 and TC24 Joint Conference
October 11-13, 2023, Madeira, Portugal

VALIDATION METHODS IN THE PREPARATION OF XML-BASED DIGITAL CALIBRATION CERTIFICATES (DCC)

G. Söylev Öktem[1]/Presenter, S. Hackel[2], B. Gloger[3], J. Loewe[4], S. Schönhals[5]

[1] Physikalisch-Technische Bundesanstalt (PTB), Braunschweig, Germany, gamze.soeylev-oektem@ptb.de
[2] Physikalisch-Technische Bundesanstalt (PTB), Braunschweig, Germany, siegfried.hackel@ptb.de
[3] Physikalisch-Technische Bundesanstalt (PTB), Braunschweig, Germany, benjamin.gloger@ptb.de
[4] Physikalisch-Technische Bundesanstalt (PTB), Braunschweig, Germany, jan.loewe@ptb.de
[5] Physikalisch-Technische Bundesanstalt (PTB), Braunschweig, Germany, shanna.schoenhals@ptb.de

Abstract:
Calibration certificates are the heart of metrological quality infrastructure and a central element of traceability of measurements. The Digital Calibration Certificate (DCC) is an endeavor to digitalize calibration certificates, developed coordinated by the PTB with the contributions of national and international partners. The DCC is implemented in XML format, and an XSD Schema is developed and maintained by PTB. The DCC schema allows validating the DCCs. Schematron is a schema language which is used to write logical rules for XML files. The PTB's DCC team has prepared a Schematron validation tool with open-source resources.

Keywords: DCC, Schematron, XML Schema, XPATH

1 INTRODUCTION

Calibration certificates are a fundamental part of metrological quality infrastructure. They document the results of calibrations. Unfortunately, they are still paper based or at least not machine-actionable when issued as simple digital documents (such as Word or PDF files). This can lead to many problems, such as missing possibility of reusing the calibration data, media break and associated errors in the transfer process from certificate to customer database, paper waste, etc. Digitalization of calibration certificates is a very important part of the digitalization efforts in metrology because of the obvious benefits like reducing errors and increasing productivity. One of the leading efforts is being undertaken by the Physikalisch-Technische Bundesanstalt (PTB) in Germany and is called the Digital Calibration Certificate (DCC). In this context, generating error-free DCCs plays a crucial role to achieve the maximum benefit and this aspect will be addressed in this paper.

In this paper, we briefly describe the DCC and touch on possible errors that may arise when using the DCC. We then explain how to validate DCCs. We discuss several options to validate DCCs, focussing specifically on schema validation and validation with Schematron. We show what kind of errors can be detected and prevented by schema validation and through Schematron.

2 DIGITAL CALIBRATION CERTIFICATE (DCC)

The PTB coordinates the development of a standard for digital calibration certificates [1]. While there exist efforts to develop PDF/A-3 based DCCs, PTB provides a DCC schema [2] which is based on the Extensible Markup Language (XML) [3]. There is also a comprehensive documentation for the DCC schema [4]. The DCC schema defines the structure for XML files, so it can be used to validate generated DCCs.

3 HOW TO VALIDATE A DCC?

Even though XML files are human readable, it can be overwhelming for the ones who are not familiar with the format. Moreover, to be able to use the full advantages of digitalization, it makes sense to use automated validation methods to make sure that the DCCs are correctly structured and are free from logical errors. The most common method is to use schema validation. Many types of errors can be caught by this method. For example, the information that must be given in the certificate according to the standard, such as an identifier for the certificate, or the name of the calibration laboratory, can be declared as a mandatory field. In this way, if this information is provided in the certificate, this can be noticed by a schema validation.

Even though there are many types of errors that can be detected by schema validation, there are some limitations of this method, because the purpose of a schema is to define the structure of XML files and not to check whether the data is

correct or whether integrity constraints are fulfilled. For instance, one may make it mandatory in the schema to enter begin and end performance dates of the calibration. However, the schema cannot check if the begin performance date is earlier than or the same date as the end performance date. Such a check may be conducted with Schematron. Schematron [5] is a schema language, which is not used for creating schemas, but rather makes assertions for specific contexts.

a. Schema Validation

The DCCs can be validated against the XSD schema provided by PTB. XSD schemas define the structure of the XML files and put constraints. In this section, we focus on what type of errors can be caught with a schema validation.

An XML file is called 'well-formed' if its syntax is correct. XML files have the typical tree structure. That means that every XML file must have one root, which is the starting element. Every element must have a starting and ending tag and can have attributes, a text content, or other elements, which are called child elements. Every element has exactly one parent, except for the root element which has no parents. A well-formed XML file can be validated against a schema.

In XML files, the element names can be freely defined in a schema. That is why schema validation allows to check if the element names are written correctly.

XML allows checking the order of child elements, allows multiple elements with the same name, and enables limiting the number of these elements. XML has built-in data types, such as 'xs:string', 'xs:date', 'xs:datetime', 'xs:boolean'. In addition, regular expressions can be used to enforce more detailed constraints on the elements. Enumeration lists can also be defined to provide the users with a list of elements to choose from. This will help with the error minimization.

Figure 1 shows the results of a schema validation with possible errors that could be caught. Many different XML software offer the schema validation with similar structure. Once errors are detected, they can be corrected subsequently.

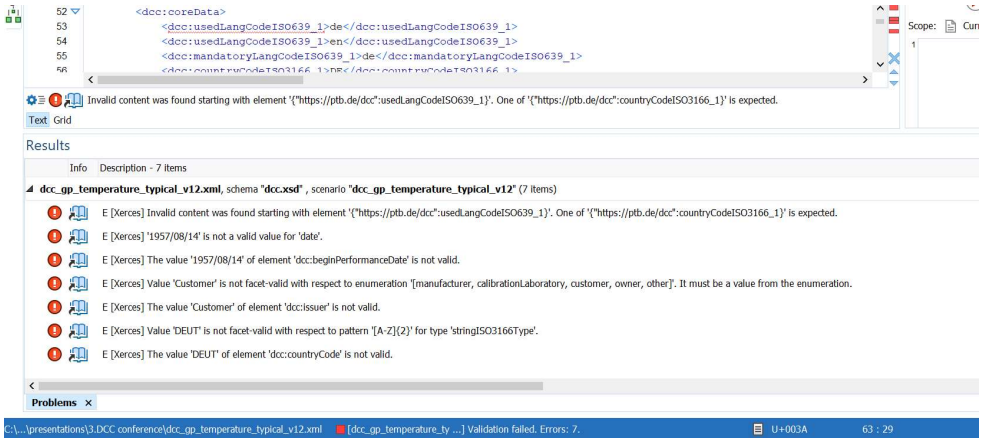

Figure 27: Schema validation results generated with 'Oxygen XML Demonstrator' Software

b. Schematron Validation

Schematron is a very simple, and very powerful language. It uses XPATH (XML Path Language) [6] based tests instead of grammar to validate XML files. In other words, a schematron schema does not generate a grammar for XML files, but rather makes assertions for specific context, in other words for specific elements of an XML file. XPATH makes it possible to conduct detailed analyses of XML files [7]. Schematron is an ISO standard. Schematron can be used among other things for constraint checking, naming and design rules, data exploration, and data reporting.

Schematron rules are written for specific contexts of an XML file. There are 6 main elements in schematron. Schematron files have 'sch' extension. Figure 2 shows the contents of an example schematron file:

```
1…….  <sch:schema xmlns="http://purl.oclc.org/dsdl/schematron">
2……..     <sch:ns uri="https://ptb.de/dcc" prefix="dcc"/>
3……..     <pattern>
4……..        <sch:rule context="dcc:content">
5……..<sch:assert role="warning" test="@lang">
6……..The language attribute is not used for this element.
7……..</sch:assert>
8……..<sch:report role="warning" test="@lang">
9……..The language attribute is used for this element.
10……..</sch:report>
11……..</sch:rule>
12……..</pattern>
13…….</sch:schema>
```

Figure 28: Schematron example

The rule is written for the context ‘dcc:content’. ‘dcc’ is the prefix for the namespace which is used in the DCC schema. ‘dcc:content’ is an element which is used in many different positions in the DCC schema.

The first line is the starting line of the schematron file. The root element of the schematron files is ‘sch:schema’.

The second line is not a mandatory line. It is used if a namespace is used in contexts to define said namespace. In the case of the DCC, this is ‘dcc’ as prefix and ‘https://ptb.de/dcc’ as namespace, which both are defined originally in the DCC schema.

The rules are written in patterns which is shown on the third line. Patterns can contain multiple rules, and schematron files can contain multiple patterns. If one needs different rules for the same context, they need to be written in different patterns, or else these rules will be ignored.

There are two different ways to apply tests: assert and report. ‘sch:assert’ on the line 5 delivers the message if the tests fails. ‘sch:report’ on the line 8 delivers the message if the test succeeds.

The role of the messages can also be defined by the user with the attribute ‘role’. There are 6 different roles to choose from. For the sake of simplicity, we chose ‘warning’, ‘information’, and ‘error’.

Tests are written using ‘test’ attribute to either ‘sch:assert’ or ‘sch:report’. In this example, there are two different tests for the same context. The messages on the lines 6 and 9, that will be delivered depending on the result of the tests, are user-defined. The two tests for this example are the same. They check the existence of the ‘lang’ attribute of the context ‘dcc:content’. In other words, the message on line 6 will be delivered in case of the absence of the attribute, because the test is attached to an assert. The message on line 9 will be delivered in cases where the ‘dcc:content’ element has the attribute ‘lang’. In both cases, the message will be classified as a ‘warning’.

As shown above, the existence of an attribute can be checked with schematron. Schematron offers the possibility to compare the content of different elements. For instance, it is possible to check that the begin performance date is earlier than or at the same date as the end performance date. The following example in Figure 3 shows measured data from an example DCC:

```
<si:realListXMLList>
        <si:valueXMLList>306.245 373.127 448.249 523.321 593.1510000</si:valueXMLList>
        <si:unitXMLList>\kelvin</si:unitXMLList>
        <si:dateTimeXMLList>1957-08-13T08:15:00Z 1957-08-13T09:15:00Z 1957-08-13T10:15:00Z 1957-08-
13T11:15:00Z 1957-08-13T12:15:00Z</si:dateTimeXMLList>
</si:realListXMLList>
```

Figure 29: DCC code example

The ‘si:dateTimeXMLList’ element contains the exact date and time when the measurements were conducted. Hence, there must be the same amount of data in both elements, which is impossible to check with schema validation, but very easy with schematron. It is also possible to compare the number of data given as reference values and measured values, even though they are descendants of different elements.

In DCCs there are some elements which are optional and can be found in different positions in the schema, but a valid certificate must contain this information, such as ambient conditions. The reason for this is that the ambient conditions can be the same for every data point in some certificates, but they also can be different for every data point in a certificate. DCC schema has both options. With schematron, it is possible to check if an ambient condition for every data point in a certificate is declared either globally or locally.

The above examples are general rules that any DCC must conform to. It is also possible to write

DCC specific tests, such as company name or length of data. In the future, PTB will provide an online schematron validation service with the general rules.

Because schematron rules are written for specific XML files, if the schema is changed, the tests might not work for the new XML files. For this reason, it might be necessary to revise existing rules when substantial changes are made to the schema. For instance, the upcoming version 4.0 of the DCC will bring many changes. Version 4.0 will be based on another schema which is called Digital SchemaX [8]. As this version will change the namespace of many elements and probably the structure of some parts of the new schema, all existing schematron rules must be revised or rewritten.

To apply the schematron rules, one can use various commercial tools, such as oXygen, Liquid Software. It is also possible to use free tools or libraries. One possible way is to use Saxon-HE [9] which allows to generate an XSLT file based on the existing schematron file. Then, this XSLT file is applied to the DCC by using a schematron processor [10]. For this, one needs two command line commands:

1. java -jar saxon-he/saxon-he-10.3.jar -s:dcc.sch -xsl:schxslt/core/src/main/resources/xslt/2.0/compile-for-svrl.xsl -o:dcc.xsl
2. java -jar saxon-he/saxon-he-10.3.jar -s:dcc_gp_temperature_simplified_v13.xml -xsl:dcc.xsl -o:result.xml

With this method, one receives an XML file (result.xml in the above example) and must extract the useful information by themselves. It is also possible to create a software. For instance, there is a Python library called 'saxonche', which uses SaxonC with a Java virtual machine. The figure 3 shows the software that is being developed by PTB using open-source resources as a demonstrator:

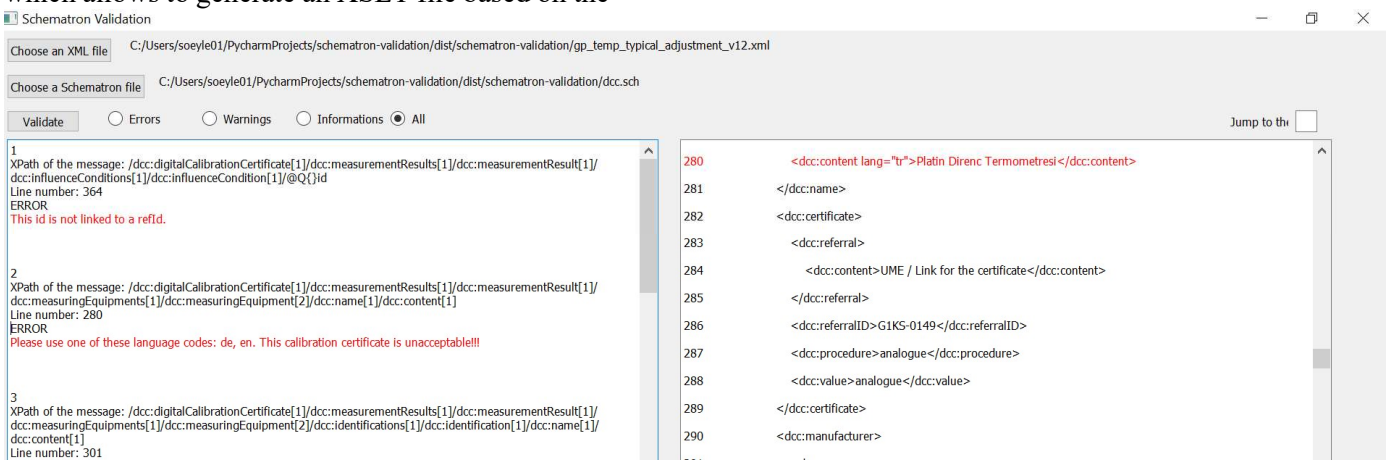

Figure 30: PTB schematron demonstrator

4 SUMMARY

The DCC provides many opportunities. However, it is crucial to generate errors free DCCs. There are different methods to manage that. First and foremost, schema validation must be used. Unfortunately, it is impossible to detect all possible errors. Thankfully, there are additional methods, such as schematron. Schematron is a very easy and elegant way to catch additional errors.

5 ACKNOWLEDGEMENT

The Project GEMIMEG II is carried out with the Grant reference of GEMIMEG 01 MT20001E from BMWK (Federal Ministry for Economic Affairs and Climate Action).

6 REFERENCES

S. Hackel et al., "The fundamental architecture of the DCC", Meas. Sens., vol. 18, p. 100354, Dec. 2021 DOI:10.1016/j.measen.2021.100354.

PTB, "DCC Schema". Online [Accessed 20230618]: https://ptb.de/dcc/v3.2.1/dcc.xsd

Extensible Markup Language (XML) 1.0 (fifth edition). Online [Accessed 20230618]: https://www.w3.org/TR/xml/

PTB, "DCC Documentation". Online [Accessed 20230618]: https://dccwiki.ptb.de/en/home

Schematron. Online [Accessed 20230618]: https://www.xml.com/pub/a/2003/11/12/schematron.html

XPATH. Online [Accessed 20230618]: https://www.w3.org/TR/1999/REC-xpath-19991116/

Schematron. Online [Accessed 20230618]: https://www.data2type.de/xml-xslt-xslfo/schematron/schematron-einfuehrung

G. Söylev Öktem et al. "Digital SchemaX and the Future of the Digital Calibration Certificate". Online [Accessed 20230830]: https://www.m4dconf2022.ptb.de/fileadmin/documents/m4dconf2022/Material/Paper/IMEKOTC6-M4Dconf-2022-P50-SOELEV-OEKTEM-et-al.pdf

Saxon-HE. Online [Accessed 20230618]: https://www.saxonica.com/html/download/java.html

Schematron Processor. Online [Accessed 20230618]: https://github.com/schxslt/schxslt

IMEKO TC8, TC11 and TC24 Joint Conference
October 11-13, 2023, Madeira, Portugal

METROLOGICAL TRACEABILITY OF MOISTURE CONTENT MEASUREMENTS IN PLANT-ORIGIN BULK MATERIALS

O. Melnykov[1], S. Kulyk[2], F. Durbiano[3], F. Rolle[4], M. Sega[5], A. Petrenko[6]/Presenter

[1] SE "Ukrmetrteststandart", Kyiv, Ukraine, amelnykov@ukrcsm.kiev.ua
[2] SE "Ukrmetrteststandart", Kyiv, Ukraine, s_kulyk@ukr.net
[3] INRIM, Torino, Italy, f.durbiano@inrim.it
[4] INRIM, Torino, Italy, f.rolle@inrim.it
[5] INRIM, Torino, Italy, m.sega@inrim.it
[6] SE "Ukrmetrteststandart", Kyiv, Ukraine, pavpostbox@gmail.com

Abstract:
This document explains advantages and disadvantages of the measurement methods for the moisture content determination of plant-based materials in order to identify the best one which can provide metrological traceability to SI units.

The term "moisture" is generic and, to have proper Calibration and Measurement Capabilities (CMCs) and Certified Reference Materials (CRMs), a better specification of the measurand should be given. Currently, no CMCs for moisture content measurement in the plant-origin bulk materials, as well as respective CRMs, are available in the KCDB. Undoubtedly, those CMCs and CRMs are crucially needed to provide metrological traceability in this area.

Keywords: Karl Fischer titration, plant matrix

1 INTRODUCTION

The moisture content is one of the most important characteristics of plant-origin bulk materials, which is necessary to support fair trade in the grain market. To determine moisture content, industrial laboratories mostly use the air-oven reference methods [1 – 5]. In the reference method, a test portion of most cereals is dried at a temperature of about 130 °C for a few hours.

Also, the absolute methods described in ISO standards [4, 5] can be used by specialized laboratories. In the absolute method a test portion is dried under reduced pressure and kept at about 50 °C for up to one month, until the constant mass is reached.

The main disadvantage of reference methods is that the completeness and specificity of moisture removal are not guaranteed [6, 7]. Absolute methods are difficult to perform and require considerable time.

Other techniques, such as the Karl Fischer titration, provide high selectivity to water determination. In this case, water molecules are usually extracted by the dried methanol [8] and it is assumed that extraction is full.

2 PURPOSE

In this paper we review methods for the moisture content measurement in plant-origin materials determination. The main aim of this work is to select a way for creating the plant matrix CRMs that would provide traceability to SI to support CMC claims.

3 MATERIALS AND METHODS

Methods described below are applied for wheat, rice (paddy, husked and milled), barley, millet, rye, oats, triticale, sorghum in the form of grains, milled grains, semolina or flour, maize, pulses, and other plant matrix objects.

a. Karl Fisher method

The Karl Fischer (KF) method is a widely used technique for the accurate determination of water content in various plant-origin materials.

The KF method is based on the chemical reaction between iodine and water in the presence of sulphur dioxide and a base. The reaction runs in a specialized titration measuring instrument. The KF reaction can be formulated as follows [9]:

$I_2 + SO_2 + 2H_2O \rightarrow 2HI + H_2SO_4$

For determining the water content, two different kinds of KF method are used: volumetric KF titration, where the injection of an iodine solution is carried out using an automatic burette (suitable for samples with high water content: 100 mg/kg - 100%); coulometric analysis according to KF, where iodine is formed in the cell as a result of electrochemical oxidation (suitable for samples in which water is present in trace or low amounts: 1 mg/kg - 5%). In modern realization of both kinds of KF methods is possible to use special supplementary equipment, such us ovens,

autosamplers, mills, temperature-controlled cells, automated filling/emptying of cells, magnetic stirrers, etc. All such supplementary equipment make the KF method more precise and reproducible, faster, ready-to-use, economically effective and environmentally friendly.

Figure 1: Karl Fischer volumetric titrator

b. Oven absolute method

A test portion of the laboratory sample is dried under reduced pressure, at a temperature in the range (45 – 50) °C, in the presence of a desiccant, until constant mass is reached.

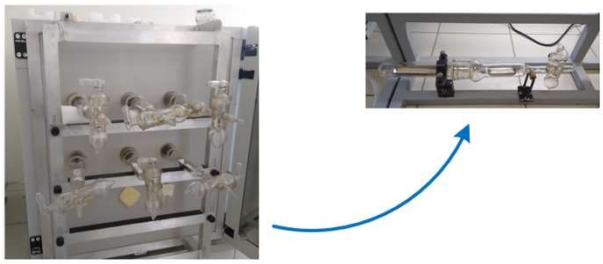

Figure 2: Oven absolute method equipment

c. Oven reference method

A test portion of the laboratory sample (previously ground and/or conditioned, if needed) is dried (100 - 135 °C) under conditions which provide a result maximally corresponding to one obtained by the absolute oven method.

4 DISCUSSION

The main disadvantage of the reference methods, described in ISO standards [4,5], is the absence of knowledge on the chemical nature of evaporated substances, that may be both water and some other volatile compounds.

In contrast to reference methods, described in ISO standards, KF method provides measurement of water content only. Using the KF titration method for moisture content measurements in plant matrix CRM would provide traceability to SI to support CMC claims.

The oven absolute method has high precision and acceptable specificity (only traces of volatile organic substances could evaporate from test portion).

Advantages and disadvantages of these methods are presented below.

Table 1: Advantages and disadvantages of reference oven method [4,5]

Advantages	**Disadvantages**
Easy to apply	Low water selectivity
Small period of time per measurement	High electricity consumption
Commercially available equipment	Low accuracy

Table 2: Advantages and disadvantages of Karl Fisher method

Advantages	**Disadvantages**
Absolute method; provide traceability to SI	Poison reagents
High water selectivity	More expensive
Small period of time per measurement	Needs skilled staff
Commercially available equipment	Medium precision
Small electricity consumption	

Table 3: Advantages and disadvantages of absolute oven method [4,5]

Advantages	**Disadvantages**
Acceptable water selectivity (expected)	Highest period of time per measurement
High precision (U (0.95; k=2; n=10) ≈ 0.03 %)	Needs skilled staff
Commercially available equipment	High electricity consumption

The comparison of the oven reference methods with KF method and the corresponding "adjustment" of working methods is a common practice [3, 11, 12]. For example, the ASAE S352.2 standard [3] includes only those oven methods for which the documented comparison with the KF titration was carried out; such studies were made for a several dozens of plant matrix measurands. Also, the absolute oven method "is intended to serve as a standard for checking and perfecting other methods for the determination of moisture content" [4].

Applying KF and absolute oven methods to the same sample and comparing the obtained results seems ~~a~~ very promising. There are many reasons to consider both methods as selective; their results are expected to be comparable. On the other hand, the questions concerning the correctness of these methods and the ways of their implementation will arise. Particularly, the comparison of both methods will allow to answer the question regarding the water selectivity of the absolute oven method. Additionally, such study will provide an estimation

of the sufficiency of water extraction in the KF method.

If the correspondence of both methods results is found to be sufficient, it will allow to produce corresponding CRMs by assigning the relevant property value by means of KF method and absolute oven one as well. In this case the traceability to SI could be provided.

In previous works the precision of KF method was not very high [10]. Nevertheless, the usage of only KF titration for such CRMs characterization seems promising by means of new KF equipment, developed in recent years; such equipment provides higher precision of the method.

5 SUMMARY

Plant matrix CRMs for measurement laboratories using KF titration method for moisture content measurements in plant-origin bulk materials are needed. With those CRMs it will be possible to establish metrological traceability and to support a fair trade in the grain market. Comparing the results of KF and absolute oven methods seems a very important and useful starting point.

6 REFERENCES

[1] G. D. Lee, "Grain Moisture Air-Oven Reference Methods in the United States", NIST Weights & Measures Connections, v. 3, issue 6, November 19, 2012.

[2] Association of Official Analytical Chemists, "Official Methods of Analysis", 13th Ed; AOAC: Washington, DC, 1980.

[3] ASAE S352.2 "Moisture Measurement – Unground Crain and Seeds", 1997.

[4] ISO 712:2009 "Cereals and cereal products – Determination of moisture content – Reference method".

[5] ISO 6540:2021 "Maize – Determination of moisture content (on milled grains and on whole grains)".

[6] J.R. Hart, L. Feinstein, C. Golumbic, "Oven methods for precise measurement of moisture content of seeds", USDA/Agricultural Marketing Service, (Marketing Research Report, 304) Washington, p. 16, 1959.

[7] P. J. Bowden, "Comparison of three routine oven methods for grain moisture content determination", Journal of Stored Products Research, vol. 20(2), p. 97-106, 1984.

[8] J.R. Hart, M.H. Neustadt, "Application of the Karl Fisher method to grain moisture determination", Cereal Chemistry, vol. 34, p. 26-37, 1957.

[9] P. Bruttel, R. Schlink, "Water Determination by Karl Fischer Titration", Metrohm Monograph, p. 4.

[10] N.J. Thiex, T. Van Erem, "Determination of water (moisture) and dry matter in animal feed, grain, and forage (plant tissue) by Karl Fischer titration: collaborative study", Journal of AOAC International, vol. 85, no. 2, p. 318–327, 2002.

[11] E. Benjamin, D. F. Grabe, "Development of oven and Karl Fischer techniques for moisture testing of grass seeds", Journal of Seed Technology, vol. 12, p. 76–89, 1988.

[12] C.D. Bormuth, "Precision and unbiasedness of an oven method and Karl-Fischer-Titration to determine the seed moisture content", Int. Agrophys., vol. 8(2), p. 191–195, 1994.

#27

IMEKO TC8, TC11 and TC24 Joint Conference
October 11-13, 2023, Madeira, Portugal

TRACEABLE IN-HOUSE PREPARATION OF RM CO_2/N_2 GAS MIXTURE USING GRAVIMETRIC STANDARDIZED METHOD

Najji H. AlYami[1], Abdullah S. AlOwaysi[1] and Khaled M. Ahmed[1,2,]*

[1] National Measurement and Calibration Center, Saudi Standards, Metrology and Quality Org. (SASO-NMCC), PO Box 3437 Riyadh 11471, Saudi Arabia,
[2]National Institute for Standards (NIS), PO Box 136 Giza, Code No 12211, Egypt,
Email: k.abdelftah@saso.gov.sa / khaled55eg@gmail.com

Abstract:

The necessity for national and international programs to monitor the levels of carbon dioxide emissions in the atmosphere has arisen as a result of the recent large greenhouse gas emissions that cause a rise in the Earth's temperature and climate changes with severe impacts. In order to give confidence in the monitoring results and enable the proper decisions to be made regarding the supply of environmental treatment and air quality through the limiting and monitoring of emission, it is required to maintain the traceability of the measurement data to SI units. Gas measurements laboratory at SASO-NMCC uses the gravimetric method to prepare reference gas mixtures of CO_2 in N_2 as primary standard mixtures (PSMs) cylinders based on universal gas law. The produced PSMs used as working standards to transfer the traceability from CRMs to customers' artefacts. The used method fully complies with ISO 6142. Description of the steps of the production process and its method verification as well as equipment used and associated uncertainty are presented in this work. In accordance with the requirements of ISO 6143, a validated gas chromatography thermal conductivity detector (GC-TCD) method was selected to verify the mole fraction of the gravimetrically prepared gas mixtures. Reproducibility of the produced concentrations is demonstrated through mid-term and long-term evaluations. Eight certified reference materials (CRMs) of different concentrations were used for the GC calibration to provide metrological traceability of the measurement results to SI units. Associated uncertainty budget, with brief description of different components and error sources, is presented.

Keywords: Reference Materials (RMs), Primary Standard Mixtures (PSMs), CRMs, CO_2, GC-TCD, ISO 6142 & 6143.

1. Introduction

According to the Global Monitoring Laboratory's annual report, the average amount of carbon dioxide in the atmosphere around the world reached a new high record in 2022 of 417.06 ppm. The increase in atmospheric carbon dioxide between 2021 and 2022 was 2.13 ppm, marking the 11th year in a row where the increase was greater than 2 ppm. The annual average carbon dioxide in 2022 at Mauna Loa Observatory in Hawaii, where the carbon dioxide record began in 1958, was 418.56 ppm [1-2].

The primary cause of the rise in carbon dioxide concentrations is the use of fossil fuels by humans as a source of energy. We are adding carbon to the atmosphere in only a few hundred years that plants removed from the atmosphere through photosynthesis over many millions of years in the form of fossil fuels like coal and oil. According to the Global Carbon Budget 2022, annual emissions from burning fossil fuels have climbed steadily since the middle of the 20th century, from roughly 11 billion tons in the 1960s to a projected 36.6 billion tons in 2022 [2].

Applications for atmospheric monitoring demand a high level of uniformity in CO_2 calibration standards. Currently, the standard uncertainties of primary gas standards, produced using a gravimetric preparation process offering traceability to the SI, are too high to be employed in measurements where minute temporal and spatial variations are significant. Due to an anticipated increase in demand based on the proliferation of atmospheric greenhouse gas (GHG) measurements globally, an international task group has been established under the Metre Convention, led by NIST, to develop a system to more efficiently disseminate accurate and consistent GHG standards [3].

In order to establish a NIST CO_2 Scale, the Gas Sensing Metrology Group is creating a new set of CO_2/Air Primary Standard Mixtures (PSMs) with

nominal concentrations ranging from 374 µmol/mol to 999 µmol/mol. The NIST CO_2 Scale will include a group of eight working standards with nominal CO_2 concentrations ranging from 385 µmol/mol to 895 µmol/mol. Additionally, CH_4, N_2O, Ar, and O_2 values will be assigned. Using the CIPM MRA process, this scale will be compared internationally, and a relationship to a standard scale, such as the WMO-Scale, will be developed for the interpretation of integrated datasets.

Seawater CO_2 measurements are crucial to attempts to monitor ocean carbon because human activities are affecting the chemistry of the ocean's carbon content. The demand for these reference resources is projected to rise as more nations step up their ocean monitoring efforts and novel technologies, including ocean carbon dioxide removal, are developed. In order to ensure SI traceability, the Gas Sensing Metrology Group is collaborating with the Inorganic Chemical Metrology Group to create the capacity to offer services for the analysis of total dissolved inorganic carbon utilizing CO_2/Air primary standard mixtures (PSMs) [3].

In this work, we show a preparation scheme of reference gas mixtures of CO_2 in N_2 as CRM cylinders using the gravimetric method in accordance with the universal gas law. The procedure being employed complies with ISO 6142 [4]. In this work, the equipment employed and the associated uncertainty, together with a description of the production process's steps and method verification, are described. To confirm the mole fraction of the gravimetrically generated gas mixtures, a validated gas chromatography thermal conductivity detector (GC-TCD) method was chosen in compliance with ISO 6143 standard [5-7, 8-13].

2. Equipment and method

A. Materials

Gas mixtures reference materials are produced from pure gases whose molecules are spread between inert nitrogen gas molecules or pure air molecules as a medium that helps stabilize the concentration of the prepared gas. It is preferable to produce the CRMs in two stages, the first includes the production of a mixture of high concentration that should have metrological traceability, then from this mixture diluted lower concentrations with traceability acquired. This scheme of production is simplified in Figure 1 a and b.

The gravimetric dilution of primary gas mixtures uses the certified reference gas mixtures (CRMs), the pure CO_2 (99.8%) and N_2 (99.9999%) gases, provided by LINDE-SIGAS, Germany as the parent gas. 5L Aluminum cylinders in which the gas mixtures were filled-in were supplied by Air Liquide, the Netherlands.

B. EQUIPMENT

Equipment comprises the evacuation system, filling system, weighing system, balance, homogenizer system, and Gas Chromatography system (GC-TCD) for verification analysis. List of the used equipment is shown in table 1.

C. SCHEME

Preparation method of the primary gas mixtures was done according to “ISO 6142-1: Gas analysis – preparation of calibration gas mixtures” [4]. Steps of the method, as per the standard, can be summarized as follows: 1- Calculate masses and uncertainties, 2- preparation composition including filling sequence, 3- perform purity analysis, 4- prepare mixture and determine masses, 5- determine molar masses, calculate mixture composition and uncertainty, 6- homogenize mixture, 7- perform verification, and 8- if verification result is positive, then report the results of concentrations and associated uncertainties (certificate).

Table 1: List of the used equipment

Name	Manufacturer	Model
VACUUM PUMP SYSTEM	PFEIFFER	HICUBE 300 CLASSIC
WEIGHING SYSTEM	METTLER TOLEDO + IDEAL MAKINE (TUBITAKUME)	XPE10003SC + RTK-10
BALANCE	METTLER TOLEDO	MS16001L01
ROLLING BENCH	HKTM (TUBITAKUME)	AGM6 80 A
GAS CHROMATOGRAPHY (GC)	AGILENT	7890B

Carbon dioxide gas with a concentration of (0.02900 ± 0.000001) mol/mol and nitrogen in balance is produced. The method used for the preparation process, as shown in Figure 1, is broken down into a number of steps, beginning with completely emptying the cylinder. To do this, the cylinder is connected to a vacuum device for a period of 12 hours, during which time all impurities were removed. When the cylinder is completely empty, the pressure indicator changes

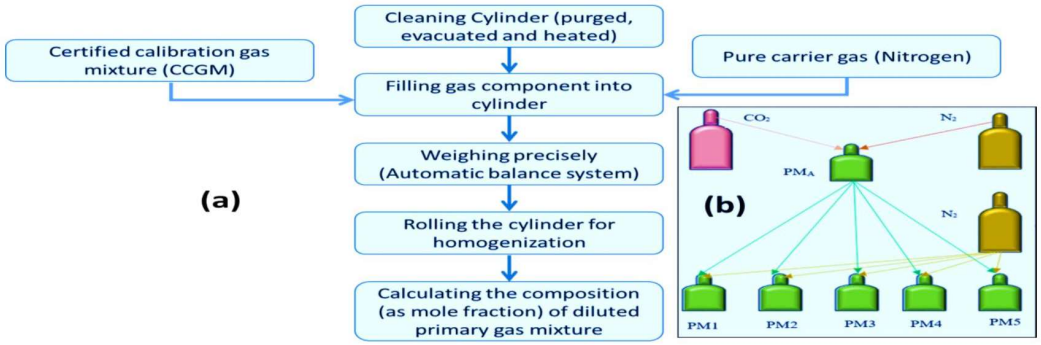

Figure 1: Scheme for the gravimetric dilution of the primary gas mixture: (a) detailed steps (flow-chart), (b) for visualization

to 1×10^{-7}, signifying that the preparation process is complete.

The Evacuation System (PFEIFFER, model: HiCUBE) is used to evacuate the sample cylinder and to purge used and new cylinder (see Figure 2). The Evacuation System is built up with a pumping station with maximum four cylinder-connections by changing the existing valve locations; See Figure 2.

Following discharge, the procedure of calculating the quantity based on the prepared target concentration using the weighing equipment commences. By contrasting the sample cylinder with the reference cylinder, the device is intended to automatically weigh the gas cylinder (Figure 3).

The ideal gas law PV=nRTz is the foundation of the system. The maximum weight and volume permitted for a cylinder are also shown in Figure 3, where the permitted weight varies from (1 mg to 10 100 g) and the size of its cylinder is (5 L).

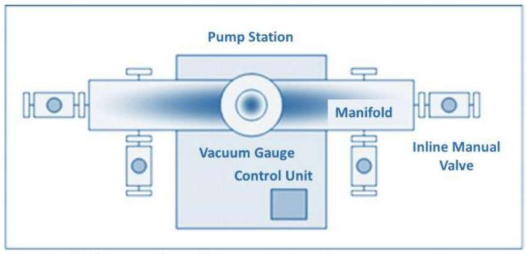

Figure 2: Schematic of the evacuation system.

Figure 3: Photograph of the weighing system.

Then, we start the filling process using a filling system after finishing the weighing procedure based on the ideal gas law, which gives us the necessary weight to achieve the desired concentrations. The primary gas mixtures are obtained by filling amounts of pure gas or gas mixtures using the gas filling mechanism. According to ISO Standard 6142-2001(E), "Gas

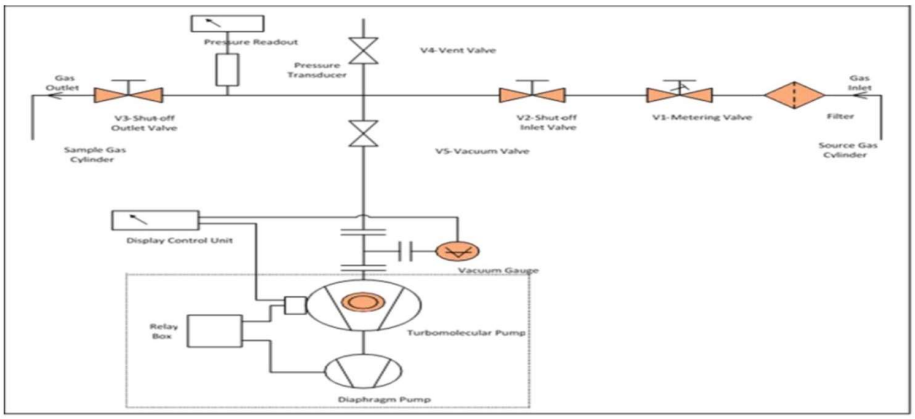

Figure 4: Schematic of gas filling system.

analysis - Preparation of calibration gas mixtures - Gravimetric method," the system is able to fill the 5L-cylinders. All gas flow lines are made of stainless steel that has been electro-polished and can resist 200 bar of pressure. All lines from pure gases down to sample cylinders can be evacuated by the system to a vacuum of approximately 1×10^{-6} mbar. Figure (4) shows the filling system schematic diagram.

Following the determination of the quantity and filling as well as the gas concentrations, the mixing stage is next to increase the homogeneity between the gases, which is a requirement of the reference material when utilizing a mixing device. Figure 5 depicts the cylinder homogenization system, which consists of three rollers on which the cylinder is put and a control panel that regulates the rollers' rotational speeds and directions. The motor turns the roller in the system's center, and the rollers on the system's edge sides move independently of one another. The technology allows for the simultaneous mixing of one or two cylinders. The center roller's rotational direction, duration, and speed can be changed via the control panel.

Figure 5: Photograph of the homogenizer.

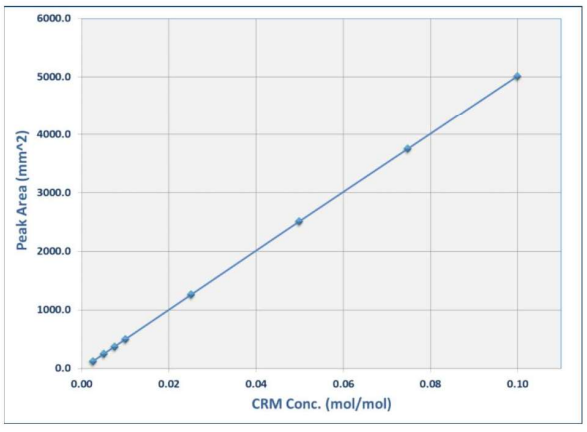

Figure 6: Calibration Curve: The relationship between the response of the device (GC) and the values of the reference materials concentrations.

3. VERIFICATION OF GAS MIXTURE COMPOSITION USING GC-TCD

The primary gas mixtures of CO_2 in N_2 propagated gravimetrically according to ISO 6142 have been verified by GC–TCD in accordance with ISO 6143. For producing and certification of eight primary mixtures, we use CRMs for verification process with concentration range (0.0100 – 0.100000) (mol/mol). So that the concentration of the unknown sample was in the middle of that range each calibration concentration was injected 10 times and the unknown was injected 10 times the average was calculated and the calibration curve was obtained by plotting the concentration (x) against the peak area (y) (see table 2). The concluded calibration curve is shown in Figure 6.

4. UNCERTAINTY ANALYSIS

The uncertainty estimation of the measurement of CO_2 concentration was carried out using the bottom-up approach based on EURACHEM/CITAC Guide CG4 [14].

The potential sources of uncertainty and how they might affect the value of the measurand are identified and preliminary analyzed; full analysis with fish bone diagram and full uncertainty budget is beyond the scope of this paper and it is part of future work for another publication. It is clear that the mass of CO_2 in the N_2 balance in the CRM, the mass of the N_2 balance gas contributed, the molecular weight of the gas components, and the uncertainty from the CRM itself are the main uncertainty sources for the preparation of PSMs by gravimetric dilution.

In addition, there are many factors affecting the GC analysis, which can be summarized in many categories as follows [15]:

A. Result of analysis: carrier gas flow rate, column temperature, sample size, and split ratio.
B. Peak area: carrier gas flow rate, baseline drift, noise, and peak resolution, among others.
C. Peak height: column temperature, detector temperature, integrator settings, and repeatability of sample injection, among others.
D. Split injection: injector liner, injector temperature, split ratio, among others.
E. TCD: detector temperature, wire temperature, carrier gas flow rate.

-The combined standard uncertainty, u_c

Taking into account the previously mentioned factors (errors), which can be categorized into type

A and Type B uncertainty, as per [16]. Since the standard uncertainties are of different units, the combined standard uncertainty, u_c is calculated as ratios and the resulting ratio is multiplied by the sample gas concentration, C_0, as shown in equation 1, to assign a unit to the calculated uncertainty.

$$u_c = C_0 \sqrt{(\frac{u_{CRM}}{C_{CRM}})^2 + (\frac{u_{PACRM}}{PA_{CRM}})^2 + (\frac{u_{PAsample}}{PA_{sample}})^2} \quad (1)$$

The expanded uncertainty at 95% confidence level (k=2) of eight PSMs was calculated in the range of 0.01 to 0.10 relative to the mole fraction of final gas mixtures from the estimation of uncertainty for the gravimetric dilution of calibration gas mixtures (CO_2 in N_2 Balance). The preliminary uncertainty budget is shown in table 3. The detailed estimation of different uncertainty components with error analysis and treatment is a topic of another on-going work.

Table 2: Verification of gas mixture composition using GC

Code	Concentration	Uncertainties associated with x-values	y-values	Uncertainties associated with y-values
CRM	0.010000	0.000004	504.000000	0.206000
CRM	0.010000	0.000002	504.000000	0.419000
CRM	0.020000	0.000002	1010.000000	1.020000
CRM	0.025000	0.000002	1260.000000	0.362000
PSM	**0.029000**	**0.000001**	**1470.615700**	**0.251250**
CRM	0.050000	0.000008	2520.000000	1.290000
CRM	0.050000	0.001104	2520.000000	1.490000
CRM	0.075000	0.000069	3780.000000	1.200000
CRM	0.100000	0.001698	5050.000000	1.660000

Table 3: Uncertainty budget (preliminary)

Cylinder	Source	X	u(X)	Unit	u(X)/X
PSM266406	**CRM**	0.010000	0.000004	mol/mol	0.000040
		0.010000	0.000002		0.000020
		0.020000	0.000002		0.000010
		0.025000	0.000002		0.000008
		0.050000	0.000008		0.000016
		0.050000	0.001104		0.002208
		0.075000	0.000069		0.000092
		0.100000	0.001698		0.001698
		u_c(CRM)			**0.00287**
		y	u(y)		u(y)/y
	Peak Area (R)	504.000000	0.206000	mm^2	0.000409
		504.000000	0.419000		0.000831
		1010.000000	1.020000		0.001010
		1260.000000	0.362000		0.000287
		2520.000000	1.290000		0.000512
		2520.000000	1.490000		0.000591
		3780.000000	1.200000		0.000317
		5050.000000	1.660000		0.000329
		u_c(PA (R))			**0.00166767**
	Peak Area (S)	1470.6157	0.2513	mm^2	**0.000170881**
C_0 (mol/mol)		**2.90E-02**			
u_c		**3.25E-03**			
C_0 x u_c		**9.43E-05**		**mol/mol**	
U_{Exp}		**1.89E-04**		**mol/mol**	
U_{Exp} %		**0.65**		**%**	

4. RESULTS AND DISCUSSION

In this work, we prepared eight PSMs with different concentrations, using the CRM (certified gas mixture) using the scheme described in section 2. The concentration range of the prepared PSMs is 0.010000 to 0.100000 mol/mol. The verification process using GC-TCD had been done as shown in table 2. The summary of the prepared concentrations and the associated uncertainties are

shown in table 4. The produced reference PGMs are used for the calibration of the customers' artefacts with maintaining the traceability of the relevant calibration activities.

Table 4. Summary of the prepared PSMs concentrations and associated uncertainties

PSM Code	Concentration mol/mol	Expanded uncertainty (%)
PSM-1	0.010000	0.000014
PSM-2	0.022000	0.000013
PSM-3	0.025000	0.000023
PSM-4	0.029000	0.000001
PSM-5	0.050100	0.000019
PSM-6	0.049000	0.001109
PSM-7	0.074900	0.000073
PSM-8	0.100000	0.001798

5. CONCLUSION AND ON-GOING WORK

Preparation scheme of primary standard mixtures of CO_2 in N_2 is presented. The prepared eight PSMs with different concentrations are used as working standards in the lab to transfer the traceability from the parent CRMs to the customers DUTs. The detailed description of the used processes; cleaning and evacuating the cylinders, automatic weighing, gas filling, mixing and homogenization processes as well as the used equipment are shown. Different sources of uncertainty, such as weighing, gas cylinder, component gas, certified calibration gas mixture, purity of N_2 balance, and molar mass of gas component, affected the uncertainty of the fraction mole of final gas mixtures, are studied, and preliminary uncertainty budget has been shown in this work. The full uncertainty analysis is beyond the scope of this paper, and under on-going preparation for another subsequent publication.

Acknowledgment

Authors thank SASO Research and Studies Center (RSC) for considering this work.

REFERENCES

[1] National Oceanic and Atmospheric Administration (NOAA), Global Monitoring Laboratory Report 2022 (https://gml.noaa.gov)

[2] Global Carbon Budget (Project), GCP 2022 Report (https://www.globalcarbonproject.org/carbonbudget/22/files/GCP_CarbonBudget_2022.pdf)

[3] NIST – Greenhouse Gas Measurements (https://www.nist.gov/greenhouse-gas measurements)

[4] ISO 6142-1:2015, "Gas analysis – preparation of calibration gas mixtures – Part 1: Gravimetric method for Class I mixtures."

[5] ISO 6143:2001, "Gas analysis – Comparison methods for determining and checking the composition of calibration gas mixtures."

[6] ISO 16664:2017, "Handling of calibration gases and gas mixtures – Guidelines."

[7] ISO/TS 29041:2008, "Gas mixtures – Gravimetric preparation – Mastering correlations in composition."

[8] A. Dubey (2013), "Studies on the air pollution around cement and lime factories", J. Environ. Earth Sci. 3, 191-194.

[9] H. Budiman and O. Zuas (2015), "Validation of analytical method for the determination of high level carbon dioxide (CO_2) in nitrogen gas (N_2) matrix using gas chromatography thermal conductivity detector", Period. Tche Quim.12,7-16.

[10] O. Zuas, H. Budiman and M. R. Mulyana (2015), "Temperature effect on thermal conductivity detector in gases (carbon dioxide, propane and carbon monoxide) analysis: a gas chromatography experimental study," Journal of Basic and Applied Research International 13(4):232-238

[11] M. Rozhnov and O. Levbarg (2007). "A way of establishing quality of measurements in gas analysis national and international aspects," Accred. Qual. Assur. 12(8), 415-417.

[12] M. J. T. Milton, G. M. Vargha and A. S. Brown (2011), Gravimetric methods for the preparation of standard gas mixtures, Metrologia 48(5), R1–R9.

[13] R. C. Geib (2005), "Calibration Standard Gases Are Key to Reliable Measurements", specialty gas report, Matheson Tri-Gas Inc.

[14] EURACHEM/CITAC Guide CG4 (2012), "Quantifying uncertainty in analytical measurement", 3rd edition.

[15] Vicki J. Barwick, "Sources of uncertainty in gas chromatography and high-performance liquid chromatography", Journal of Chromatography A, 849 (1999) 13–33.

[16] JCGM 100:2008, "Guide to the expression of uncertainty in measurement (GUM)".

#30

IMPLEMENTATION AND VALIDATION OF CALIBRATION METHODS IN THE AREA OF HIGH FREQUENCIES

M. Cundeva-Blajer[1]/Presenter, Gj. Dimitrovski[1], K. Demerdziev[1]

[1] Ss. Cyril and Methodius University in Skopje, Faculty of Electrical Engineering and Information Technologies - Skopje, Republic of North Macedonia, mcundeva@feit.ukim.edu.mk

Abstract:

The paper presents a methodology for calibration of high-frequency instruments, such as oscilloscopes, counters and function generators operating above 1 MHz up to GHz level. The methods were developed at the Laboratory for Electrical Measurements at Ss. Cyril and Methodius University in Skopje, following the Calibration Guide EURAMET cg-7. The paper also discusses the challenges of setting up measurement traceability chain and uncertainty evaluation. These methods are important for the region of Southeast Europe, where the metrology facilities for calibration/testing of high frequency electronic devices are not sufficiently developed to meet the needs of the fast-growing automotive supply chain sector.

Keywords: high frequencies calibration, EURAMET cg-7, oscilloscope, electronic components testing

1. INTRODUCTION

The expansion of production facilities in the automotive supply chain in recent years in the region of Southeast Europe has increased the need for the development of testing and calibration facilities for advanced electronic components. However, the conformity assessment bodies in the field of electronic devices are insufficient in the region of Southeast Europe, [1]. This implies the necessity of upgrading the capacities of testing and calibration infrastructure in the area of testing electronic components. One of the most demanding fields is the calibration of high frequency testing devices, such as oscilloscopes, counters and function generators. In this paper, novel calibration methods for instruments for high frequencies over 1 MHz up to GHz level, in compliance with the Calibration Guide EURAMET cg-7 Version 1.0 (06/2011), [2], developed at the Laboratory for Electrical Measurements (LEM) at Ss. Cyril and Methodius University in Skopje (UKIM), will be presented. The establishment of an unbroken measurement traceability chain at high frequencies is an international metrological challenge, [3]. The evaluation of uncertainty due to significant and with unknown properties contributing influential factors, represents a computationally intensive modeling task. As a result of the lack of appropriate metrological facilities, the validation of the developed calibration methods poses further implementation obstacles. In this contribution, the methodology for overcoming these issues and the obtained metrology outputs in the Laboratory of Electrical Measurements at Ss. Cyril and Methodius University in Skopje, are elaborated and discussed.

2. NEEDS ANALYSIS IN THE FIELD OF HIGH FREQUENCY METROLOGY

The field of high frequencies has less developed calibration infrastructure in comparison to other electrical quantities, [5], [8-13]. Furthermore, most of the National Metrology Institutes and accredited calibration laboratories in their published calibration & measurement capabilities (CMCs) demonstrate restricted scopes in the field of high frequencies (mostly up to 1 MHz), [6].

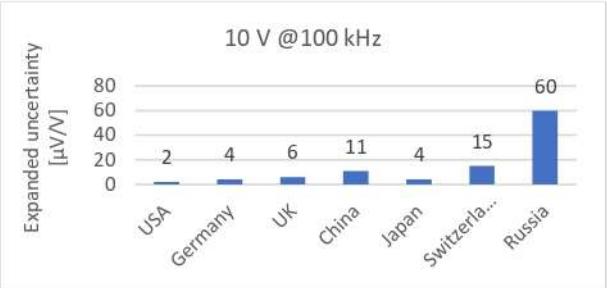

Figure 1. Expanded measurement uncertainties of 10 V voltage @100 kHz at the international NMIs

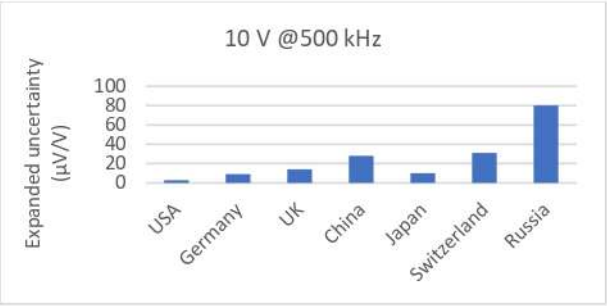

Figure 2. Expanded measurement uncertainties of 10 V voltage @500 kHz at the international NMIs

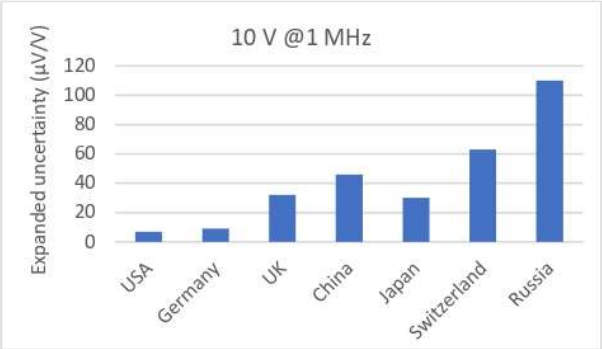

Figure 3. Expanded measurement uncertainties of 10 V voltage @1 MHz at the international NMIs

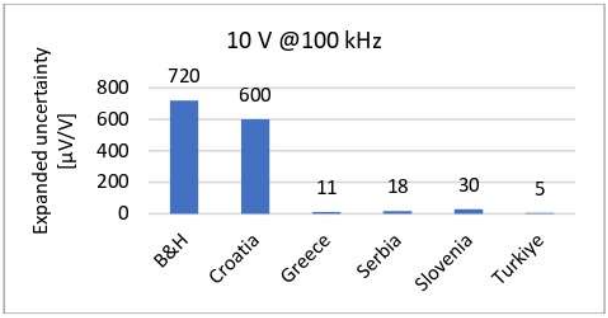

Figure 4. Expanded measurement uncertainties of 10 V voltage @100 kHz at labs in Southeast Europe

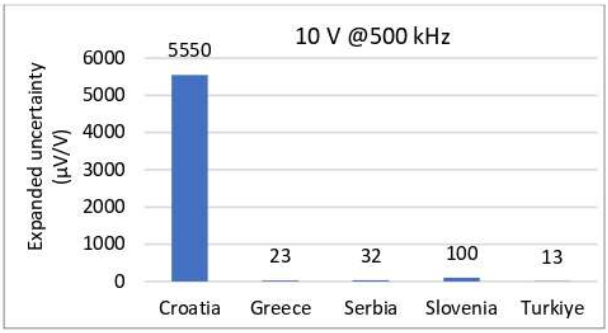

Figure 5. Expanded measurement uncertainties of 10 V voltage @500 kHz at labs in Southeast Europe

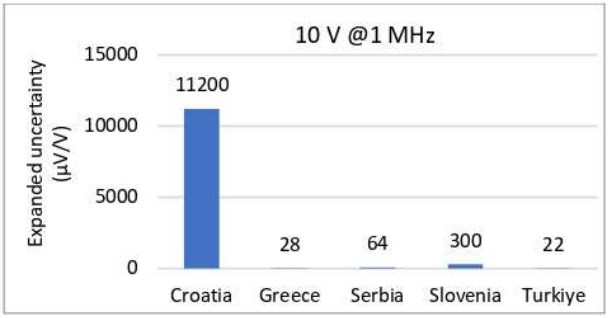

Figure 6. Expanded measurement uncertainties of 10 V voltage @1 MHz at labs in Southeast Europe

The current state-of-the-art in the field of high frequency metrology is presented bellow through the comparison of the best CMCs at international and at regional level of Southeast Europe, where the LEM laboratory is located. In Figures 1-3, a comparison of the best CMCs at international level and in Figure 4-6 at regional level of Southeast Europe for frequencies of 100 kHz, 500 kHz and 1 MHz, are presented, based on the available data in the KCDB database of BIPM, [6]. High frequencies above 1 MHz introduce challenges in the process of calibration and the number of National Metrology Institutes (NMIs) and accredited calibration laboratories which perform these calibrations is restricted, [6], [8-13].

Figure 7. LEM reference standard multifunctional calibrator Transmille 4015 with oscilloscope calibration option SPC600

LEM has been an accredited calibration laboratory for electrical quantities instruments according to ISO 17025:2017 since 2015, [4]. Its personnel is developing a new calibration method for calibration of high frequency instruments (oscilloscopes, counters and function generators), [3] in compliance to the Calibration Guide EURAMET cg-7 Version 1.0 (06/2011), [2].

Table 1. Technical specification of the reference standard for electrical inductance of LEM

Multifunctional Calibrator Transmille 4015	
Supplement to the multifunctional calibrator for calibration of oscilloscopes with frequency range up to 600 MHz Transmille SPC600	
Range	Resolution
2 mV/Div to 10 mV/Div	10 nV
20 mV/Div to 100 mV/Div	100 nV
200 mV/Div to 2 V/Div	1 µV
5 V/Div to 20 V/Div	10 µV
50 V/Div	100 µV
Range:	Best annual accuracy:
DC Voltage 2mV to 50V/Div	0.01 %
AC Voltage 2mV to 50V/Div	0.1 %
Time Base 2ns/Div. to 5s/Div.	5 ppm
Frequency (reference frequency 50 kHz)	30 ppm
Rise time/fall	1 ns
Wave forms	Combined at least up to 100 ns

LEM has recently acquired a reference standard for calibration of oscilloscopes, the Transmille 4015 Multifunctional Calibrator with the option SPC600 for calibration of high frequency instruments i.e., oscilloscopes and counters with frequency range up

to 630 MHz illustrated in Figure 7, with technical specification as presented in [7] and in Table 1. It is calibrated in the oscilloscope measurement range at the producer's accredited calibration laboratory with established measurement traceability to national (NPL) and international primary reference standards (BIPM), with an accompanying calibration certificate. The SPC600 option is a built-in black box option of the Transmille 4015 Multifunctional Calibrator and there is no publicly available information on the physical system of the realisation of the reference standard [7].

3. CALIBRATION PROCEDURE FOR HIGH FREQUENCY INSTRUMENTS DEVELOPED IN LEM

The national metrology institutes and the calibration laboratories in the field of electrical quantities develop diverse calibration methods for high frequency instruments i.e. oscilloscopes, counters or function generators, [8-13]. According to the Calibration Guide EURAMET cg-7 Version 1.0 (06/2011), [2] the calibration procedure of oscilloscopes obligatory includes two main stages:

- calibration of the vertical deflection (measurement of the voltage amplitude along the vertical axis),
- frequency bandwidth calibration (frequency measurement along the horizontal axis).

The two stages are independent of each other, but both are necessary to perform a complete oscilloscope calibration procedure. Each set value, generated by the reference standard, is measured repeatedly 12 times according to [2].

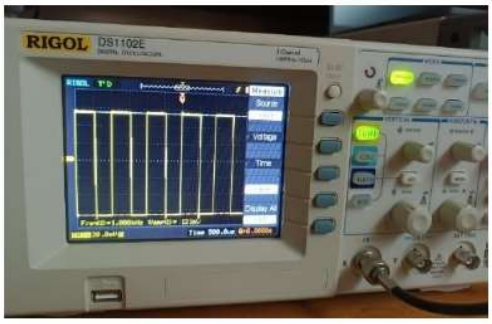

Figure 8. UUT 100 MHz RIGOL DS1102E Oscilloscope calibrated with the Transmille 4015 Multifunctional Calibrator

In this case study, the Laboratory for Electrical Measurements (LEM), validates the developed calibration procedure through real case calibration of a 100 MHz digital oscilloscope RIGOL DS1102E, with technical specification in [14] and presented in Figure 8.

The uncertainty budget, for the both calibration stages (calibration of the vertical deflection and of the frequency bandwidth), is derived by combing data from a component of type A and components of type B, as in GUM, [5] and [15]. The uncertainty of type A, u_A, is calculated from the experimental data subjected to statistical processing, i.e. the mean value, X_{mean}, and the standard deviation of the measurement, s_A, as in:

$$s_A = \sqrt{\frac{1}{n-1}\sum_{i=1}^{n}(X_{icor} - X_{mean})^2} \quad (1)$$

where

$$X_{mean} = \frac{1}{n}\sum_{i}^{n} X_{icor} \quad (2)$$

$$X_{icor} = X_i - X_{ref} \quad (3)$$

X_i is the measured value in the particular point and X_{ref} is the reference value from the calibrator. The following uncertainty components are fused in the uncertainty budget of type B, u_B:

u_{res_instr} – from calibrated instrument resolution,
u_{res_refst} – from reference standard resolution
u_{d_refst} – from reference standard drift
u_{c_refst} – from the reference standard calibration

The combined uncertainty of type B equals:

$$u_B = \sqrt{u^2_{res_{instr}} + u^2_{res\_refst} + u^2_{d\_refst} + u^2_{c\_refst}} \quad (4)$$

The total combined uncertainty is:

$$u_c = \sqrt{u_A^2 + u_B^2} \quad (5)$$

The expanded uncertainty deployed in the particular rules for conformity of statement is:

$$U = 2 \cdot u_c \quad (6)$$

The delivery of the combined uncertainty is shown in the Ishikawa diagram in Figure 8.

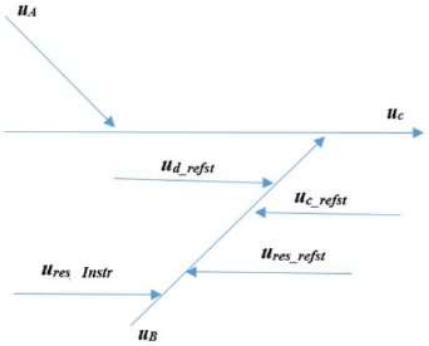

Figure 9. Ishikawa fishbone diagram of the factors in the combined uncertainty budget in calibration of high frequency instrument (valid for the two main oscilloscope parameters - the vertical deviation and the frequency band)

Table 2. Inputs of combined uncertainty budget for calibration of the digital oscilloscope RIGOL DS1102E at 12 V, @1 kHz

U_{ref} [V]	U_{mean} [V]	u_A [V]	u_{res_instr} [V]	u_{d_refst} [V]	u_{c_refst} [V]
12.000	11.97	0.0225	0.00289	0.00842	0.000005

The results of the calculation by using the data fusion concept, [5] at the measurement point of 12 V at frequency of 1 kHz are given in Table 2, with

values expressed in V. The derived combined uncertainty is:

$u_c = 0.024$ V (7)

and the expanded uncertainty is:

$u = 0.048$ V (8)

Similar methodology for uncertainty calculation in the calibration of the frequency bandwidth at 100 kHz, 500 kHz, 1 MHz and 50 MHz (results above the maximal frequency range of the publicly available CMC) at 1 V voltage, is applied. The results the concrete measurement setting are presented in Table 3.

Table 3. Inputs of combined uncertainty budget for calibration of the frequency bandwidth at different measurement points

f_{ref}	f_{mean}	u_A	u_{res_instr}	u_{d_refst}	u_{c_refst}
100 [kHz]	99.88333 [kHz]	0.50779 [kHz]	0.00289 [kHz]	0.0006 [kHz]	0.00005 [kHz]
500 [kHz]	498.5833 [kHz]	1.0037 [kHz]	0.00289 [kHz]	0.003 [kHz]	0.00005 [kHz]
1 [MHz]	0.998667 [MHz]	0.00604 [MHz]	0.00029 [MHz]	0.000006 [MHz]	0.0000005 [MHz]
50 [MHz]	50.06333 [MHz]	0.04560 [MHz]	0.00289 [MHz]	0.0003 [MHz]	0.000005 [MHz]

The derived combined and expanded uncertainties are provided in Table 4.

Table 4. Combined and expanded uncertainty for calibration of the frequency bandwidth at different measurement points

f_{ref}	u_c	U
100 [kHz]	0.51 [kHz]	1.02 [kHz]
500 [kHz]	1.004 [kHz]	2.008 [kHz]
1 [MHz]	0.006 [MHz]	0.012 [MHz]
50 [MHz]	0.046 [MHz]	0.091 [MHz]

4. SUMMARY AND CONCLUSIONS

The paper provides an analysis of the state-of-the-art CMCs available at international NMIs and laboratories in Southeast Europe for calibration of high frequency instruments. The restrictions of the publicly available CMC at high frequencies level i.e. over 1 MHz, are evident and the metrology gap is clearly identified.

The Laboratory of Electrical Measurements in Skopje has acquired and installed high accuracy class reference standard for high frequency instruments calibration (oscilloscopes or counters), and suitable calibration methods, with experimental validation presented in this contribution, has been developed. The extension of the accreditation scope of LEM over 1 MHz up to 630 MHz, will significantly improve the available high frequency calibration infrastructure. This will contribute to increased quality of the electronic components test facilities in the region, supporting and impacting the specific industries, like the automotive supply chain and wider.

5. ACKNOWLEDGEMENT

The research is conducted in the scientific project "Development and Upgrade of Laboratory Resources for Research and Introduction of New Analytical Methods in Electrical Metrology", Contract No. 15-15590/22, 22.11.2021, financed by the Ministry of Education and Science of Republic of North Macedonia.

6. REFERENCES

[1] "Automotive Industry in Southeast Europe", 2023 Report, SeeNext, seenext.org

[2] EURAMET cg-7 "Calibration of Measuring Devices for Electrical Quantities Calibration of Oscilloscopes", Calibration Guide, Version 1.0 (06/2011).

[3] M. Čundeva-Blajer, Gj. Dimitrovski, V. Sapundžiovski, V. Dimčev, K. Demerdžiev „Infrastructure Development For Extreme Electrical Metrology", Jour. Elect. Eng. and Inf. Tech., Vol. 7, No. 2, pp. 101–109 (2022). DOI: https://doi.org/10.51466/JEEIT2272201101chb

[4] K. Demerdziev, M. Cundeva-Blajer et. al. "Improvement of the FEIT Laboratory of Electrical Measurements Best CMC Through Internationally Traceable Calibrations and Inter-Laboratory Comparisons", Int. Conf. ETAI 2018, Struga, R. Macedonia, 20-22 Sept. 2018 (ETAI 6-4)

[5] M. Cundeva-Blajer "Data Fusion for Uncertainty Evaluation in Extreme Electrical Metrology", Proc. Int. Con. Measurement, Quality and Data Science MQDS 2023, 5-7.06.2023, Bordeaux, France

[6] www.bipm.org (retrieved on 28.06.2023)

[7] "Transmille 4015 Multiproduct Calibrator Extended Specifications", Transmille, UK 2022

[8] Y. Kuojun, P. Zhixiang, S. Jiali and Y. Peng, "A fast baseline and trigger level calibration method in digital oscilloscope," 2019 IEEE I2MTC, Auckland, New Zealand, 2019, pp. 1-6, doi: 10.1109/I2MTC.2019.8827158.

[9] C. Cho et al., "Calibration of channel mismatch in time-interleaved real-time digital oscilloscopes," 2015 85th Microwave Measurement Conf. (ARFTG), Phoenix, AZ, USA, 2015, pp. 1-5, doi: 10.1109/ARFTG.2015.7162896.

[10] W. Weifeng, Z. Yijiu, Y. Zhonghao, H. Hui and Z. Shanshan, "Design of automatic calibration in digital oscilloscope," 2019 14th IEEE Int. Conf. on Electronic Measurement & Instruments (ICEMI), Changsha, China, 2019, pp. 79-85, doi: 10.1109/ICEMI46757.2019.9101611.

[11] M. Bieler et al., "Rise-Time Calibration of 50-GHz Sampling Oscilloscopes: Intercomparison Between PTB and NPL," in IEEE Trans. on Instrumentation and Measurement, vol. 56, no. 2, pp. 266-270, April 2007, doi: 10.1109/TIM.2007.890609.

[12] C. Cho, J. -G. Lee, T. -W. Kang and N. -W. Kang, "Calibration of sample-time error in a sampling oscilloscope and uncertainty analysis," CPEM 2016, Ottawa, Canada, pp. 1-2, doi: 10.1109/CPEM.2016.7540669.

[13] Dongju Kim, Joo-Gwang Lee, Dong-Joon Lee and Chihyun Cho "Traceable calibration for a digital real-time oscilloscope with time interleaving architecture", 2018 *Meas. Sci. Tech.* 29 015003 https://doi.org/10.1088/1361-6501/aa892c

[14] Rigol, User's Guide, DS1000E, DS1000D Series, Digital Oscilloscopes, Sept.2010.

[15] "Evaluation of measurement data-Guide to the expression of uncertainty in measurement", JCGM 100:2008 GUM

#31

EXTREME IMPEDANCE CALIBRATIONS: ENHANCEMENT OF METROLOGY INFRASTRUCTURE

M. Cundeva-Blajer[1]/Presenter, M. Nakova[1], V. Sapundziovski[1], K. Demerdziev[1]

[1] Ss. Cyril and Methodius University in Skopje, Faculty of Electrical Engineering and Information Technologies-Skopje, Republic of North Macedonia, mcundeva@feit.ukim.edu.mk

Abstract:

The metrology infrastructure for electrical quantities in Southeast Europe is underdeveloped as certain areas of electrical instruments' calibrations are not well covered by the existing laboratories, even though there are economic and scientific needs. The paper shows the improvement of the calibration and measurement capabilities for extreme electrical impedance in the accredited Laboratory for Electrical Measurements at the Ss. Cyril and Methodius University in Skopje by deploying new calibration methods of instruments for extreme electrical resistance and inductance. The validation/verification of methods for traceability establishment and the innovative estimation of measurement uncertainty in impedance instruments calibration for improved metrology infrastructure capacity, are presented.

Keywords: extreme impedance, calibration of inductance, calibration of high resistance, CMC

1. INTRODUCTION

Metrology's main goal is to perform the most accurate measurements possible and to interpret the results properly. Metrology infrastructure keeps improving in two ways: 1-it allows measuring very high or very low physical quantities that the current labs cannot provide, or 2-it makes the measurements more accurate by reducing the uncertainty with new, better, or altered methods that already exist, [1]. In Southeast Europe the metrology infrastructure for electrical quantities is underdeveloped i.e., certain essential areas of electrical instruments' calibrations are not sufficiently covered by the existing metrology laboratories, [2]. However, the regional economy and science are expressing evident needs for this kind of calibration and testing facilities. The paper aims to present the boost of the calibration and measurement capabilities (CMCs) for extreme electrical impedance. It presents some challenges faced in developing this infrastructure and how they are being overcome. The accredited Laboratory for Electrical Measurements (LEM) at the Ss. Cyril and Methodius University (UKIM) in Skopje is introducing novel calibration procedures addressing instruments for instruments for very high and very low electrical resistance and inductance, which have not been covered by the existing laboratory scope of accreditation. The validation and verification procedures for establishment of traceability and the innovative techniques for estimation of measurement uncertainty for calibration of impedance instruments are conducted. The final objective of the research is the accreditation of novel calibration methods in the LEM, and contributing to the capacity building of the metrology infrastructure in the field of extreme electrical impedance, in particular in the region of Southeast Europe.

2. CURRENT STATE OF THE ART IN THE FIELD OF EXTREME ELECTRICAL IMPEDANCE METROLOGY

The electrical impedance is presented by the combined effect of resistance and reactance in a circuit of alternating current. The reactance can be predominantly inductive or capacitive. So, when talking of metrology of electrical impedance, it is an issue of measurement of electrical resistance, and measurement of reactance. Therefore, the current state of the art in calibration of instruments for electrical impedance is composed of best calibration and measurement capabilities (CMC) of electrical resistance, and best CMC of electrical inductance or capacitance. In this contribution the best CMC for electrical inductance and very high electrical resistance will be presented.

The field of electrical inductance has less developed calibration infrastructure than other electrical quantities, and showing metrological progress in calibrating devices for electrical inductance would be a contribution to the extreme electrical metrology, [3], [7]-[11]. Furthermore, most of the National Metrology Institutes and accredited calibration laboratories in their published CMCs demonstrate restricted scopes in the field of electrical inductance, [4]. The current state-of-the-art in the field of electrical inductance metrology is presented bellow through the comparison of the best CMCs at international level and at regional level of Southeast Europe, where the LEM laboratory is

located. In Figure 1, a comparison of the best CMCs at international level and in Figure 2 the best CMCs at regional level of Southeast Europe for electrical inductance of 10 mH are presented, based on the data in the KCDB database of BIPM, [4]. The electrical inductance of 10 mH introduces challenges in the process of calibration and the number of National Metrology Institutes (NMIs) and accredited calibration laboratories which perform these calibrations is rather low, [7]-[11].

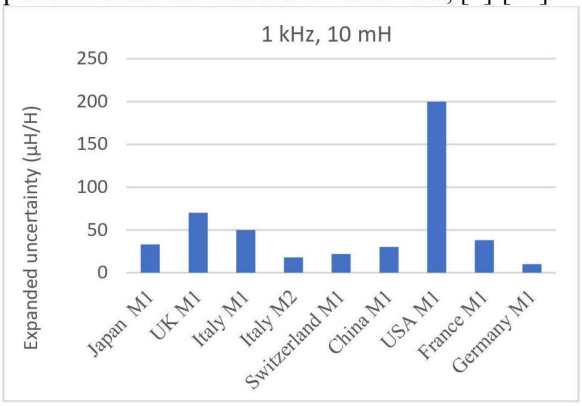

Figure 1. Expanded measurement uncertainties of inductance of 10 mH @1 kHz at the international NMIs

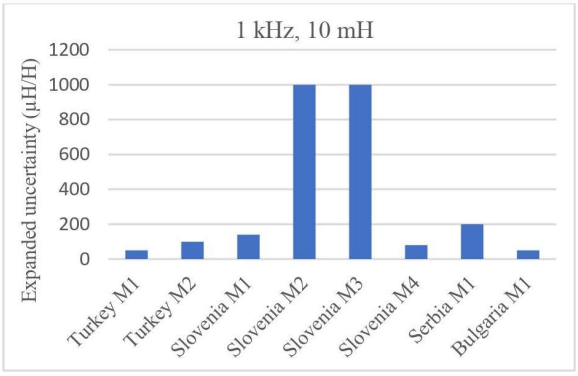

Figure 2. Expanded measurement uncertainties of inductance of 10 mH @1 kHz at the regional NMIs

Figure 3. LEM reference standard multifunctional calibrator Transmille 4015 with inductance calibration option

LEM has been an accredited calibration laboratory for electrical quantities instruments according to ISO 17025:2005 since 2015, and later according to ISO 17025:2017, but it does not have accreditation for electrical inductance instruments. LEM is working on establishment of a new calibration method for inductance instruments examination, [1]. A reference standard for electrical inductance, Transmille 4015 Multifunction calibrator, with an option IND for inductance generation, has recently been acquired. It is illustrated in Fig. 3, while the technical specification [5] is presented in Table 2, at a frequency of 1 kHz. It is calibrated in the electrical inductance measurement range at the producer's accredited calibration laboratory with established measurement traceability to national (NPL) and international primary reference standards (BIPM). As the presented results bellow are for the case study of calibration at 10 mH electrical inductance, some additional technical specification of the reference standard are:, Q-factor 8,6, display resolution 10 µH. The recommended measurement method in the range from 1 mH to 100 mH is L_s – serial reference impedance modelling [5]. The IND option is a built-in black box option of the Transmille 4015 Multifunctional Calibrator and there is no publicly available information on the physical system realisation of the inductance reference standard [5].

Table 1. Technical specification of the reference standard for electrical inductance of LEM

Multifunctional Calibrator Transmille 4015			
Supplement for calibration of instruments for inductance with specifications for 1 kHz and accuracy of ± 50 µH Transmille IND			
Electrical Inductance	**Q-factor**	**Display resolution**	**Best annual accuracy:**
1 mH	1	100 nH	0.5 %
10 mH	2.8	1 µH	0.5 %
19 mH	3.8	1 µH	0.5 %
29 mH	4.7	1 µH	0.5 %
50 mH	6.1	1 µH	0.5 %
100 mH	8.6	10 µH	0.5 %
1 H	29	100 µH	0.5 %
10 H	110	1 mH	0.5 %

In Fig. 4 and 5, the comparison of the expanded measurement uncertainties of the national metrology institutes at the international and regional level when measuring high electrical resistance of 1 TΩ, are shown, [4]. As a result of the perceived gap in measurement and calibration possibilities between top international laboratories, and considering the regional state of the metrological infrastructure in the area of electrical quantities, an analysis of the international supply of reference standards for electrical quantities that are not covered by the existing LEM reference standards has been carried out. Based on that, LEM has defined a detailed technical specification for the procurement of high accuracy class artefact, for significant expansion of the LEM's CMC. Table 2 shows the detailed technical specifications of the newly acquired reference standards in LEM for very high electrical resistance 5 kV IET Labs HRRSQ.

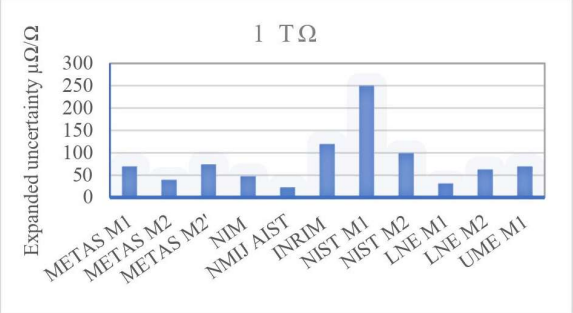

Figure 4. Expanded measurement uncertainties of electrical resistance of 1 TΩ at the international NMIs

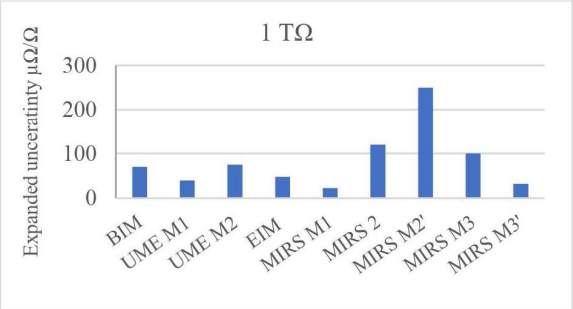

Figure 5. Expanded measurement uncertainties of electrical resistance of 1 TΩ at the regional NMIs level

Table 2. Technical specification of the reference standard for high electrical resistance of LEM

Reference standard resistance decade from 100 MΩ to 1 TΩ for voltage of 5 kV IET Labs HRRSQ	
Characteristics	**Value**
Electrical resistance	from 100 MΩ to 1 TΩ
Accuracy class	0.1% to 0.5%
Voltage level	5 kV
Temperature coefficient	25 ppm/°C to 100 ppm/°C
Voltage coefficient	1 ppm/V to 5 ppm/V

3. CALIBRATION PROCEDURES FOR EXTREME ELECTRICAL IMPEDANCE INSTRUMENTS DEVELOPED IN LEM

The national metrology institutes and the calibration laboratories in the field of electrical quantities develop diverse calibration methods for instruments for impedance i.e. inductance, [7-11] and resistance measurement, [12-14].

Figure 6. Test set-up in LEM for calibration of ROHDE & SCHWARZ HM8118 LCR-Bridge with the Transmille 4015 Multifunctional Calibrator

In this case study, the Laboratory for Electrical Measurements (LEM), develops a calibration procedure of LCR bridges i.e., more precisely a calibration procedure of meters for electrical inductance and calibration procedure of the electrical inductance measurement range of a LCR-meter is conducted for validation/verification. The UUT is ROHDE & SCHWARZ HM8118 - Programmable LCR-Bridge, with technical specification in [6] and test set-up as in Figure 6.

The developed calibration procedure for extreme i.e. very high electrical resistance is verified by calibration of a Metrel MI 2077 TeraOhm 5kV tera-ohmmeter with the technical specifications in [15] with reference standard resistance decade from 100 MΩ to 1 TΩ for voltage of 5 kV IET Labs HRRSQ.

Figure 7. Test set-up in LEM for calibration of Metrel MI 2077 TeraOhm 5kV with the 5 kV IET Labs HRRSQ resistance reference standards decade

The uncertainty budget, for the both calibration procedures, is built by fusing data from a component of type A and components of type B, as in GUM, [16]. The uncertainty of type A u_A is calculated from the experimental data subjected to statistical processing, i.e. the mean value X_{mean} and the standard deviation of the measurement s_A, as in:

$$s_A = \sqrt{\frac{1}{n-1}\sum_{i=1}^{n}(X_{icor} - X_{mean})^2} \quad (1)$$

where

$$X_{mean} = \frac{1}{n}\sum_{i}^{n} X_{icor} \quad (2)$$

$$X_{icor} = X_i - X_{ref} \quad (3)$$

X_i is the measured value in the particular point and X_{ref} is the reference value from the calibrator or the resistance reference standard. The following uncertainty components are fused in the uncertainty budget of type B, u_B:

u_{res_instr} – from calibrated instrument resolution,
u_{res_refst} – from reference standard resolution
u_{d_refst} – from reference standard drift
u_{c_refst} – from the reference standard calibration

The combined uncertainty of type B is:

$$u_B = \sqrt{u_{res\_instr}^2 + u_{res\_refst}^2 + u_{d\_refst}^2 + u_{c\_refst}^2} \quad (4)$$

The total combined uncertainty is:

$$u_c = \sqrt{u_A^2 + u_B^2} \quad (5)$$

With dominant type A uncertainty and sufficient high number of repeated measurements, the expanded uncertainty deployed in the particular rules for conformity of statement is:

$$U = 2 \cdot u_c \quad (6)$$

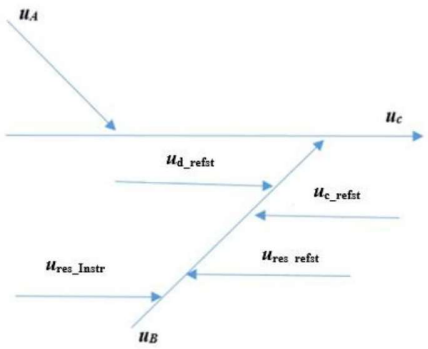

Figure 8. Ishikawa fishbone diagram of the factors in the combined uncertainty budget in calibration of impedance instrument (inductance-meter or tera-ohmmeter)

The results of the calculation by using the data fusion concept at the measurement point of 10 mH are in Table 3, with values expressed in mH:

Table 3. Inputs of combined uncertainty budget for calibration of the RLC-meter at 10 mH, @1 kHz

L_{ref} [mH]	L_{mean} [mH]	u_A [mH]	u_{res_instr} [mH]	u_{res_refst} [mH]	u_{d_refst} [mH]	u_{c_refst} [mH]
10.412	10.557	0.001	0.00003	0.00003	0.036	0.037

The derived combined uncertainty is:

$$u_c = 0.037 \text{ mH} \quad (7)$$

and the expanded uncertainty is:

$$U = 0.073 \text{ mH} \quad (8)$$

Similar methodology for calculation of the uncertainty of the calibration of the tera-ohmmeter at the measurement point of 1 TΩ, is applied.

Table 4. Inputs of combined uncertainty budget for calibration of the tera-ohmmeter at 1 TΩ, @1 kV

R_{ref} [TΩ]	T_{mean} [TΩ]	u_{res_instr} [TΩ]	u_{res_refst} [TΩ]	u_{d_refst} [TΩ]	u_{c_refst} [TΩ]
1.0	0.969	0.00003	0.002887	0.000289	0.0019

The derived combined uncertainty is:

$$u_c = 0.00348 \text{ TΩ} \quad (9)$$

and the expanded uncertainty equals:

$$U = 0.007 \text{ TΩ} \quad (10)$$

4. SUMMARY AND CONCLUSIONS

The contribution gives an overview of the current best CMCs for inductance and very high electrical resistance at the global level, and identifies the existing gap of the metrology infrastructure in Southeast Europe.

The Laboratory of Electrical Measurements in Skopje has acquired and installed high accuracy class reference standards for inductance and high electrical resistance and has developed suitable calibration methods. With the expansion of the accreditation scope, the available calibration facilities, contributing to the upgrades of the metrological infrastructure, are improved. The methodology presented is universal and can be used for further development of calibration methods in the field of extreme electrical metrology.

5. ACKNOWLEDGEMENT

The research is conducted in the scientific project "Development and Upgrade of Laboratory Resources for Research and Introduction of New Analytical Methods in Electrical Metrology", Contract No. 15-15590/22, 22.11.2021, financed by the Ministry of Education and Science of Republic of North Macedonia.

6. REFERENCES

[1] M. Čundeva-Blajer, Gj. Dimitrovski, V. Sapundžiovski, V. Dimčev, K. Demerdžiev „Infrastructure Development For Extreme Electrical Metrology“, Jour. Elect. Eng. and Inf. Tech., Vol. 7, No. 2, pp. 101–109 (2022). DOI: https://doi.org/10.51466/JEEIT2272201101chb

[2] Demerdziev K., Cundeva-Blajer M., Dimcev V., Srbinovska M., Kokolanski Z. “Improvement of the FEIT Laboratory of Electrical Measurements Best CMC Through Internationally Traceable Calibrations and Inter-Laboratory Comparisons”, Int. Conf. ETAI 2018, Struga, R. Macedonia, 20-22 Sept. 2018 (ETAI 6-4)

[3] M. Cundeva-Blajer “Data Fusion for Uncertainty Evaluation in Extreme Electrical Metrology”, Proc. Int. Con. Measurement, Quality and Data Science MQDS 2023, 5-7.06.2023, Bordeaux, France

[4] www.bipm.org (retrieved on 28.06.2023)

[5] “Transmille 4015 Multiproduct Calibrator Extended Specifications”, Transmille, UK 2022

[6] “HM8118 LCR-Bridge User Manual”, Rohde&Schwarz, München, Germany, 2016

[7] N. Sakamoto, "Long-term calibration results of 10 mH and 100 mH standard inductors using a reactance compensation method," CPEM 2012, Wash. DC, USA, 2012, pp. 582-583, doi: 10.1109/CPEM.2012.6251063.

[8] J. Bohacek, R. Sedlacek "Calibration of Inductance Standards," CPEM 2004, London, UK, 2004, pp. 37-38, doi: 10.1109/CPEM.2004.305408.

[9] M. Marzano et. al. "Primary Realization of Inductance and Capacitance Scales with a Fully Digital Bridge," IEEE Trans. Instr.&Meas. vol. 71, pp. 1-8, 2022, doi: 10.1109/TIM.2022.3214498.

[10] T. Skubis et. al. "Coherence of Comparison Results for 10 mH Inductance Standards," IEEE Conf. IMTC 2007, Warsaw, Poland, 2007, pp. 1-3, doi: 10.1109/IMTC.2007.379060.

[11] M. Ortolano et al, "A Comprehensive Analysis of Error Sources in Electronic Fully Digital Impedance Bridges," IEEE Tran. Instr.&Meas, vol. 70, pp. 1-14, 2021, doi: 10.1109/TIM.2020.3034115.

[12] P. P. Capra, F. Galliana, R. Cerri, M. Lanzillotti, F. Francone and A. Pollarolo, "Portable DC Voltage and Resistance Reference with Switching Unit for Calibration of Electrical Precision Multifunction Instruments," CPEM 2018, Paris, France, 2018, pp. 1-2, doi: 10.1109/CPEM.2018.8501092.

[13] K. -T. Kim et. al. "The Establishment of High DC Shunt Calibration System at KRISS and Comparison With NRC," IEEE Tran. Instr.&Meas. vol. 64, no. 6, pp. 1364-1368, June 2015, doi: 10.1109/TIM.2015.2399022.

[14] B. Schumacher and J. Melcher, "Automated high-value resistance calibration up to 1 PΩ," CPEM 2010, Daejeon, Korea (South), 2010, pp. 635-636, doi: 10.1109/CPEM.2010.5543482.

[15] https://www.metrel.si/assets/Metrel/PDF_dokumentacija/Single_leaflets/MI_2077_TeraOhm_5_kV/Ang/Single_2018_MI2077TeraOhm5kV_Ang.pdf (retrieved on 28.06.2023)

[16] “Evaluation of measurement data-Guide to the expression of uncertainty in measurement”, JCGM 100:2008 GUM

IMEKO TC8, TC11 and TC24 Joint Conference
October 11-13, 2023, Madeira, Portugal

THE DIGITAL NIST: STEPS TOWARD THE DIGITAL TRANSFORMATION OF NIST'S MEASUREMENT SERVICES

R.J. Hanisch,[1] J. Fedchak,[2] C. Cooksey,[3] K. Delak,[4] S. Choquette,[5]
W.D. Camara,[6] K. Rimmer,[7] I. Dominguez Mendoza[8]

[1] Material Measurement Laboratory, NIST, USA, robert.hanisch@nist.gov
[2] Physical Measurement Laboratory, NIST, USA, james.fedchak@nist.gov
[3] Physical Measurement Laboratory, NIST, USA, catherine.cooksey@nist.gov
[4] Information Technology Laboratory, NIST, USA, katya.delak@nist.gov
[5] Material Measurement Laboratory, NIST, USA, steven.choquette@nist.gov
[6] Material Measurement Laboratory, NIST, USA, william.camara@nist.gov
[7] Material Measurement Laboratory, NIST, USA, catherine.rimmer@nist.gov
[8] Informática, CENAM, Mexico, idomingu@cenam.mx

Abstract:
Beginning in 2022, NIST began a project called *The Digital NIST* which aims to make our measurement services—calibrations, standard reference materials, standard reference data--fully digital and fully FAIR [1]. We reported on this work previously [2] but provide here an update on further progress and prospects for future developments.

Keywords: calibrations; reference materials; reference data; measurement services; digitalization

1 INTRODUCTION

NIST is in the early phases of the digital transformation of metrology within its measurement services. Two key NIST services are the calibrations, of which there are over 400 services in nine different areas, and the standard reference materials (SRMs), of which NIST has more than 1100 in its catalog. Two separate but related projects are underway in each of these services: first, to develop a tool to both produce human readable calibration reports and NIST digital calibration reports (NDCR); the second is to produce a digital reference material certificate (DRMC) for our SRMs. Challenges for the calibration projects include the wide variety of reports NIST produces; a standard template must be developed for the human readable reports, and the elements of the reports must also be mapped into a digital report. NIST will leverage the XML schema DCC presently under development by PTB for calibration reports as much as possible. For the DRMCs, the metadata descriptors for reference materials are quite different and the DCC schema will need certificate-specific extensions. Demonstrating traceability to the SI is fundamental to both SRM products and calibration services and a digital representation of this traceability could be an important feature of digital certificates. Concerns regarding privacy and business identifiable information (BII) is particularly a challenge to calibration services. We describe here the NIST progress and status of these projects with a perspective of some of the key challenges regarding the digital representations of traceability that are presently perceived.

2 THE DIGITAL TRANSFORMATION OF METROLOGY FOR CALIBRATIONS

NIST calibration services is developing an application to produce both human readable and digital calibration reports from calibration data and metadata. Increasing internal efficiency of metrology organizations is one of the advantages to the digital transformation of metrology. To that end, NIST has a strong desire to both support its calibrations customers and increase the efficiency of the calibration services. NIST's stakeholders have expressed the desire to have a consistent format for the calibration reports that NIST produces from its many calibration services. Some of NIST's stakeholders also have need of calibration reports in a digital format. Creating an application that produces a human readable calibration report from calibration data and metadata in a consistent format is a first step toward a digital transformation of NIST's calibration services. Such an application can subsequently be used to produce a digital

calibration report based on, for example, an XML schema.

There are several challenges for this current effort. NIST reports tend to give extensive details on the measurement methodology, the data analysis, the apparatus, and, often, the calibration measurement history. NIST calibrations are traceable to NIST primary standards and are often unique. The technique, procedures, and equipment used give the best quality data at the lowest uncertainty. Consequently, NIST calibration reports have evolved to be customized and unique to each service. Even so, the NIST quality manual complies with reporting requirements of the ISO/IEC 17025:2017, and therefore the data and metadata in the reports do follow a common model. One of the challenges of this project is to define elements for the information contained in the reports that are not specified in the ISO/IEC 17025:2017 and to produce the reports in a consistent format.

Another challenge is pulling the metadata from various sources into the report. NIST customers place orders through an e-commerce system. Much of the customer metadata can be obtained from that system. However, metadata describing the equipment is often missing or incomplete, and so this metadata is typically provided by the technical expert performing the calibration. The technical expert also provides the metadata describing the calibration and calibration data. Presently, most of the NIST-provided data and metadata is stored in non-centralized locations. The calibration data is typically acquired and analyzed automatically with acquisition software such as LabVIEW or Python. In some cases, the analysis is performed separately from the acquisition software in spreadsheets. An application for report generation needs to be able to pull data from these various sources. Options for manual entry must also be included.

We have developed a standard template for calibration reports, but the display of data, such as in tables or graphs, is still under development. With so many unique services, there are many ways to display data. Initially, graphical representation of data will be embedded into the report as an image. Pictures or other graphics depicting equipment or apparatus are also common in NIST reports.

Once the calibration reports are broken into its fundamental elements, producing a NIST digital calibration report (NDCR) is somewhat straight forward. The data model and schema are taken from the DCC XML schema maintained by PTB [3]. Various enhancements are likely to be used by NIST; this is in nascent development and will evolve with the needs of NIST and its stakeholders.

A consideration by NIST throughout this development is security. NIST calibration reports are not public facing document. Business identifiable information is protected. Internally, even the metadata can only be accessed by authorized users with proper credentials.

3 DIGITAL CERTIFICATES OF ANALYSIS FOR REFERENCE MATERIALS AND TRACEABILITY

It was determined that to digitize the certificates of analysis, their information, mainly the values contained, must be stored in a database. For this, these data must be analyzed to classify and structure them in a way that leads to the design of the database and eventually to the design of a standard Digital Reference Material Certificate.

The first classification that was carried out was in a general way according to the types of values contained in the certificate and the mode of certification [4]; the classification was made according to the knowledge of those who handle this information. The classification is shown in Table 1.

Table 1. Value type classifications.

			Certification Mode		
			Batch non-continuous	Batch continuous (lot)	Serialized
Value type	Value and uncertainty	Single value	✓	✓	✓
		Multiple value	✓	n/a	✓
	Sequencing		✓	n/a	n/a
	Formula		✓	✓	✓

A random sample of around 130 certified reference materials (considering the current classification areas in NIST: chemical composition, physical properties, and engineering material) was taken to verify the classification and begin with the analysis of the information contained for a first attempt at database design.

The decision was made to focus, as a first objective, on the analysis and design of the database only for those reference material certificates whose type of value is, according to the general classification, "value and uncertainty" since they represent the bulk of existing SRMs. These are values of the measurands and associated information, such as their unit, uncertainty, traceability, type (certified or non-certified), identification, classification, and conversions. To create the model for reference materials, sample certificates were analyzed. In consultation with people responsible for the content of those

certificates, a specific and structured proposal was designed for this type of reference material certificates. Additional certificates were then added to the analysis and compared against the model design to determine whether they fit the model or the model needed to be adapted. This design includes the following:

- Value of the measurand.
- Unit: expressed as currently stated on the certificate (i.e., could be derived units) but includes information to make a conversion easier if necessary.
- Uncertainty: symmetric and non-symmetric, value of k, level of confidence, and type of uncertainty.
- Type of measurement: certified, non-certified, detection limit.
- Properties of the measurands: such as molar mass, to carry out conversions between mass fraction and concentration; minimum sample size to ensure homogeneity; traceability statements; whether the measurement is on a dry-mass basis; whether the measurement is dependent on a specific method.
- Identification and Synonyms: allowing for multiple ways of identifying what is being measured such as the common name, chemical name, CAS, chemical structure, InChi Key, etc.; all of them can be specified per measurand.
- Groups, allowing infinite ways to group values together such as elements, amino acids, vitamins, fats, tocopherols, etc.
- Statements: additional specific information to the measurand.
- Method(s) for obtaining the value, as well as who performed the measurement.

A test database has been generated with this design and testing carried out with real certificate information within the original sample of 130. The initial tests were satisfactory and now we are working on inserting information beyond that sample.

One of the challenges in the analysis of the reference materials is separating the data from the formatting. For many certificates the values are grouped and presented in ways that are easier for the human reader to understand. For example, a certificate may split the certified values into three separate tables so that Fats, Elements, and Tocopherols are grouped together. However, a good design will accommodate and record appropriate metadata about the value so that the information can be processed, analysed, and grouped in various ways in the future.

Dynamic future uses of certificates can be achieved by focusing the model on the value and its associated data. The values, units, and uncertainties can be evaluated in a systemic and consistent way when the data is stored discreetly. Machine programs can be written to take data from the Digital Reference Material Certificate and combine it with measured data from the user to allow the user to make claims of traceability more easily.

4 SUMMARY

Following a successful pilot project conducted in 2022, in which we confirmed that the PTB Digital Calibration Certificate construct could be adapted for NIST calibration reports and form the basis for NIST reference material certificates of analysis, we are continuing to develop the tools to routinely produce these digital artifacts. We have not yet set a schedule for production, and in any case digital calibration reports and digital reference material certificates will need to be phased in over a period of several years. We also intend to fully modernize NIST's measurement services such that we achieve full traceability to the SI in digital form.

5 REFERENCES

[1] M. Wilkinson et al., "The FAIR Guiding Principles for Scientific Data Management and Stewardship," Nature Scientific Data, vol. 3, article no.160018,2016.DOI: 10.1038/sdata.2016.18

[2] W. D. Camara et al., "Digital NIST: An Examination of the Obstacles and Opportunities in the Digital Transformation of NIST's Reference Materials," Acta IMEKO, vol. 12, no.1, 2023.DOI: 10.21014/actaimeko.v12i1.1403

[3]https://www.ptb.de/dcc/v3.0.0/ [accessed June 2023]

[4] C. R. Beauchamp et al., "Metrological Tools for the Reference Materials and Reference Instruments of the NIST Material Measurement Laboratory," NIST Special Publication 260-136, 2021 edition; National Institute of Standards and Technology, Gaithersburg, MD (2021); available at https://nvlpubs.nist.gov/nistpubs/SpecialPublications/NIST.SP.260-136-2021.pdf [accessed July 2023].

IMEKO TC8, TC11 and TC24 Joint Conference
October 11-13, 2023, Madeira, Portugal

VALIDATION OF A METHOD FOR THE EXTRACTION AND QUANTIFICATION OF WATER-SOLUBLE CHLORIDE IN CEMENT BY ION CHROMATOGRAPHY

C. Daniel[1], A.R. Dablio[1], R. Damian[1], M. Lagmay[1], J.A. Valdueza[1], J.E. Guerrero[1], M.A. Principe[1]

[1]Standards and Testing Division, Industrial Technology Development Institute, Department of Science and Technology, Bicutan, Taguig City, Philippines, csdaniel@itdi.dost.gov.ph

Abstract:
Chloride is a corrosive anion that can attack steel and other metal embedded materials in concrete structures leading to its degradation. Chloride in concrete may come from the materials used for making concrete such as cement. Hence, it is important to have a reliable method for determining chloride in cement, in this case the water-soluble chloride which is representative of chloride that may pose corrosion risk. In this study, ASTM C1218/C1218M-20 was used as a guide for sample extraction and the water-soluble chloride was later quantified by ion chromatography. Validation of this method from extraction to instrumental determination was conducted by assessment of the linear range, detection limit, precision, and trueness. It was found that the method was suitable for the determination of water-soluble chloride content in cement.

Keywords: water-soluble chloride; cement; method validation

1. INTRODUCTION

Concrete is a composite construction material consisting of a filler and a binder. Cement paste (cement + water) acts as the binder, while aggregates serve as the filler [1-2]. One of the major degradation mechanisms of concrete is the corrosion of reinforcing steel bars (rebars). Chloride is one of the deleterious species of reinforced concrete [3,6]. The mechanism by which it corrodes the rebar is based on the destruction of the protective thin layer of steel due to the changes in pH. It is usually caused by the thermal transformation products of calcium oxychloride salts. This action is collectively referred to as chloride penetration [4,7].

Chloride may be introduced into the concrete via internal and external sources. Internal sources include inherently chloride-containing mixing-water, cement and aggregates, while external sources come from the surrounding environment. Since it may affect the structural integrity at excessive levels, it is crucial to test the concrete and its primary ingredients for their chloride content. This is to assess the condition of concrete cover around reinforcement, and forecast the corrosion risk of reinforced concrete where chlorides penetrate [6].

On the basis of how they are tightly held in the material, chloride may be present in two states - chemically bound and free ions. As only the latter primarily influences the corrosion process, the free chloride ion content must be determined to assess risk of corrosion. In essence, the free ions are the ones that can be extracted by water. For this reason, they may also be referred to as the water-soluble chloride [5].

Regulatory bodies have set the maximum permissible level of chloride in concrete. For instance, the American Concrete Institute (ACI) has set the maximum water-soluble chloride content in concrete at 0.06 - 1.00 percent by weight of cement, depending on the type of concrete [8]. Meanwhile, the European Standards (EN 206-26) has a recommendation of 0.1-0.4 percent by weight of cement, depending on the type of concrete [9].

A reliable and accurate analytical method is essential to support this regulation. There are already existing methods used for quantification of water-soluble chloride from the American Society of Testing Materials (ASTM), American Association of State Highway and Transportation Officials (AASHTO), and International Union of Laboratories and Experts in Construction Materials, Systems and Structures (RILEM) [10-11]. They differ in the extraction conditions and quantitation methods. Potentiometric titration, Volhard method, and Ion Chromatography are some of the analytical techniques that can be utilized.

In this study, a method for extraction and quantification of water-soluble chloride in cement was developed and subsequently validated. ASTM C1218/C1218M-20 was used as the main guide for the extraction procedure. Specifically, the objectives of the study are as follows: (1) to harmonize the extraction procedure used in the

laboratory and the next steps in sample preparation prior to instrumental determination, and (2) to validate the extraction procedure and ion chromatographic method to assess its suitability for water-soluble chloride determination in cement.

2. METHODOLOGY

2.1 Materials and reagents

All solid chemical reagents are analytical reagent (AR) grade. Type 1 water was used as diluent to standard solutions and mobile phase and as an extracting solvent.

Calibration stock standard solution used was Supelco Certripur Anion multi-element standard II with 1000 mg/L chloride concentration. Calibration solutions were prepared following the instrument working range of 0.25 - 12.0 mg/L with at least 6 concentration points. The spiking standard solution of 2126 mg/L Cl^- was prepared from solid potassium chloride.

Eluent solution or mobile phase was 8.0 mM sodium carbonate (Na_2CO_3)/1.0 mM sodium bicarbonate ($NaHCO_3$), prepared by dilution of Dionex AS14A eluent concentrate (0.8 M sodium carbonate Na_2CO_3/0.1 M $NaHCO_3$). The mobile phase was filtered in cellulose nitrate 1.0 um membrane filter using a vacuum filtration system.

The ordinary portland cement samples (grayish fine powder) were obtained from various local cement plants.

2.2 Sample extraction

The ASTM C1218/C1218M-20 Standard Test Method for Water-Soluble Chloride in Mortar and Concrete [10] was used as a reference for method development of the sample extraction procedure. The general procedure involved weighing 10 g of cement sample, followed by the addition of 50 mL of Type 1 water and boiling the mixture for not more than 5 minutes to extract the water-soluble chloride. Four different conditions (see Table 1) were studied to know the effect of 24 h standing, washing, and dilution to the amount of chloride extracted. All mixtures were filtered using Whatman #42 filter paper and dilutions were made to obtain a 100 mL solution.

2.3 Instrumental determination

Chloride quantification was performed using a Dionex IonPac AS14A analytical column (4 x 250 mm) with Dionex IonPac AG14A guard column (4 x 50 mm) on a Dionex ICS-1000 Ion Chromatography System. The ion chromatograph is equipped with an isocratic pump, a chemical suppressor and conductivity detector. The instrument conditions used (Table 2) were the same as that already established by the laboratory for the analysis of chloride in water. The standards and samples were manually injected with 0.45 µm acrodisc syringe filter. The chloride ion was eluted 4.4 minutes after sample injection.

Table 1: Different conditions employed for extraction of water-soluble chloride after boiling

Treatment	Sample preparation conditions		
	stand 24 h	washing	dilution
A	Yes	Yes	Yes
B	No	Yes	Yes
C	No	No	No
D	Yes	No	No

Table 2: Ion chromatographic conditions employed for chloride determination

Parameter	Value
Pump flow rate	0.90 mL/min
Suppressor current	50 mA
Cell temperature	30 °C
Injection volume	1 mL
Run time	15 minutes

2.4 Volhard titration method

For the comparison of ion chromatography and argentometric chloride titration, the cement sample was prepared by following ASTM C1218. To the cement water extract, 3 mL of (1:1) HNO_3 was added, followed by 3 mL of 30% hydrogen peroxide. After standing for 1-2 minutes, the solution is heated to near boiling then cooled.

For back titration, 5.00 mL of 0.025 N $AgNO_3$ was added to precipitate the chloride as silver chloride. Afterwards, 3 mL of benzyl alcohol was added and 2 mL of ferric ammonium sulfate indicator. The unreacted silver ion was titrated with 0.025 N NH_4SCN.

2.5 Method validation studies

Validation of the extraction method and ion chromatographic analysis was performed by using the Eurachem Guide [12] as a reference. Linearity and working range and detection limit was already established in the ion chromatography system for water analysis. Hence the calibration standards were prepared by considering these already established parameters. For repeatability assessment, two cement samples with different chloride

concentrations were used. Since there is no available certified reference material, the trueness of the method was assessed by spiking the sample at around 100% level with 2126 mg/L Cl^- which was prepared from solid potassium chloride. The concentration of the laboratory prepared spiking solution was confirmed by ion chromatography.

3. RESULTS AND DISCUSSION

3.1 Effect of different sample preparation conditions

In the initial studies, two ordinary portland cement samples were used to determine the effect of different sample processing conditions after boiling the cement-water mixture on the extracted chloride. ASTM C1218 requires the sample to stand for 24 hours prior to filtration and instrumental determination. Treatment A and D follow the ASTM method in the sense that the sample was allowed to stand for 24 h prior to filtration. Treatment B and C was included in the study to know if the additional solvent used for washing and thereafter dilution will affect the chloride values significantly.

The results in Table 3 show that the different processing conditions after boiling have a significant effect on the obtained chloride values. Samples that were allowed to stand for 24 hours and were diluted afterwards had the lowest chloride concentration while those samples that were filtered after cooling down to room temperature had relatively higher chloride extracted. The final volume after extraction has a great influence on the calculated amount of chloride. For Treatment C and D, the final volume after extraction is less than the original amount of water added (water absorption capacity differ per cement sample) hence this reduction in volume after extraction caused the higher chloride values than Treatment A. Additional amount of water for washings has no effect on Treatment A since the cement has already hardened after 24 hours thereby no additional chloride can be extracted. But for Treatment B, there is a possibility for additional extraction from the washing solvent for the quantitative filtration and dilution hence results for Treatment B are higher compared to Treatment A wherein both employ the washing and dilution step. These results show that the extraction and final sample preparation steps prior to injection in the ion chromatography system have a significant effect on the chloride values. Hence, one can only make a good comparison of results if similar preparation steps were followed.

For consistency in the sample preparation workflow for routine laboratory analysis, the extraction procedure that was followed in the method validation study was Treatment A. The chloride value obtained by this method was comparable to the acid-soluble chloride content of the cement sample.

Table 3: Effect of different extraction conditions on the water-soluble chloride by ion chromatography

Treatment	Sample 1		Sample 2	
	Average Cl (mg/kg)	%RSD (n=7)	Average Cl (mg/kg)	%RSD (n=3)
A	62.1	2.5	54.1	1.9
B	96.7	1.1	107.6	4.6
C	122.5	6.3	100.5	3.7
D	102.2	2.4	72.3	1.7

3.2 Comparison of ion chromatography and Volhard titration results

The results of ion chromatography were compared with the results obtained by Volhard titration. Using a representative water-extract sample (Sample 1, Treatment B), Volhard titration was performed by following the procedure described in 2.4. The titration results showed an average chloride value of 94.2 mg/kg (%RSD= 4.63). There is a good agreement between ion chromatography and Volhard titration results.

Although the results are comparable, the ion chromatography method offers the advantage of being able to detect lower chloride concentrations. Through instrumental determination, operator error in visual endpoint detection during titration is eliminated, removing this bias during chloride determination.

3.3 Method validation results

The suitability of a method is assessed by evaluating various figures of merit which include but are not limited to the following: linear working range, method detection limit, precision, and trueness. The method must pass certain analytical requirements, as shown in Table 4, to consider it fit for the intended purpose.

The maximum permissible level set for water-soluble chloride in concrete is 60 mg/kg. This means beyond this level the chloride may trigger degradation of concrete. Those cement products that contain chloride concentrations below this regulation limit are said to conform to this standard specification. In order to come up with a correct and sound conformity assessment of cements based on their chloride content, a method capable of detecting chloride concentration way below this regulation limit must be in place.

Linear working range is the interval over which the method provides results with an acceptable

uncertainty. The ion chromatography system has an already established working range of 0.25 - 12.0 mg/L. This was based on linear regression analysis and residual plots.

Table 4: Summary of method performance characteristics for water-soluble chloride in cement determination by ion chromatography

Parameter	Acceptance criteria	Experimental Value
linear range (mg/L)	0.25 - 12	0.25 - 12
method detection limit (mg/kg)	60	11
repeatability (%RSD)	5.3 (100 mg/kg)	2.54 (62.1 mg/kg, n=7)
		2.74 (75.2 mg/kg, n=7)
trueness by spiking (% recovery)	90 – 107 (100 mg/kg)	95.5 – 105.5 (100 % spiking level; n=4)

Method detection limit (MDL) is the lowest concentration of the analyte that can be detected by the method at a specified level of confidence. MDL was assessed by analyzing 11 blank samples that underwent the whole analytical procedure. The calculated average chloride concentration and standard deviation (s) was 7.38 and 4.06 mg/kg, respectively. Corrected standard deviation was computed and found to be 3.52 mg/kg. This was multiplied by the factor '3' (as suggested in the Eurachem Guide [12]) to finally determine the MDL which was found to be 11 mg/kg. This is way below the 60 mg/kg acceptance criteria.

Precision is a measure of how close the results are to one another. This can be assessed through the percent relative standard deviation (%RSD). A low %RSD indicates a good agreement of data with one another. Two samples, seven replicates each, were analyzed using the method under repeatability conditions. The %RSD were calculated as 2.54 and 2.74% for sample 1 and 2, respectively. These values passed the 5.3% acceptance criteria at 100 mg/kg concentration level.

Trueness is an expression of how close the mean of an infinite number of results is to a reference value. This was assessed through the percent recovery of spiked samples. The percent recoveries ranged from 95.5 - 105.5%. This is within the 90-107% limit at 100 mg/kg concentration level.

In summary, the method passed the requirements for the four mentioned method validation parameters, as shown in Table 4. Hence, the method is suitable for the analysis of water-soluble chloride in cement.

3.4 Application of the method to various cement samples

The validated method was used to determine the water-soluble chloride content of different ordinary portland cement samples (mostly Type 1) that are either produced locally or supplied by various cement suppliers. As shown in Table 5, all the cement samples have chloride values that are below the regulatory limit.

Table 5: Water-soluble chloride content of different cement samples from local cement plants and cement suppliers.

Cement sample	Water-soluble chloride (mg/kg)
1	62.1
2	54.1
3	84.2
4	37.7
5	33.2
6	40.2
7	56.8
8	49.4
9	50.3
10	77.6

4. CONCLUSIONS

It was demonstrated in this study that different sample preparation procedures after hot water extraction of the cement would give different chloride values. Hence, only when similar extraction procedures are followed we can expect a good comparability of results. The water-soluble chloride content varied greatly with treatment. Treatment A, which is consistent with ASTM C1218, is the chosen method for the extraction of water-soluble chloride in cement. This was the sample preparation method used in the method validation.

Based on its performance characteristics, the method is suitable for the determination of water-soluble chloride in cement. Linear working range was from 0.25 - 12 mg/L. The method detection limit (MDL) was found to be 11 mg/kg. Method precision (repeatability) was below the 5.3 %RSD acceptance criteria. Method trueness by recovery was within 90-107% requirement.

For further validation, the method can be tested using a certified reference material. Also, other figures of merit such as intermediate precision,

selectivity, among others, should be assessed to further evaluate the method.

5. SUMMARY

The laboratory used ASTM C1218 method to come up with the final procedure for the extraction of the water-soluble chloride in cement. The method involved boiling the cement sample in water and allowing it to stand for 24 h prior to filtration and dilution. Afterwards, the extracted chloride ion was quantitated using ion chromatography. The performance characteristics of this method were assessed and was found to be fit for use in a routine chemical testing laboratory.

6. REFERENCES

[1] University of Illinois, "Concrete: Scientific Principles." Online [Accessed 20230510]: http://matse1.matse.illinois.edu/concrete/prin.html

[2] Penn State College of Engineering, "Composition of Cement." Online [Accessed 20230510]: https://www.engr.psu.edu/ce/courses/ce584/concrete/library/construction/curing/Composition%20of%20cement.htm

[3] N. Klein, E. D. Gómez, G. S. Duffó, and S. B. Farina, "Effect of sulphate on the corrosion of reinforcing steel in concrete," Constr Build Mater, vol. 354, Nov. 2022, doi: 10.1016/j.conbuildmat.2022.129214.

[4] U.A. Birnin-Yauri, S. Garba, "The effect and mechanism of chloride ion attack on portland cement concrete and the structural steel reinforcement", IFE Journal of Science, vol. 8, no. 2, pp. 131-134, 2006.

[5] C. Arya, N.R. Buenfeld, J.B. Newman, "Assessment of Simple Methods of Determining the Free Chloride Ion Content of Cement Paste", Cement and Concrete Research, vol. 17, pp. 907-918, 1987.

[6] T. Chaussadent, G. Arliguie, "AFREM test procedures concerning chlorides in concrete: Extraction and titration methods", Materials and Structures, vol. 32, pp. 230-234, April 1999.

[7] A.A. Ahmed, D. Trejo, "Quantifying Conservativeness of Water-Soluble Chloride Testing", ACI Materials Journal, vol. 120, no. 2, March 2023.

[8] ACI Committee, "Chloride limits in the ACI 318 building code requirements", 1998.

[9] European Standards, "National Annex — EN 206 — Concrete - Specification, performance, production and conformity", Draft, Rev. 10, 2014

[10] ASTM C1218. (2008). Standard Test Method for Water-Soluble Chloride in Mortar and Concrete, American Society for Testing and Materials (ASTM) Philadelphia, PA.

[11] RILEM TC 178-TMC, "Analysis of water soluble chloride content in concrete (Recommendation)", Materials and Structures, vol. 35, pp. 586-588, November 2002.

[12] B. Magnusson, U. Örnemark (eds.), "Eurachem Guide: The Fitness for Purpose of Analytical Methods – A Laboratory Guide to Method Validation and Related Topics", 2nd ed. 2014. ISBN 978-91-87461-59-0. Online [Accessed 20230530]: https://www.eurachem.org/images/stories/Guides/pdf/MV_guide_2nd_ed_EN.pdf